

**RATIONAL DESIGN OF A NEW CLASS OF  
CYCLODEXTRIN-CONTAINING POLYMERS FOR GENE DELIVERY**

Thesis by  
Suzie Jean Hwang

In Partial Fulfillment of the Requirements  
for the Degree of

Doctor of Philosophy

California Institute of Technology

Pasadena, California

2001

(Submitted December 19, 2000)

© 2001

Suzie Jean Hwang

All Rights Reserved

## **Dedication**

To my family for all their love and support

## Acknowledgments

I thank God for many people who have been blessings to me during my time at Caltech.

I am particularly grateful to the following people for their support and assistance:

My sincerest gratitude to my advisor, Mark Davis, for all of his support and encouragement throughout my time at Caltech. His dedication and excitement about the work carried this project and motivated me through the “dry spells” of experimental research. His greatest lessons to me were from his example as an advisor and scientist.

Many thanks to Dr. Hector Gonzalez, for setting the foundations of this project with his chemistry expertise, and for his helpful advice to me throughout my time at Caltech. Thanks also to Dr. Nathalie Bellocq, for her invaluable input to this project and for being such a good friend and fun officemate.

My committee members have been generous with their time and advice: Doctor Mark Farbstein, Professor David Tirrell, Professor Timothy Triche, and Professor Scott Fraser.

I am grateful to the Whitaker Foundation for their financial support.

My appreciation to Pat Koen of the Electron Microscopy Facility, Rochelle Diamond of the Flow Cytometry Facility, the Biological Imaging Center staff, and the staff at Peptide Synthesis Facility for their assistance throughout the project.

Thanks to the members of the Davis group for a wonderful work environment. Special thanks to Patricia, my aerobics buddy, for getting me in touch with my Texan roots, Geraldo, for his unparalleled and frequently amusing straight-talk, and Lin, for her friendship throughout graduate school. Best wishes to the new students, Swaroop, John, Jeremy, Andrea and Steve.

The following people enhanced my quality of life here with their much appreciated friendship: Aileen – my sister in Christ, thank you for your love and prayers, Swee – my dear roomie, I miss our late-night food runs to Monterey Park, and Dorothy, Ning, Lintong, Jie-Hui – for hours of ba sze fen fun, and more importantly, for friendships beyond a lifetime. I am also indebted to Perlita and Roland Uyboco and Thomas and Carmen Hall for their guidance and friendship.

Thanks to Winston, who walked beside me the entire way. His love and friendship is an irreplaceable part of my life.

Most of all, I thank my family for their constant love and support. To my mom and dad who struggle and work to make it easy for me to follow my dreams - their selflessness and sacrifice will always remain with me. Thanks also to Stephanie, my sister and closest friend, for all of her encouragements.

## Abstract

The transfer of gene therapy from an academic exercise to a clinical setting demands the development of an efficient, biocompatible gene delivery vector. Current non-viral systems suffer from toxicity, low transfection efficiency, and in vivo instability. In this work, a new class of polymers was designed to address these issues. Linear, polyamidine,  $\beta$ -cyclodextrin ( $\beta$ CD)-containing polymers ( $\beta$ CDPs) are synthesized by polymerizing difunctionalized cyclodextrins with other difunctionalized comonomers. The inclusion of  $\beta$ CD in the backbone of the polyamidine polymers decreases the  $IC_{50}$ s by three orders of magnitude, resulting in a polymer with very low in vitro and in vivo toxicity. The cationic  $\beta$ CDPs are able to self-assemble with and condense DNA into small particles (100-150 nm in diameter). When formulated at a positive charge, the complexes are readily internalized by nearly all exposed cultured cells.

The transgene expression from the delivered complexes was increased by fine-tuning the  $\beta$ CDP structure for optimum reporter gene activity and by modifying the polymer to enhance endosomal release. The function of the  $\beta$ CDPs was found to be highly dependent on the polymer structure; changes in position of the amidine charge centers by a few angstroms resulted in transfection and toxicity differences of one order of magnitude. The highest transfection is achieved with the  $\beta$ CDP6 polymer, that contains a 2 methylene spacer between the cyclodextrin and amidine group and a 6 methylene spacer between adjacent amidine functionalities. The conjugation of a pH-sensitive moiety, histidine, to  $\beta$ CDP6 endgroups also increases transgene expression by 20-fold without a change in polymer toxicity. Flow cytometry and confocal microscopy experiments with fluorescently-labeled DNA suggest that histidylation of  $\beta$ CDP6 enhances transfection by buffering the endosomal pH, thereby delaying lysosomal degradation and allowing for more endosome release.

The  $\beta$ CDP-based particles ( $\beta$ CD-polyplexes) were modified for in vivo stability by using the ability of cyclodextrins to form inclusion complexes with hydrophobic guest molecules. Various compounds were conjugated to adamantane, a molecule that has a high cyclodextrin association constant. The adamantane conjugates, when added to preformed  $\beta$ CD-polyplexes, are able to self-assemble with the  $\beta$ CD-polyplexes without disrupting the polymer/DNA binding interactions. Using this method,  $\beta$ CD-polyplexes were modified with adamantane-polyethylene glycol (PEG) conjugates. The PEGylated particles were salt stabilized in a PEG length-dependent manner. In a second example, modification of  $\beta$ CD-polyplexes with anionic peptide-adamantane conjugates prevented non-specific cellular uptake in cultured cells. The assembly of the three components, DNA,  $\beta$ CDP, and adamantane-based modifier, results in a particle with the potential for achieving systemic, in vivo gene delivery. Finally, a small molecule, fluorescein, was conjugated to adamantane and co-delivered with  $\beta$ CD-polyplexes to cultured cells, thus demonstrating the possibility for therapeutic pouches of small molecule and gene-drugs.

## Table of Contents

<b>1. INTRODUCTION.....</b>	<b>1</b>
<b>1.1 OBJECTIVES.....</b>	<b>1</b>
<b>1.2. HUMAN GENE THERAPY.....</b>	<b>2</b>
1.2.1. Methods of Genetic Intervention.....	2
1.2.2. History of Human Gene Therapy.....	4
1.2.3. Current Status of Gene Therapy.....	6
<b>1.3. GENE DELIVERY.....</b>	<b>8</b>
1.3.1. The need for a DNA carrier.....	9
1.3.2. Receptor-mediated delivery.....	9
1.3.3. The ideal gene delivery system.....	10
1.3.4. Viral delivery systems.....	12
1.3.5. Nonviral delivery systems.....	13
<b>1.4. CYCLODEXTRINS.....</b>	<b>16</b>
<b>1.5. LITERATURE CITED.....</b>	<b>20</b>
 <b>2. A NEW CLASS OF POLYMERS FOR THE DELIVERY OF MACROMOLECULAR THERAPEUTICS.....</b>	 <b>23</b>
<b>2.1. ABSTRACT.....</b>	<b>23</b>
<b>2.2. INTRODUCTION.....</b>	<b>24</b>
<b>2.3. MATERIALS AND METHODS .....</b>	<b>25</b>
2.3.1. Polymer synthesis and characterization.....	25
2.3.2. Solid phase DNA binding assay.....	28
2.3.3. Polyplex formation and characterization.....	29
2.3.4. Cell culture and transfections.....	30
<b>2.4. RESULTS.....</b>	<b>31</b>
2.4.1. Binding of functionalized CD monomers to DNA.....	31
2.4.2. DNA binding of CD-polymer.....	32
2.4.3. In vitro transfection and toxicity of DNA complexes.....	33
2.4.4. Particle characterization.....	39
<b>2.5. DISCUSSION.....</b>	<b>42</b>
<b>2.6. ACKNOWLEDGMENTS.....</b>	<b>46</b>
<b>2.7. LITERATURE CITED.....</b>	<b>46</b>

<b>3. EFFECTS OF STRUCTURE OF <math>\beta</math>-CYCLODEXTRIN-CONTAINING POLYMERS ON GENE DELIVERY.....</b>	<b>50</b>
<b>3.1. ABSTRACT.....</b>	<b>50</b>
<b>3.2. INTRODUCTION.....</b>	<b>51</b>
<b>3.3. MATERIALS AND METHODS.....</b>	<b>52</b>
3.3.1. $\beta$ -Cyclodextrin-polymers.....	52
3.3.2. Polyamidine polymers.....	57
3.3.3. Polymer characterization.....	58
3.3.4. Polyplexes.....	59
3.3.5. Cell culture and polyfections.....	60
3.3.6. IC <sub>50</sub> determination.....	61
<b>3.4. RESULTS.....</b>	<b>61</b>
3.4.1. $\beta$ CDPs synthesis and characterization.....	61
3.4.2. Polyplex characterization.....	62
3.4.3. DNase protection.....	65
3.4.4. In vitro transfection and toxicity of $\beta$ CDP polyplexes.....	65
3.4.5. Polymer displacement by heparan sulfate.....	69
<b>3.5. DISCUSSION.....</b>	<b>71</b>
<b>3.6. LITERATURE CITED.....</b>	<b>77</b>
<b>4. INCREASED TRANSFECTION BY HISTIDYLATION OF A CATIONIC CYCLODEXTRIN-BASED POLYMER .....</b>	<b>80</b>
<b>4.1. ABSTRACT.....</b>	<b>80</b>
<b>4.2. INTRODUCTION.....</b>	<b>81</b>
<b>4.3. MATERIALS AND METHODS.....</b>	<b>82</b>
4.3.1. Polymer synthesis.....	82
4.3.2. Polyplexes.....	83
4.3.3. Cells and transfections.....	84
<b>4.4. RESULTS.....</b>	<b>86</b>
4.4.1. Histidylated $\beta$ -cyclodextrin-DMS.....	86
4.4.2. Polyplex formation.....	86
4.4.3. Transfection ability of Hist-CDP6.....	88
4.4.4. Plasmid Delivery by Hist-CDP6.....	90
4.4.5. Intracellular distribution of Hist-CDP6-delivered oligos.....	90
4.4.6. Transfections in the presence of chloroquine.....	94
<b>4.5. DISCUSSION.....</b>	<b>95</b>
<b>4.6. LITERATURE CITED.....</b>	<b>100</b>

<b>5. MODIFICATION OF <math>\beta</math>-CYCLODEXTRIN POLYMER-BASED POLYPLEXES BY CYCLODEXTRIN-ADAMANTANE INCLUSION COMPLEX FORMATION .....</b>	<b>103</b>
<b>5.1. ABSTRACT.....</b>	<b>103</b>
<b>5.2. INTRODUCTION.....</b>	<b>104</b>
<b>5.3. MATERIALS AND METHODS.....</b>	<b>106</b>
5.3.1. Polymer and peptide preparation.....	106
5.3.2. Polyplexes and modifications with GALA peptide.....	107
5.3.3. Cells and transfection.....	108
<b>5.4. RESULTS.....</b>	<b>109</b>
5.4.1. Particle size of modified complexes.....	109
5.4.2. Zeta potential of modified complexes.....	110
5.4.3. DNA delivery efficiency of modified complexes.....	112
5.4.4. Transfection efficiency of modified complexes.....	114
5.4.5. Toxicity of modified complexes.....	117
<b>5.5. DISCUSSION.....</b>	<b>118</b>
<b>5.6. LITERATURE CITED.....</b>	<b>123</b>
<b>6. APPLICATIONS OF <math>\beta</math>-CYCLODEXTRIN POLYMER-CONTAINING POLYPLEXES MODIFIED BY INCLUSION COMPLEX FORMATION.....</b>	<b>126</b>
<b>6.1. ABSTRACT.....</b>	<b>126</b>
<b>6.2. INTRODUCTION.....</b>	<b>127</b>
<b>6.3. MATERIALS AND METHODS.....</b>	<b>129</b>
6.3.1. Synthesis of adamantane conjugates.....	129
6.3.2. Synthesis of cyclodextrin-based polymers.....	131
6.3.3. Polyplex preparation and characterization.....	132
6.3.4. Cell culture and transfection experiments.....	133
<b>6.4. RESULTS AND DISCUSSION.....</b>	<b>135</b>
6.4.1. Polyplex stabilization by pegylation.....	135
6.4.2. Adamantane-mediated co-delivery of small molecules and peptides.....	145
6.4.3. Galactose conjugation for targeted delivery to hepatocytes.....	147
<b>6.5. ACKNOWLEDGMENTS.....</b>	<b>153</b>
<b>6.6. LITERATURE CITED.....</b>	<b>154</b>

<b>7. SUMMARY AND RECOMMENDATIONS.....</b>	<b>158</b>
<b>7.1. SUMMARY OF RESULTS.....</b>	<b>158</b>
<b>7.2. RECOMMENDATIONS.....</b>	<b>163</b>
<b>7.3. LITERATURE CITED.....</b>	<b>167</b>

## List of Figures

Figure 1.1	Antisense gene therapy.....	3
Figure 1.2	Targets for oligonucleotide therapeutics.....	4
Figure 1.3	Gene therapy publications over the past two decades.....	6
Figure 1.4	Receptor-mediated delivery.....	9
Figure 1.5	Schematic illustration of $\beta$ -cyclodextrin.....	16
Figure 1.6	Polymer design strategy.....	19
Figure 2.1	Schematic of $\beta$ -cyclodextrin.....	25
Figure 2.2	$\beta$ -Cyclodextrin comonomers.....	26
Figure 2.3	Schematic of $\beta$ -cyclodextrin polymer synthesis.....	27
Figure 2.4	$\beta$ -CD polymer/DNA binding.....	32
Figure 2.5	$\beta$ -CD polymer-mediated transfection to BHK-21 and CHO-K1.....	34
Figure 2.6	PEI-mediated transfection to BHK-21 and CHO-K1.....	36
Figure 2.7a	Comparison of transfection efficiency of various non-viral vectors.....	38
Figure 2.7b	Comparison of the toxicities of various non-viral vectors.....	39
Figure 2.8	TEM of polymer/DNA complexes.....	40
Figure 2.9	Particle size and zeta potential.....	41
Figure 3.1	Synthesis of the comonomer A.....	53
Figure 3.2	Polymerization scheme for $\beta$ -cyclodextrin polymers.....	57
Figure 3.3	Hydrodynamic diameter of $\beta$ CDP-based polyplexes.....	63
Figure 3.4	Electron micrograph of $\beta$ CDP6 polyplexes at 50+/- charge ratio.....	64
Figure 3.5	DNase protection of plasmid DNA by $\beta$ CDP complexation.....	65
Figure 3.6	Transfection and toxicity of $\beta$ CDP5 and $\beta$ CDP6 to BHK-21.....	66
Figure 3.7	Comparison of transfection and toxicity of $\beta$ CDP6-based polyplexes.....	67
Figure 3.8	IC <sub>50</sub> s of $\beta$ CDPs of BHK-21 cells.....	68
Figure 3.9	Determination of binding constants by heparan sulfate displacement.....	70
Figure 4.1	Synthesis of Hist-CDP6.....	86
Figure 4.2	Zeta potential and hydrodynamic diameter of Hist-CDP6 polyplexes.....	87
Figure 4.3	Comparison of $\beta$ CDP6 and Hist-CDP6-mediated transfection to BHK-21.....	88
Figure 4.4	Relative transfection efficiencies of Hist-CDP6 and $\beta$ CDP6.....	89
Figure 4.5	Rhodamine-labeled plasmid uptake mediated by Hist-CDP6 and $\beta$ CDP6.....	91
Figure 4.6	Transfection of fluorescein-labeled oligos to BHK-21 cells with Hist-CDP6 and $\beta$ CDP6.....	92
Figure 4.7	Confocal images of BHK-21 cells transfected with fluorescently-labeled oligos complexed with Hist-CDP6 and $\beta$ CDP6 at 10 +/-.....	93
Figure 4.8	Effect of chloroquine on $\beta$ CDP6 and Hist-CDP6-mediated transfections.....	95

Figure 5.1	Schematic illustration of inclusion complexation of adamantane with $\beta$ -cyclodextrin.....	105
Figure 5.2	Hydrodynamic diameter of GALA and GALA-Ad-modified polyplexes.....	110
Figure 5.3	Zeta potential of GALA and GALA-Ad-modified polyplexes.....	111
Figure 5.4	Uptake of GALA-Ad and GALA modified polyplexes by BHK-21 cells.....	113
Figure 5.5	Uptake of GALA-Ad and GALA modified polyplexes by HUH-7 cells.....	115
Figure 5.6	Luciferase transfection of BHK-21 cells with $\beta$ CDP6-based polyplexes modified with GALA and GALA-Ad.....	116
Figure 5.7	Toxicity of GALA and GALA-Ad modified polyplexes to BHK-21 cells.....	117
Figure 5.8	Proposed structures of GALA and GALA-Ad modified polyplexes.....	120
Figure 6.1	Structure of $\beta$ CDP6-Peg <sub>3400</sub> .....	135
Figure 6.2	Scheme for post-DNA-complexation pegylation by grafting.....	137
Figure 6.3	Structures of various adamantane-PEG molecules.....	141
Figure 6.4	Salt stabilization of polyplexes by pegylation.....	142
Figure 6.5	Steric stabilization versus dispersion stabilization.....	143
Figure 6.6	Co-delivery of $\beta$ CDP6 polyplexes with PEG <sub>3400</sub> -FITC.....	146
Figure 6.7	Structure of Lactose-CDP6.....	148
Figure 6.8	Transfection of $\beta$ CDP and Lac-CDP6 polyplexes to HUH-7 cells.....	149
Figure 6.9	Structure of Lac-C6-CDP6.....	150
Figure 7.1	Toxicity comparison of non-viral vectors.....	159
Figure 7.2	Stabilization and cell targeting component.....	164
Figure 7.3	Endosomal release component.....	164
Figure 7.4	Nuclear localization component.....	165
Figure 7.5	Proposed delivery vehicle for liver targeting.....	167

## List of Tables

Table 1.1	Disease targets in human gene therapy trials.....	7
Table 1.2	Gene therapy clinical trials as of June 2000.....	8
Table 1.3	Barriers and ideal vector characteristics.....	11
Table 1.4	Comparison of viral and nonviral vectors.....	16
Table 3.1	Effect of the length of comonomer B on the polymerization.....	62
Table 6.1	Particle sizes of PEI and $\beta$ CDP6 polyplexes during post-DNA-complexation pegylation by grafting.....	138
Table 6.2	Lactose-mediated uptake into HUH-7 cells.....	152

# Chapter 1

## Introduction

### 1.1 OBJECTIVES

The potential for providing new disease treatments by gene-based therapies has been hampered by limitations in gene delivery. Viral vectors, extensively studied in both *in vitro* and *in vivo* settings, have shown problems in host immunogenicity, manufacturing, and scale-up. Non-viral vectors, while bypassing many problems encountered with viral vectors, have suffered in clinical progress due to their toxicity, low transfection efficiency, and *in vivo* instability. The objective of this research was to develop a non-toxic, polymeric gene delivery system capable of accomplishing efficient gene delivery and adaptable for *in vivo* applications.

The following design strategy was adopted in order to meet these goals. First, a new family of cationic polymers was designed from non-toxic starting materials. These polymers are capable of condensing and delivering DNA while maintaining the low toxicity characteristic of the monomeric materials. Next, transfection efficiency and *in vivo* stability of the delivery system were independently addressed. Delivery efficiency was optimized by studying the effect of polymer structure on gene delivery and by providing methods to enhance intracellular trafficking. A modification method capable of providing salt stability and preventing non-specific cell interactions is described. The polymer can also be modified with this method to incorporate a targeting ligand to accomplish cell specific delivery. The three components – therapeutic gene, polymer and modifier – can be self-assembled to yield a polymeric delivery system for *in vivo* gene delivery.

A review of gene-based therapeutic intervention and current delivery technologies is important to better understand the motivation behind this work. Therefore, an

introduction to gene therapy and gene delivery is presented here. Methods of genetic intervention for human gene therapy are discussed, followed by a brief synopsis of the status of clinical gene therapy trials. The current viral and nonviral delivery vectors are described, including advantages and disadvantages for each vector and their progress as delivery agents for human gene therapy. Finally, some background information important for the development of the  $\beta$ -cyclodextrin polymer-based delivery system is discussed.

## **1.2. HUMAN GENE THERAPY**

Rapid advances since the mid-1970s in molecular genetics along with near completion of the Human Genome Project are paving the way for a revolution in medical therapy. Techniques allowing identification and characterization of genetic mutations give scientists the ability to better understand the cause of many diseases. The development of gene-based therapies will continue to improve on conventional treatments, and may provide treatments for genetic diseases such as adenosine deaminase deficiency, cystic fibrosis, or hemophilia. The list will continue to expand as the genetic basis of more diseases are determined.

### **1.2.1. Methods of Genetic Intervention**

Genetic diseases result from one or more DNA mutations that are felt on the protein level. Gene therapy provides an opportunity to address the root causes of diseases by targeting and correcting faulty DNA instead of the mutated protein products. This approach has the advantage in that it prevents disease progression rather than postponing or masking deterioration. The type of genetic intervention used depends on the effect of the mutation on the protein product. One possible effect is altered protein activity that can be treated by short sequences of DNA or RNA known as antisense oligonucleotides

(oligos). The oligos are used to inhibit mutant protein production by binding to their complementary sequence, thus preventing proper RNA splicing, halting mRNA translation, or triggering RNase cleavage of the mRNA (Fig. 1.1)(1). For example, 90% of chronic myelogenous leukemia patients have a mutation of the *abl* gene resulting in a hybrid protein p210. Antisense oligos directed to the altered gene reduce growth of malignant cells in leukemia patients while having no effect on normal cells (2).

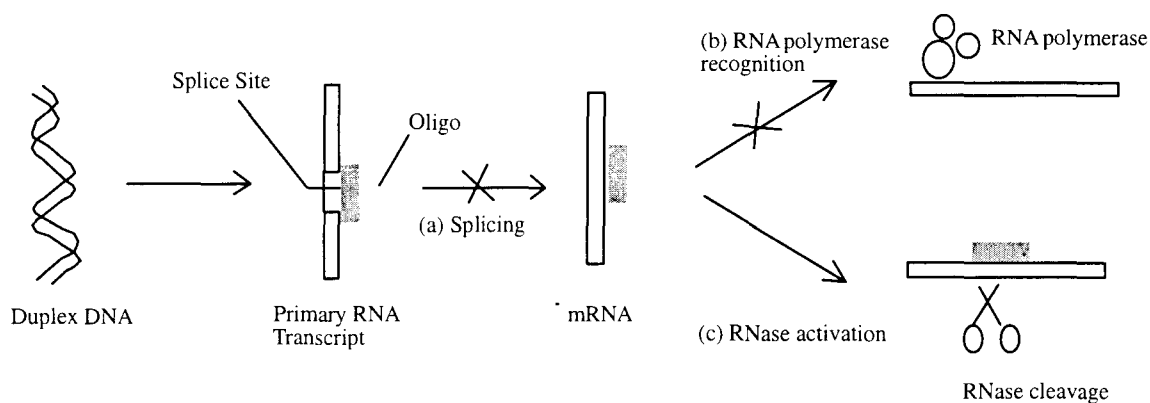


**Figure 1.1. Antisense gene therapy.** Antisense oligos can prevent protein production by (a) interfering with splicing, (b) blocking RNA polymerase recognition of promoter sites, or (c) triggering degradation of duplex mRNA by RNase activation.

Other anticode drugs can also prevent protein production. Triplex-forming oligonucleotides (known as antigene oligos) bind to duplex DNA and block transcription. Ribozymes are RNA molecules that have a sequence capable of recognizing and binding complementary mRNA and a catalytic subunit to cleave the bound mRNA. Thus, antisense oligos, antigene oligos, and ribozymes can all be used to disable a potential disease-causing protein (Fig. 1.2) (3).

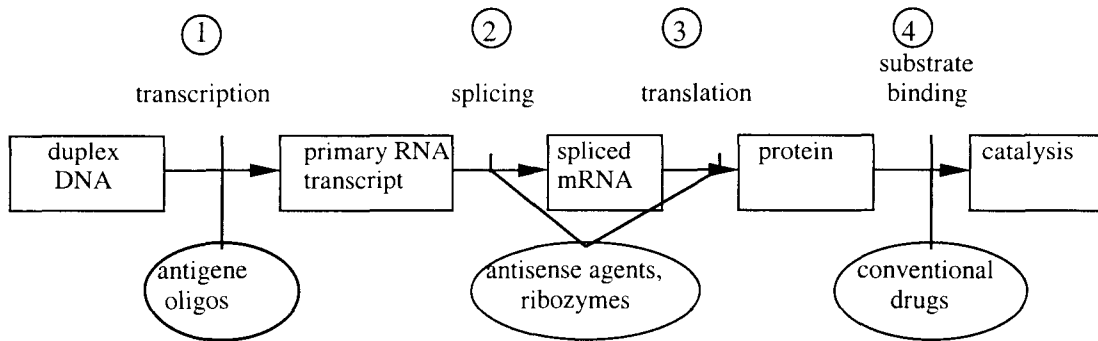


**Figure 1.2(3). Targets for oligonucleotide therapeutics.** The four steps to gene expression are represented in the rectangles. Conceptual targets for intervening drugs are represented in the ovals.

Adverse genetic mutations can also result in decrease or knockout of protein activity. In this case, the missing or flawed protein product can be replaced by the introduction of a gene, either by integration into the chromosome or episomally in plasmid form, that codes for an active protein. For example, p53, a tumor suppressor protein, is inactivated in over half of all human cancers (4, 5). Because p53 prevents cell proliferation in response to DNA damage, p53 inactivation allows the damaged cells to replicate, often resulting in tumor growth. Therefore, reintroduction of a wild-type p53 gene into tumor cells may serve to control tumor growth or sensitize cells to radiation and chemotherapy. Indeed, delivery of p53 to several tumor cell lines and cancer xenographs prevents cell growth (6, 7).

### 1.2.2. History of Human Gene Therapy

The vision for human gene therapy emerged in the late 1960s with the new understanding of the genetic information flow from DNA to RNA to protein. With this knowledge, scientists began to reach beyond the traditional metabolic approach to disease treatment in search of methods directed at the causative genetic defects (8). Rogers hypothesized in 1968 that viruses, that deliver DNA to cells with high efficiency, could

be modified and used to deliver unnatural genetic information (9). The technology to realize this goal was developed in the 1970s as recombinant DNA techniques revolutionized biochemistry by providing a way to alter and replicate DNA.

The first recombinant viruses, viruses modified to contain an unnatural gene of interest while remaining infectious, were produced in 1981 (10). The work was followed in 1984 by Willis et al. who demonstrated correction of an enzymatic defect by a recombinant retroviral vector delivered to cells derived from patients with Lesch Nyhan syndrome (8, 11). Other viruses, including adenovirus, adeno-associated virus, and herpes simplex virus were added to the list of possible delivery vectors by the early 1990s (12-15). Wu et al. and Felgner et al. began the study of non-viral approaches for gene delivery in 1987 by using a polycation, poly-L-lysine, and cationic lipids, respectively, to mediate DNA delivery (16-17). The gene delivery tools available by the end of the 1980s set the stage for the first clinical human gene therapy trial.

The first approved clinical gene therapy trial began in 1990 at the NIH with a protocol for treating a form of severe combined immunodeficiency (SCID) resulting from a defect in the adenosine deaminase gene (ADA-SCID). A deficiency in the purine catabolic enzyme ADA results in decreased T and B lymphocytes (18). The clinical manifestation of this defect is a greatly weakened immune system; patients with ADA-SCID are not able to combat minor infections and, left untreated, rarely have a lifespan over 2 years. ADA-SCID is an ideal gene therapy target for several reasons: the biological basis for the disease is well understood, the disease is caused by a single gene defect, and correction to 1-5% of normal activity results in disease attenuation (19). The first trial involved ex vivo treatment of two ADA-SCID patients (20). Peripheral T cells were collected from the patients, transduced with a retroviral vector expressing human ADA, expanded, and reinfused back into the patients. The T-cell count in both patients rose to normal range after the treatment. The effect remained stable in one patient but fell to original enrollment levels for the second patient, probably due to the low *gene transfer*

efficiency achieved in the second patient. Both patients are alive 10 years after the initial gene therapy treatment. Although the patients continued to receive traditional ADA protein injections, the results from the trial were encouraging and provided impetus for the rapidly expanding field of human gene therapy.

### 1.2.3. Current Status of Gene Therapy

The interest in gene therapy rose quickly after the ADA-SCID trials. A Web of Science search under “gene therapy” reveals that the number of publications after 1990 nearly doubles every two years (Fig. 1.3). In addition, the target diseases expanded to include other monogenic diseases, various forms of cancer, and infectious diseases (Table 1.1). Major pharmaceutical companies now include either in-house gene therapy divisions or have partnered with other companies specializing in gene therapy. The search for gene-based treatments has continued with enthusiasm.

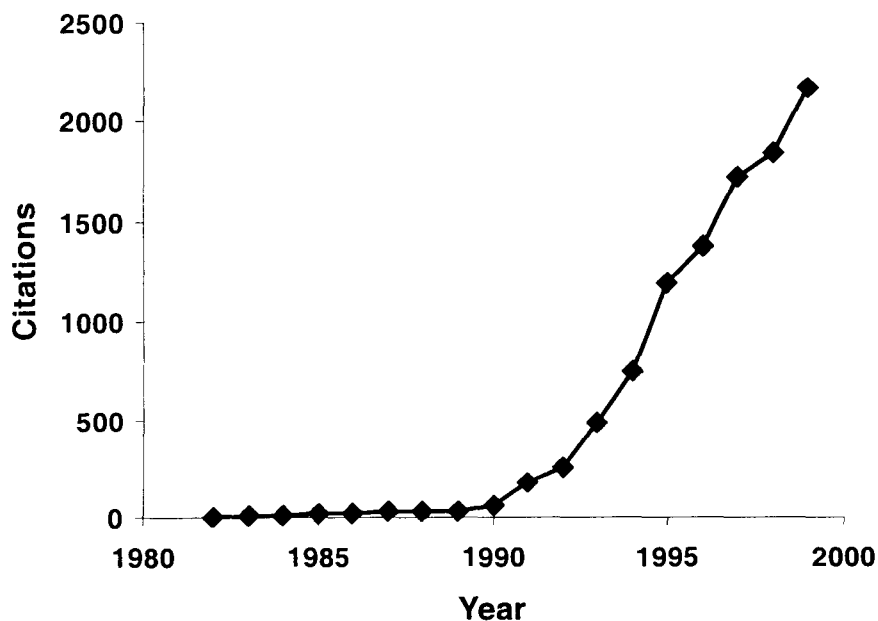


Figure 1.3. Gene therapy publications over the past two decades.

<b>Monogenic Diseases</b>	<b>Cancer</b>	<b>Other Diseases</b>
AAT deficiency	Gynecological tumors	HIV infection
ADA-SCID/X-linked SCID	Nervous system tumors	Amyotrophic lateral sclerosis
Canavan disease	Gastrointestinal tumors	Coronary artery disease
Chronic granulomatous disease	Genito-urinary tumors	Cubital tunnel syndrome
Cystic fibrosis	Skin tumors	Peripheral artery disease
Familial hypercholesterolemia	Head and neck tumors	Restenosis
Fanconi's anemia	Lung tumors	Rheumatoid arthritis
Gaucher's disease	Mesothelioma	
Hemophilia B	Hematological malignancies	
Hunter's/Hurler syndrome	Sarcomas	
Leukocyte adherence deficiency	Germ cell cancers	
OTC deficiency		
Purine nucleoside phosphorylase deficiency		

**Table 1.1. Disease Targets in Human Gene Therapy Trials**  
([www.wiley.co.uk/genetherapy](http://www.wiley.co.uk/genetherapy))

The number of clinical gene therapy trials as of June 2000 exceeds 400 (Table 1.2). Upon first glance, the gene therapy field appears to be burgeoning fruitfully; however, closer inspection reveals that only 2 of the 425 trials are Phase III protocols and over 90% of the trials are Phase I or I/II. Indeed, ten years after the first trial, gene therapy remains largely in the research stage with only one approved antisense molecule for treating CMV retinitis in AIDS patients.

Phase	Number
Phase I	288
Phase I/II	98
Phase II	37
Phase III	2
Total	425

**Table 1.2. Gene Therapy Clinical Trials as of June 2000.**  
[www.wiley.co.uk/genetherapy](http://www.wiley.co.uk/genetherapy)

### 1.3. GENE DELIVERY

Dr. Harold Varmus, the director of the NIH, along with other investigators, realized the unforeseen difficulties in gene therapy by 1995 (21-23). The road to the new genetic medicines would not be as straight as expected. Varmus assembled two advisory committees to assess the progress of gene therapy. The report from the first committee, chaired by Drs. Orkin and Motulsky, delivered a stinging diagnosis of gene therapy:

“The Panel finds that. . . while the expectations and the promise of gene therapy are great, clinical efficacy has not been definitively demonstrated at this time in any gene therapy protocol, despite anecdotal claims of successful therapy and the initiation of more than 100 Recombinant DNA Advisory Committee (RAC)-approved protocols. Significant problems remain in all basic aspects of gene therapy. Major difficulties at the basic level include shortcomings in all current gene transfer vectors and an inadequate understanding of the biological interaction of these vectors with the host.”(24)

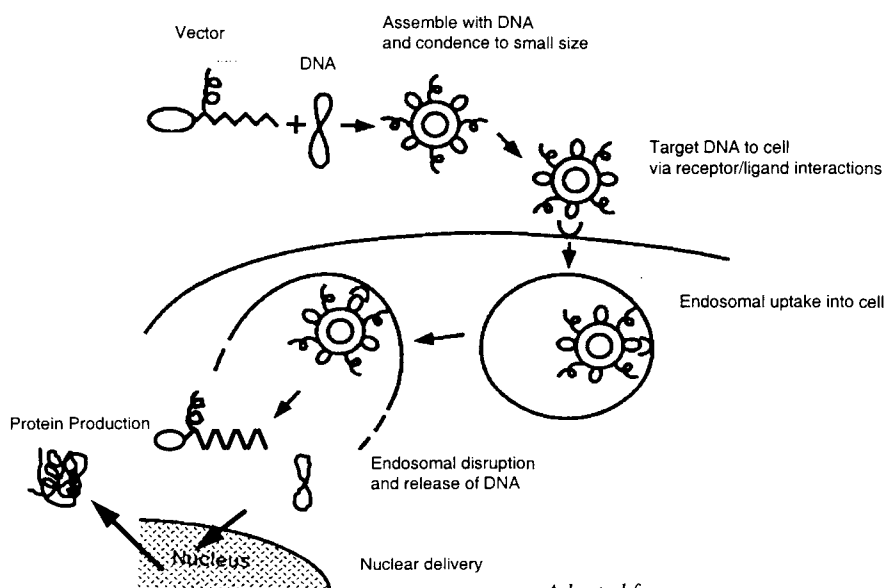
Although harsh, the assessment of the NIH advisory committee rang true. Five years after the report publication, gene delivery remains the bottleneck in gene therapy. In the words of J.P. Behr, “the weak link of gene therapy is paradoxically the vehicle rather than the ‘drug’ itself.”(25)

### 1.3.1. The Need for a DNA Carrier

Unlike traditional small molecule medicines that can easily diffuse into target cells, gene-based therapeutics are large, highly anionic entities. The size of these molecules prevents passive diffusion into cells; the charge of the molecules results in nonspecific binding to cationic serum proteins instead of the desired interaction with anionic cell surfaces. In addition, nucleases in the body rapidly digest any free DNA found outside of cell nuclei. Finally, the desired destination for most genetic drugs is the cell nuclei; thus, the essence of gene delivery lies in the intricate design of the delivery system (vector) and its ability to facilitate DNA delivery, not only to the cell but also to the nucleus. One method for cell-specific internalization and intracellular trafficking is receptor-mediated endocytosis.

### 1.3.2. Receptor-mediated Delivery

The basic mechanism for receptor mediated delivery is shown in Fig.1.4.



Adapted from:  
Cristiano, et al. *Cancer Gene Therapy* v3:1 pp.49-57

**Figure 1.4. Gene delivery to the cell via receptor-mediated endocytosis.**

The vector and attached ligand interacts with the DNA and directs the complex to receptors on the cell. The receptor and bound ligand-complex is endocytosed into the cell and brought into endosomes. At this point, gene transfer is maximized if there is a mechanism for the DNA to escape from the endosomal vesicle and detach from the vector. Without endosomal escape, the DNA is shuttled to the Golgi network or delivered to lysosomes where it is rapidly degraded by nucleases. Finally, the DNA needs to be delivered to the nucleus for transcription to take place.

### **1.3.3. The Ideal Gene Delivery System**

The ideal gene carrier therefore needs to have several characteristics in order to overcome barriers encountered in vivo (Table 1.3). The barriers are divided into three categories: extracellular, intracellular, and development barriers. Extracellular barriers include physiological salt conditions, serum and cell-associated proteins, and the immune system. The carrier should therefore condense the DNA to small particles, be serum-stable, not aggregate in 150 mM salt solutions, and be stealthy to the immune system. Intracellular barriers include the cell, endosomal and nuclear membranes. An efficient carrier would provide mechanisms for traversing the cell membrane, escaping endosomal vesicles and delivering the therapeutic load to the nucleus. In order to become part of a commercial therapeutic drug, the delivery vehicle would have to be manufactured at large scales under cGMP (current good manufacturing practice) conditions. The delivery vehicle should also be well defined, both under formulation conditions and after administration. Preferably, the carrier would also be easily applied to different nucleic acid drugs without much modification to the basic carrier. Finally, the carrier should have a substantial shelf-storage time and, if necessary, straightforward formulation methods.

<b>Type of Barrier</b>	<b>Barrier</b>	<b>Vector Characteristic</b>
Extracellular	Serum Proteins	Protects DNA from proteases, prevents nonspecific protein interactions
	Physiological Ionic Conditions	Non-aggregating in 150 mM salt
	Adaptive Immune System	No foreign peptide sequences
	Humoral Immune System	Not highly charged to prevent opsonization or complement activation
	Extracellular Matrices	Condenses DNA to small particles
	Toxicity	Nontoxic both intact and after biodegradation
Intracellular	Cell Membrane	Able to enter cells, preferably by receptor-mediated endocytosis
	Endosomal Membrane	Capable of releasing DNA from endosomal vesicles
	Cytoplasm	Mobile in the cytoplasm
	Nuclear Membrane	Traverses nuclear pores
Development	Versatility	Can be easily applied to different nucleic acids
	Holding Capacity	Large nucleic acid holding capacity
	Production	Able to be manufactured at cGMP conditions
	Scale-up	Able to be produced in large scales
	Storage	Has a long shelf-life

**Table 1.3. Barriers and Ideal Vector Characteristics**

### 1.3.4. Viral Delivery Systems

Viruses are natural DNA deliverers, and therefore contain efficient processes for specific targeting to cells, endosomal uptake, endosomal release, and nuclear trafficking (26). Not surprisingly, viral vectors were the first gene delivery agents to be developed. Viral vectors are shells of the virus made replication incompetent by using recombinant DNA techniques to replace viral genes with genes of interest. The two most commonly used viral vectors, retroviruses and adenoviruses, are briefly described here. Together, these two vector types account for over 90% of the viral vectors used in clinical trials.

Retroviruses were the first viruses studied for gene delivery (11), and remain the most popular delivery vector in clinical trials (used in 38% of protocols in gene therapy trials). Although retroviruses are very efficient at overcoming intracellular barriers, they are limited by low cellular uptake. In addition, retroviruses suffer from many safety issues, including random chromosomal integration that may disrupt protein functions and the possibility of replication competent retroviruses arising during manufacturing (27). Another major impediment in retroviral vector development is the difficulty in producing high titers of retroviruses. Purification of recombinant viruses is difficult, making it challenging to produce the vectors under cGMP standards.

Adenoviruses have received a lot of attention as a possible viral alternative to retroviral vectors. Unlike retroviruses, adenoviruses are able to transduce a wide range of both dividing and quiescent cell types. Adenoviruses can also be grown to high titers and are easier to purify than retroviruses. Transgene expression is usually high due to efficient endosomal release, cytoplasmic trafficking, and nuclear localization available in adenoviral delivery. However, any achieved expression is usually transient as a result of immune responses to viral proteins displayed on transduced cells. Repeat administrations of the viruses are therefore necessary but are unfortunately generally rendered ineffective by the humoral immune system. In addition to silencing transgene expression, immune

responses pose a significant health threat to patients. For example, in 1999, J. Gelsinger, a young patient in gene therapy trials, passed away suddenly after treatment. The incident was highly publicized because the cause of death was found to be an immune response to the adenoviral vector used in the treatment.

Many second and third generation viral vectors are being developed to address the issues discussed above. However, a trouble-free viral vector is not expected in the near future. While significant progress is being made in viral vector refinement, viable alternatives are being developed in nonviral delivery methods.

### **1.3.5. Nonviral Delivery Systems**

The two major approaches to nonviral gene delivery involve the use of cationic lipids and/or cationic polymers. These synthetic systems are cationic to facilitate the self-assembly with anionic DNA that results in DNA condensation to small particles. Thus, cationic lipids and polymers assist DNA delivery on a basic level by neutralizing the highly anionic charge associated with DNA and by reducing the size of the DNA macromolecules. The self-assembly of cationic lipid/DNA and cationic polymer/DNA complexes results in simple formulation procedures. In addition, the non-specific assembly by electrostatic interaction allows the systems to be applied for different genes without alterations in the delivery vectors. The ease of use and versatility of these synthetic systems have made them a standard as molecular biology transfection reagents. However, application to human in vivo systems is not nearly as straightforward. The hurdles that are faced by cationic lipid and cationic polymer systems are described in the following paragraphs.

### *Lipoplexes: cationic lipid/DNA complexes*

Felgner et al. demonstrated in 1987 the use of cationic lipids as DNA transfection agents (17). Since then, scores of cationic lipids have been developed and tested as transfection agents. The cationic lipids interact with negatively charged DNA to facilitate cellular entry. Since lipoplexes do not involve foreign proteins or peptide sequences, they do not elicit immune responses. Cationic lipids are also capable of delivering DNA of nearly any size. Like viruses, delivery occurs by endosomal uptake. The basic lipoplexes studied in the early 1990s have been modified to include “smart” functions, including receptor-mediated targeting (28), pH-sensitive lipids that assist in endosomal release, and stabilization to serum proteins (29). These modifications have increased the in vivo compatibility of lipoplexes.

Cationic lipids are the most advanced non-viral vector in clinical trials, accounting for 20% of approved protocols. The Allovectin-7 Phase III clinical trials (developed by Vical) involve direct injection of a lipoplex product to a tumor site. However, despite the improvement in design, current cationic lipids are not suitable for systemic delivery due to their in vivo instability and low delivery efficiency. Cationic lipoplexes interact with serum proteins. The new physiological environment encountered by the lipoplexes upon injection also causes dynamic changes in their structure. Felgner et al. used fluorescently labeled plasmids to quantitate cationic lipid-mediated DNA uptake in cultured cells and found that less than 0.1% of plasmid DNA is successfully delivered to cell nuclei (30). In addition, the toxicity associated with the cationic lipid remains a problem for in vitro and in vivo applications.

### *Polyplexes: cationic polymer/DNA complexes*

Lipoplexes and polyplexes debuted almost concomitantly in 1987 with Wu et al.’s work demonstrating poly-L-lysine (PLL)-mediated gene transfection. PLL was followed

by other cationic polymer systems, the most popular ones being dendrimers and polyethylenimine. However, while many cationic lipids were designed de novo, most of the studied cationic polymers are commercially available chemicals adapted for gene delivery and are therefore not optimized for biological use.

Cationic polymers self-assemble with DNA and condense into small particles suitable for cellular uptake. When formulated at a positive charge, the particles interact readily with the cell surface and are internalized by endocytosis. Like cationic lipids, cationic polymers are generally non-immunogenic and can be easily applied to nucleic acid-based macromolecules of varying sizes. Polyplexes tend to be more stable than lipoplexes because their multivalent interaction with DNA is not readily reversed. However, polyplexes also suffer from high toxicity and low transfection efficiencies. While 100 viral particles (in the absence of an immune response) can transfect 100 cells, polyplex delivery requires over 100 million plasmid copies to achieve transgene expression in 100 cells (30). Cationic polymers simply do not have the efficient viral mechanisms for cell entry and trafficking. Each membrane encountered (cell, endosome and nucleus) represents a major barrier for the non-viral delivery systems. Polyplexes are also colloidal particles and suffer from colloidal stability problems. For example, polyplexes aggregate quickly under high concentrations and physiological salt conditions. The aggregation problem prevents the possibility of systemic delivery of polyplexes.

Although cationic polymers are useful in in vitro settings, their current in vivo applications are few and have mainly been limited to direct injections. Systemic delivery has been difficult owing to the aggregation of the polyplexes and interaction with blood components upon injection. In addition, toxicity of the polyplexes remains a major issue. Hence, there are currently no cationic polymers in clinical gene therapy trials.

A summary of the advantages and disadvantages of viral and non-viral vectors is presented in Table 1.4. The immunogenicity of viruses and their difficulty in large scale manufacture have plagued viral gene delivery since its inception. It is evident that the

development of a nontoxic, efficient non-viral delivery vector is essential for the implementation of genetic intervention as a method of medical therapy. We address this issue in this work by developing novel cyclodextrin-based polymers for gene delivery applications.

VIRAL VECTORS		NON-VIRAL VECTORS	
Advantages	Disadvantages	Advantages	Disadvantages
Efficient cellular entry	Host immune response	Ease of use	Toxic to cells
Efficient intracellular trafficking	Difficult to scale up and manufacture	Versatility	Low delivery efficiency
Generally non-toxic	Safety issues	Non-immunogenic	Low in vivo stability

**Table 1.4. Comparison of Viral and Non-viral Vectors**

#### 1.4. CYCLODEXTRINS

Cyclodextrins (CDs) are cyclic oligomers of 6,7, or 8 glucoses (called  $\alpha$ ,  $\beta$ , and  $\gamma$ -cyclodextrin, respectively). The structure of  $\beta$ -cyclodextrin ( $\beta$ -CD) is shown in Fig 1.5. Cyclodextrins are cup-shaped molecules with a hydrophobic cavity that forms inclusion complexes with guest molecules.

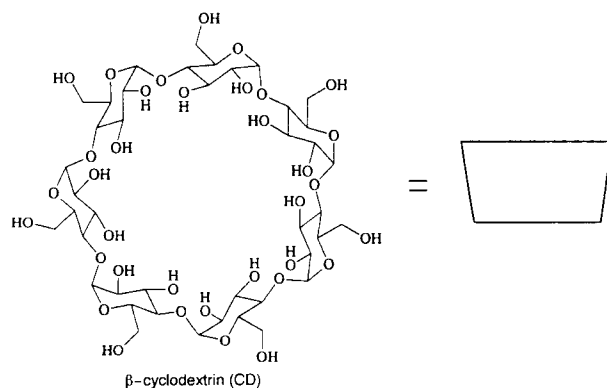


**Figure 1.5. Schematic illustration of  $\beta$ -cyclodextrin. (31)**

Cyclodextrins and cyclodextrin derivatives are used in several pharmaceutical formulations, generally as solubilizing agents for their complexation ability with hydrophobic compounds. Thus, the safety of CDs for drug use is well established; CDs are non-immunogenic and have low toxicity. In addition, CD chemistry is well studied with significant literature precedence for various functionalization procedures. Finally, CDs are available on large scales in pharmaceutical grade.

Cyclodextrins therefore possess many advantageous properties: non-immunogenic, non-toxic, available in large quantities at pharmaceutical grade, and capable of forming inclusion complexes. The first objective of this work was to incorporate CDs in a polymeric form that is able to self-assemble with and condense DNA without eliminating these advantageous properties. The development of a linear,  $\beta$ -cyclodextrin-based polymer ( $\beta$ CDP) that mediates gene delivery with low toxicity is described in Chapter 2. The polymers are synthesized by modular assembly, that allows for detailed structure-function studies. Therefore, Chapter 3 describes the synthesis of a family of  $\beta$ CDPs with various charge densities. The effect of polymer structure on gene delivery and toxicity is elucidated and an optimal polymer structure for transfection efficiency is determined.

In addition to toxicity, traditional non-viral vectors also suffer from low transfection efficiencies. One of the major limiting steps in achieving transgene expression is escape from vesicular compartments after the particles are endocytosed by cells. Confocal microscopy of fluorescently-labeled plasmids delivered by cationic polymers generally show punctate staining indicative of endosomal trapping. Viruses and certain polymers such as polyethylenimine take advantage of endosomal acidification to assist in release from these vesicles. Chapter 4 discusses the incorporation of a pH-sensitive moiety, histidine, in the  $\beta$ CDP to enhance endosomal release and increase transgene expression.

The ultimate application for the  $\beta$ -cyclodextrin polymers is systemic gene delivery. In order to achieve this, the  $\beta$ CDP-based polyplexes need to be stabilized against salt-induced aggregation, serum proteins, and non-specific cell interactions. PEGylation, that involves grafting of polyethylene glycol (PEG) to polyplexes, is a commonly used strategy to impart particle stability to colloidal systems (32). Because PEGylation prevents particle uptake by cells, the polyplexes would need to enter cells by receptor-mediated endocytosis. Therefore, the polyplexes also need to be modified with a ligand for cell targeting. Chapter 5 presents a new method for modifying polyplexes by taking advantage of the ability of cyclodextrins to complex with hydrophobic molecules.  $\beta$ CDP-based polyplexes are modified with adamantane-peptide conjugates. The modification does not interfere with DNA binding and condensation but is able to prevent non-specific cellular uptake. Chapter 6 studies further applications of the modification method, including salt stabilization by PEGylation and co-delivery of genes and small molecules.

Thus, the application of the initial design strategy taken by this work (Fig 1.6) resulted in the development of a non-toxic polymer capable of binding, condensing and protecting DNA and a modifier molecule for providing additional functionalities such as stabilization and targeting. The assembly of the three components – therapeutic gene,  $\beta$ CDP, and modifier – to provide a non-viral, systemic gene delivery system is discussed in Chapter 7.

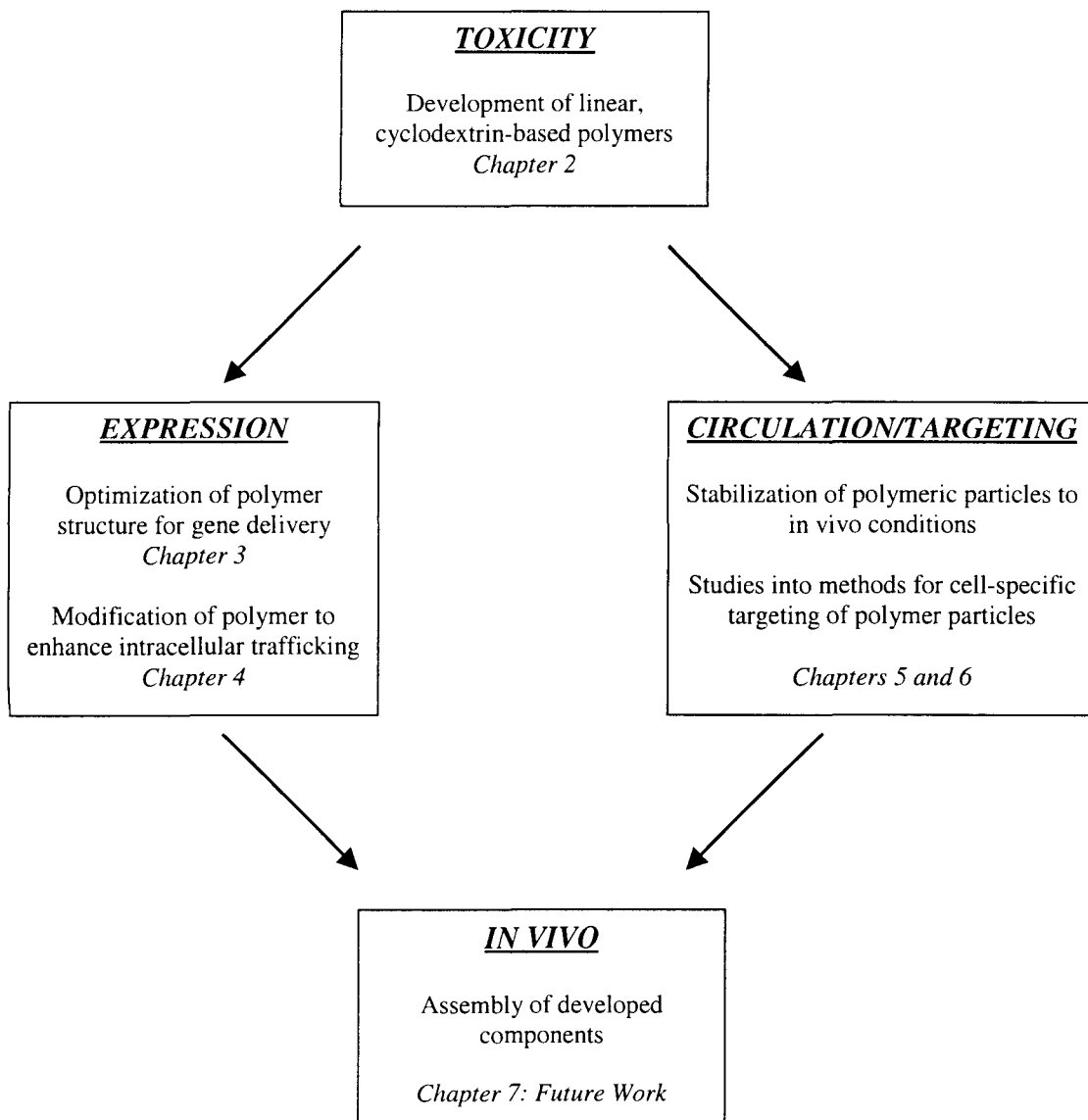


**Figure 1.6. Polymer Design Strategy.**

## 1.5. LITERATURE CITED

1. Uhlmann, E. and Peymann, A. (1990). *Chemical Rev.*, **90**, 544-579.
2. Tonkinson, J. L. and Stein, C. A. (1996). *Cancer Investigation*, **14**, 54-65.
3. Maher, C. J. (1996). *Cancer Investigation*, **14**, 66-82.
4. Levine, A. (1997) p53, the cellular gatekeeper for growth and division. *Cell*, **88**, 323-331.
5. Vogelstein, B. and Kinzler, K. (1992) p53 function and dysfunction. *Cell*, **70**, 523-526.
6. Nielsen, L., Dell, J., Maxwell, E., Armstrong, L., Maneval, D. and Catino, J. (1997) Efficacy of p53 adenovirus-mediated gene therapy against human breast cancer xenografts. *Cancer Gene Therapy*, **4**(2), 129-138.
7. Nielsen, L. and Maneval, D. (1998) p53 tumor suppressor gene therapy for cancer. *Cancer Gene Therapy*, **5**(1), 52-63.
8. Friedmann, T. In *The Development of Human Gene Therapy*; T. Friedmann, Ed.; Cold Spring Harbor Laboratory Press: New York, 1999; pp 1-20.
9. Rogers, S. and Pfuderer, P. (1968) Use of viruses as carriers of added genetic information. *Nature*, **219**, 749-751.
10. Shimotohno, K. and Temin, H. (1981) Formation of infectious progeny virus after insertion of herpes simplex thymidine kinase gene into DNA of an avian retrovirus. *Cell*, **26**, 67-77.
11. Willis, R., Jolly, D., Miller, A., Plent, M., Esty, A., Anderson, P., Chang, H., Jones, O., Seegmiller, J. and Friedmann, T. (1984) Partial phenotypic correction of human Lesch-Nyhan (hypoxanthine-guanine phosphoribosyltransferase-deficient) lymphoblasts with a transmissible retroviral vector. *J. Biol. Chem.*, **259**, 7842-7849.
12. Podsakoff, G., Wong, K. and Chatterjee, S. (1994) Efficient gene transfer into nondividing cells by adeno-associated virus based vectors. *J Virol*, **68**, 5656-5666.

13. Geller, A., Keyomarsi, K., Bryan, J. and Pardee, A. (1990) An efficient deletion mutant packaging system for defective herpes simplex virus vectors: potential applications to human gene therapy and neuronal physiology. *Proc Natl Acad Sci USA*, **87**, 8950-8954.
14. Rosenfeld, M., Siegfried, W., Yoshimura, K., Yoneyama, K., Fukayama, M., Stier, L., Paakko, P., Gilardi, P., Stratford-Perricaudet, L., Perricaudet, M., Jallat, S., Pavirani, A., Lecocq, J.-P. and Crystal, R. (1991) Adenovirus-mediated transfer of a recombinant  $\alpha$ 1-antitrypsin gene to the lung epithelium in vivo. *Science*, **252**, 431-434.
15. Flotte, T., Zeitlin, P., Solow, Afione, S., Owens, R., Markakis, D., Drumm, M., Guggino, W. and Carter, B. (1993) Expression of the cystic fibrosis transmembrane conductance regulator from a novel adeno-associated virus promoter. *J Biol Chem*, **268**, 3781-3790.
16. Wu, G. and Wu, C. (1987) Receptor-mediated in vitro gene transformation by a soluble DNA carrier system. *J. Biol. Chem.*, **262**, 4429-4432.
17. Felgner, P., Gadek, T., Holm, M., Roman, R., Chan, H., Wenz, M., Northrop, J., Ringold, G. and Danielsen, M. (1987) Lipofection: A highly efficient, lipid mediated DNA-transfection procedure. *Proc Natl Acad Sci USA*, **84**, 7413-7417.
18. Fisher, A. (1991) Severe combined immunodeficiencies. *Immunodefic Rev*, **3**, 83-100.
19. Hirschhorn, R. (1990) Adenosine deaminase deficiency. *Immunodefic Rev*, **2**, 175-198.
20. Blaese, R., Culver, K., Miller, A., Carter, C., Fleisher, T., Clerici, M., Shearer, G., Chang, L., Chiang, W., Tolstshev, P., Greenblatt, J., Rosenberg, S., Klein, H., Berger, M., Mullen, C., Ramsey, W., Muul, L., Morgan, R. and Anderson, W. (1995) T lymphocyte-directed gene therapy for ADA-SCID: initial trial results after 4 years. *Science*, **270**, 475-480.

21. Varmus, H. (1995) NIH review of gene therapy protocols. *Science*, **267**, 1889.
22. Verma, I. (1994) Gene therapy: hopes, hypes, and hurdles. *Mol Med*, **1**, 2-3.
23. Friedmann, T. (1994) The promise and overpromise of gene therapy. *Gene Ther*, **1**, 217-218.
24. Orkin, S. and Motulsky, A. In; 1995.
25. Behr, J. (1994). *Bioconj Chem*, **5**, 382-389.
26. Ledley, F. (1994). *Curr Op Biotech*, **5**, 626-636.
27. Cannon, P. and Anderson, W. In *Gene Therapy*; N. Templeton and D. Lasic, Eds.; Marcel Dekker: New York, 2000; pp 1-16.
28. Xu, L., Pirrolio, K. and Chang, E. (1997) Transferrin liposome mediated p53 sensitization of squamous cell carcinoma of the head and neck to radiation in vitro. *Hum Gene Ther*, **6**, 467-475.
29. Hong, K., Zheng, W. and Baker, A. (1997) Stabilization of cationic complexes by polyamines and PEG-phospholipid conjugates for efficient in vivo delivery. *FEBS Lett*, **400**, 233-237.
30. Felgner, P., Zelphati, O. and Liang, X. In *The Development of Human Gene Therapy*; T. Friedmann, Ed.; Cold Spring Harbor Laboratory Press: New York, 1999; pp 241-460.
31. Szejtli, J. and Osa, T. *Comprehensive Supramolecular Chemistry*; Elsevier Science: Oxford, 1996.
32. Ogris, M., Brunner, S., Schuller, S., Kircheis, R. and Wagner, E. (1999) PEGylated DNA/transferrin-PEI complexes: reduced interaction with blood components, extended circulation in blood and potential for systemic gene delivery. *Gene Ther*, 595-605.

## Chapter 2

### A New Class of Polymers for the Delivery of Macromolecular Therapeutics

#### 2.1 ABSTRACT

Cationic polymers show promise for the *in vitro* and *in vivo* delivery of macromolecular therapeutics. Known cationic polymers, e.g., poly-(L)lysine (PLL) and polyethylenimine (PEI), have been employed in native and modified forms for the delivery of plasmid DNA (pDNA) and reveal varying levels of toxicity. Here, we report the preparation of a new class of cationic polymers that are specifically designed to deliver macromolecular therapeutics. Linear, cationic, beta-cyclodextrin ( $\beta$ -CD)-containing polymers (CD-polymers) are synthesized by copolymerizing difunctionalized  $\beta$ -CD monomers (AA) with other difunctionalized comonomers (BB) such that an AABBAABB product is formed. The  $\beta$ -CD polymers are able to bind  $\sim 5$  kbp pDNA above polymer to DNA (+/-) charge ratios of 1.5, compact the bound pDNA into particles of approximately 100-150 nm in size at charge ratios above 5 +/-, and transfect cultured cells at charge ratios above 10 +/- . *In vitro* transfections with the new  $\beta$ -CD-polymers are comparable to the best results obtained in our hands with PEI and Lipofectamine. Some cell line-dependent toxicities are observed for serum-free transfections; however, no toxicity is revealed at charge ratios as high as 70 +/- in transfections conducted in 10% serum. Single IV and IP doses as high as 200 mg/kg in mice showed no mortalities.

---

The contents of this chapter were published in *Bioconjugate Chemistry* (1999) **10**, 1068-1074 and were reprinted with permission of the publisher.

## 2.2 INTRODUCTION

Methodologies currently under investigation for the *in vivo* delivery of macromolecular therapeutics, e.g, proteins, oligonucleotides, ribozymes, plasmid DNA, etc., include both viral and non-viral constructs. Viral transfection systems can produce efficient expression of transgenes within cells of interest. However, they have several disadvantages, e.g., adenoviruses have high immunogenicity, retroviruses produce random genomic integration and both vectors have severely limiting capacities for the size of a foreign transgene. Additionally, scaled-up manufacture of replication-deficient viral constructs in the absence of recovered replication-competency is problematic (1). In contrast, non-viral transfection systems have low immunogenicity, the capacity to handle larger sizes of DNA than viruses, and are amenable to large-scale manufacture. A recent review has appeared on non-viral gene delivery constructs (2). In spite of the advantages of non-viral delivery systems, they reveal numerous problems such as substantially less gene expression than viral vectors and toxicity.

The goal of our work was to synthesize new non-viral vectors for the delivery of therapeutic macromolecules. Our approach was to construct a completely new family of materials specifically prepared for this application. We chose to work with polymeric materials and attempted to specifically address the issue of toxicity. To this end, we synthesized a new class of cyclodextrin-containing polymers in the hope of creating a relatively non-toxic vector for the delivery of macromolecules since numerous cyclodextrins are known to have low toxicity (3).

Cyclodextrins (CDs) are cup-shaped molecules formed by cyclic oligomers of glucose (see Fig. 2.1). Cyclodextrins comprised of 6, 7, and 8 glucose units are called  $\alpha$ -,  $\beta$ - and  $\gamma$ -cyclodextrins, respectively. The three-dimensional structure of CDs is such that the cavity is relatively hydrophobic when compared to the exterior and thus can be used to imbibe hydrophobic compounds to form host-guest complexes. The ability of CDs to

form inclusion complexes has been exploited in CD drug formulations throughout the world (including the US -- the first drug formulation to contain a CD, Sporanox®, was approved by the FDA in 1997). Because of this, it is known that CDs have relatively low toxicity and lack immunogenicity (3). The question addressed here is whether these desirable features can be maintained in polymeric form in order to deliver macromolecules.

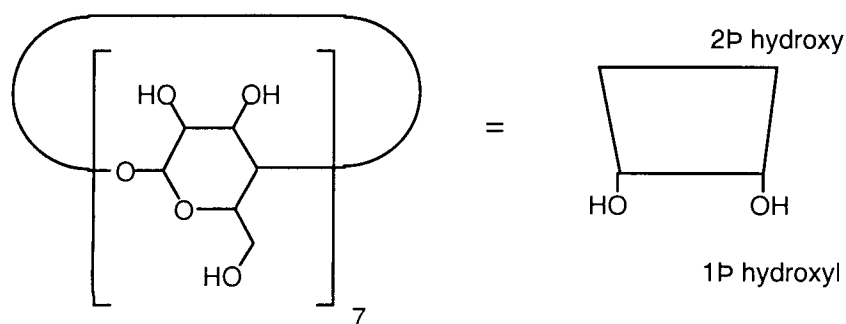


**Figure 2.1. Schematic of beta-cyclodextrin.**

In this paper, the synthesis and characterization of a new family of  $\beta$ -CD containing polymers is presented. Numerous polymers have been prepared (4), and here we provide several representative examples. It is shown that these polymers can bind and condense pDNA and transfect cells with a low level of toxicity.

## 2.3 MATERIALS AND METHODS

### 2.3.1. Polymer Synthesis and Characterization

*Monomers.* 6A,6D-Dideoxy-6A,6D-diamino- $\beta$ -cyclodextrin (**1**, Figure 2.2) and 6A,6D-Dideoxy-6A,6D-di(2-aminoethanethio)- $\beta$ -cyclodextrin (**2**, Figure 2.2) were synthesized according to literature procedures (4) and had satisfactory NMR, mass spectral and elemental analyses. All reagents were purchased from the Aldrich Chemical Co.

(Milwaukee, WI) and used as received except for dimethylsuberimidate·2HCl (DMS) and dithiobis(succinimidyl propionate) (DSP), which were purchased from Pierce Chemical Co. (Rockford, IL), and used as received. The degree of hydration of the cyclodextrin samples was determined by measuring the weight loss on a TA Instruments TGA 951 thermogravimetric analyzer operating from 25 °C to 140 °C at a 5°/min heating rate.

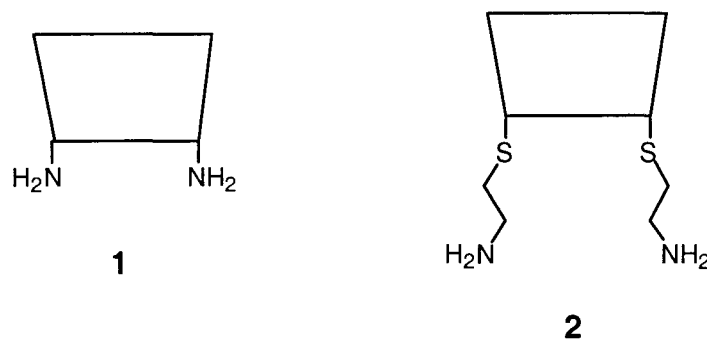


**Figure 2.2.**  $\beta$ -Cyclodextrin comonomers.

*Polymers containing  $\beta$ -Cyclodextrin (3-5).*  $\beta$ -CD copolymers **3-5** were prepared by the polymerization of a difunctionalized  $\beta$ -CD (AA) monomer with a difunctionalized comonomer (BB) to give an AABBAABB product (Figure 2.3). One procedure to form **4** is provided below. Additional synthetic methodologies can be found elsewhere (4). An 8 mL vial was charged with a solution of the bis(hydrogen carbonate) salt of 6A,6D-dideoxy-6A,6D-di(2-aminoethanethio)- $\beta$ -cyclodextrin hexahydrate (184.6 mg,  $1.36 \times 10^{-4}$  mol) dissolved in 0.5M  $\text{Na}_2\text{CO}_3$ . DMS (37.0 mg,  $1.36 \times 10^{-4}$  mol) was added and the solution was centrifuged briefly to dissolve the components. The resulting mixture was stirred at 25 °C for 15 h. The mixture was then diluted with ca. 10 mL of water and the pH brought to 4 with 10% HCl. This material was then dialyzed against a Spectra/Por® 7 MWCO 3,500 dialysis membrane (Spectrum, Houston, TX) in  $\text{dH}_2\text{O}$  for 24 h. The dialyzed solution was lyophilized to dryness yielding 51 mg (24%) of a white amorphous solid. Calculated for  $\text{C}_{54}\text{H}_{94}\text{N}_4\text{Cl}_2\text{O}_{33}\text{S}_2 \cdot 7\text{H}_2\text{O}$ ; C:40.83, H: 6.85, N: 3.53; Found C:

40.77, H: 6.52, N: 3.46.  $^1\text{H}$  NMR (500MHz,  $\text{D}_2\text{O}$ )  $\delta$  1.39 (br, 4H), 1.69 (br, 4H), 2.49 (br, 4H), 2.92 (br, 4H), 3.16 (br, 4H), 3.5-4.0 (m, 42H), 5.05 (m, 7H).  $^{13}\text{C}$  NMR (125 MHz,  $\text{D}_2\text{O}$ )  $\delta$  27.5, 28.6, 31.5, 33.8, 39.6, 42.6, 61.6, 73.2, 74.2, 82.7, 85.2, 103.2, 169.4. IR (KBr) 1652 (C=N).

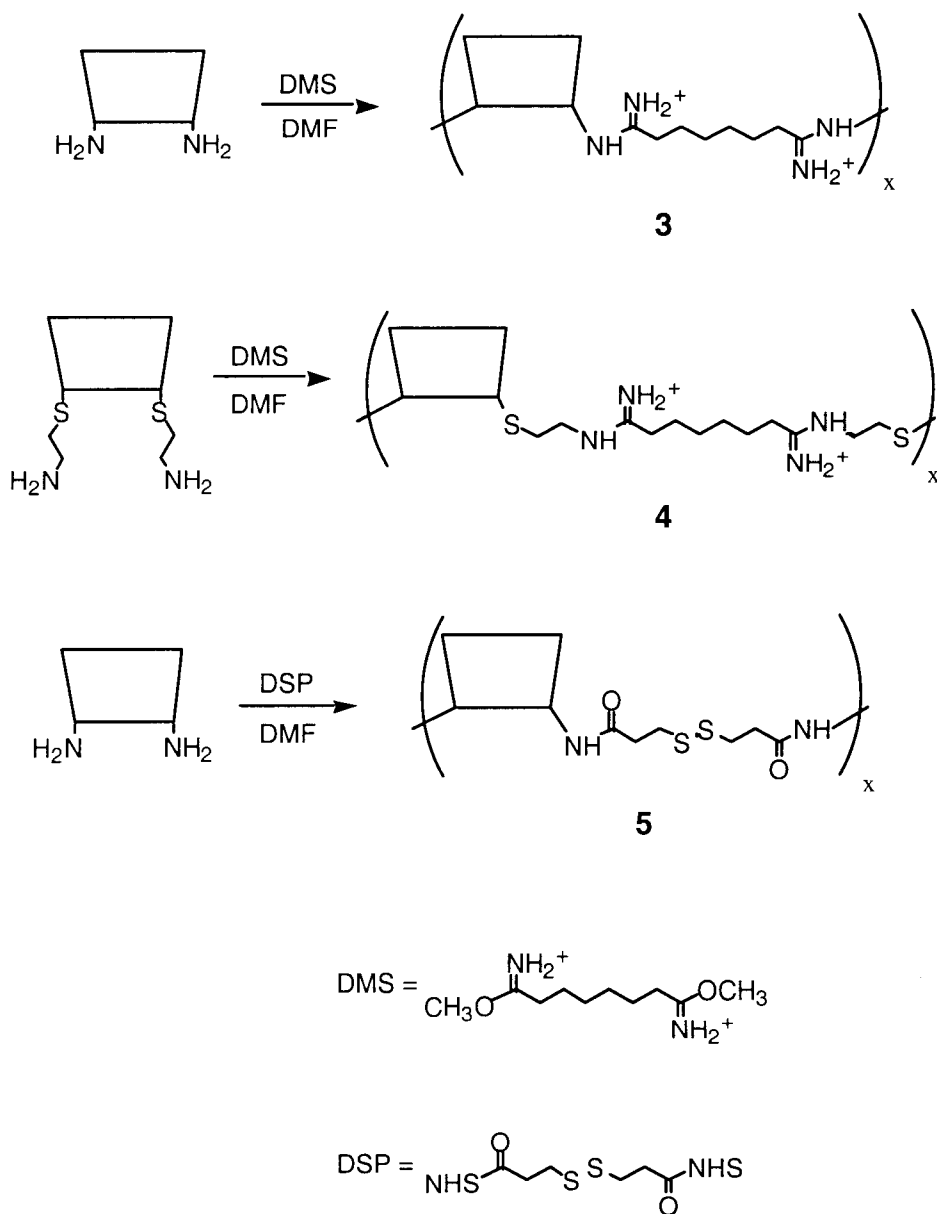


**Figure 2.3. Schematic of  $\beta$ -cyclodextrin polymer (3 - 5) syntheses.**

*Light Scattering and Molecular Weight Determination.* The specific refractive index increment,  $dn/dc$ , was measured in 0.3 M NaCl using a Waters 2410 differential refractive index detector at a flow rate of 1.0 mL/min. The value of  $dn/dc$  for **4** in 0.3 M NaCl at  $\lambda = 930$  nm and 25 °C was 0.155 mL/g. Polymer samples were then analyzed on a Hitachi D6000 HPLC system equipped with a ERC-7512 RI detector, a Precision Detectors PD2020/DLS light scattering detector and a Progel-TSK G2000 SWXL column using 0.3 M NaCl as eluant at a 0.7 mL/min flow rate. The weight average molecular weight,  $M_w$ , was determined to be 8.8 KDa, with a polydispersity index,  $M_w/M_n$  of 1.10.

**2.3.2. Solid Phase DNA Binding Assay.** A 5'-amino-modified 50-mer oligonucleotide (5'-Amino-AAA ACT GCT TAC CAG GGA TTT CAG TGC ATG TAC ACG TTC GTC ACA TCT CA -3', "NMODSOL") and its complementary oligonucleotide ("COMPSOL") were synthesized by the Biopolymer Synthesis and Analysis Research Center at Caltech (Pasadena, CA). NMODSOL was covalently coupled to magnetic porous glass (MPG) supports according to manufacturer's instructions (Solid Phase Oligo COUPLE-IT Kit, CPG. Inc, Lincoln Park, NJ). UV absorption analysis revealed successful coupling of 190  $\mu$ g of oligo to 10 mg of MPG particles. The complementary oligo, COMPSOL, was then annealed to the coupled strand by heating a solution of COMPSOL in 45 mM NaCl with the MPG-coupled oligo in boiling water for 2 minutes and then allowing the solution to slowly cool to room temperature. UV analysis confirmed successful annealing of the complementary strand.

Primary amine-containing compounds to be analyzed for DNA binding capability were added at a 1:5 (+/-) charge ratio in 1 mL of distilled water to the MPG-supported DNA (dsDNA-MPG) and incubated with gentle rotation for 2 h. The particles were magnetically separated and the supernatant removed. Unbound molecules remaining in the supernatant were quantified by amine reaction with TNBS at pH 8.5 (6) and

compared to amine quantification of the solution before exposure to dsDNA-MPG to determine extent of DNA binding.

### **2.3.3. Polyplex Formation and Characterization**

*Plasmids.* pGL3-Control Vector (pGL3-CV) plasmid, which contains the luciferase gene under the control of the SV40 promoter, was purchased from Promega (Madison, WI). Plasmids were amplified by *E. Coli* strain DH5 $\alpha$  and purified using Qiagen's Endotoxin-free Megaprep Kit (Valencia, CA).

*Preparation of DNA/polymer complexes and DNA Gel Retardation Assay.* One microgram of pGL3-CV (0.1  $\mu\text{g}/\mu\text{L}$  in distilled water) was mixed with an equal volume of polymer (10  $\mu\text{L}$  in distilled water) at the appropriate charge ratios. After a 15-30 minute incubation, the samples were pipetted with 1  $\mu\text{L}$  of loading buffer into wells of a 0.6% agarose gel containing 6  $\mu\text{g}$  ethidium bromide/100 mL TAE buffer (40 mM Tris-acetate, 1 mM EDTA) and electrophoresed.

*Transmission Electron Microscopy.* Polymer/DNA complexes were prepared at different charge ratios as described above for the gel retardation assay. After one hour incubation, five microliters of sample were applied in duplicate to 400-mesh carbon-coated copper grids for 45 seconds, after which excess liquid was removed by blotting with filter paper. The 400-mesh carbon-coated copper grids were glow-discharged immediately prior to sample loading. One set of samples was then rotary shadowed at a 6° angle with a 3 cm tungsten wire while the duplicate set was negatively stained with 2% uranyl acetate for 45 seconds before blotting. Images were recorded using a Philips 201 electron microscope operated at 80 kV.

*Dynamic Light Scattering (DLS) and Zeta Potential.* For determination of particle size and charge, 2  $\mu\text{g}$  of pGL-CV3 (0.1 $\mu\text{g}/\mu\text{L}$  in dH<sub>2</sub>O) was mixed with an equal volume of polymer (20  $\mu\text{L}$  in dH<sub>2</sub>O) and allowed to stand for 30 minutes before diluting to a final volume of 1.3 mL for measurements. Particle size and zeta potential of the complexes were measured using a ZetaPals dynamic light scattering detector (Brookhaven Instruments Corporation, Holtsville, NY). Three measurements were taken for each sample and data reported as average size and zeta potential.

#### **2.3.4. Cell Culture and Transfections.**

*Cell Lines and Cell Culture.* BHK-21 cells were purchased from ATCC (Rockville, MD) and maintained in Dulbecco's Modified Eagle Medium supplemented with 10% fetal bovine serum (FBS), 100 units/mL penicillin, 100  $\mu\text{g}/\text{mL}$  streptomycin and 0.25  $\mu\text{g}/\text{mL}$  amphotericin. CHO-K1 cells were purchased from ATCC and maintained in Ham's F-12 medium with the above listed supplements. All cells were cultured at 37 °C in a 5% CO<sub>2</sub> humidified atmosphere and passaged every 4-5 days. Media and supplements were purchased from Gibco BRL (Gaithersburg, MD).

*Cell Transfections and Luciferase Assay.* BHK-21 cells were plated at 60,000 cells/well in 24-well plates 24 hours before transfection. Immediately prior to transfection, cells were rinsed once with PBS (pH 7.4) and 200  $\mu\text{L}$  of Optimem (Gibco), for serum-free transfections, or complete media, for transfections in 10% serum, were added to each well. Polymer 4/DNA complexes were prepared as described above. Lipofectamine (Gibco) and Superfect (Qiagen) complexes were prepared according to manufacturers' instructions. PEI (branched 25 kDa, Sigma) and polylysine (35 kDa, Sigma) complexes were prepared as described above, except in 150 mM NaCl at pH 7.0 instead of distilled water. Thirty minutes was allowed for complex formation before addition to cells. After 5 h, 800  $\mu\text{L}$  of appropriate media with 10% FBS were added to cells. Twenty-four hours

after transfection, the medium in each well was replaced with 1 mL of culture media per well. After another 24 hours, medium was removed by aspiration, cells were washed twice with PBS (pH 7.4), and lysed by one freeze-thaw cycle in 50  $\mu$ L Cell Culture Lysis Buffer (Promega, Madison, WI). Cell lysates were analyzed for luciferase activity with Promega's luciferase assay reagent and for vector toxicity as described below. Light units were integrated over 10 seconds in duplicate with a luminometer (Monolight 2010, Analytical Luminescence Laboratory, San Diego, CA).

*Toxicity.* The amount of protein in cell lysates obtained 48 hours after transfection was used as a measure of cell viability. Protein levels of transfected cells were determined by Biorad's DC protein assay (Hercules, CA) and normalized with protein levels of cells transfected with naked DNA. A protein standard curve was run with various concentrations of bovine IgG (Biorad) in Cell Culture Lysis Buffer.

## **2.4. RESULTS**

**2.4.1 Binding of Functionalized CD Monomers 1 and 2 to DNA.** DNA is not retarded in the electrophoresis assay by contact with the functionalized CD monomers **1** and **2** (data not shown) and this is most likely due to weak binding interactions that are disrupted by the presence of salts. Therefore, a solid phase DNA binding assay conducted in deionized water was developed as described in Materials and Methods. Using this assay, the CD-monomer **1** does not bind to DNA (0% binding), possibly due to the steric hinderance of the bulky cyclodextrin cups that are in very close proximity to the positive charge center. In order to test this hypothesis, **2** was prepared to specifically remove the amine further from the CD. CD-monomer **2** readily binds to DNA, with 88% binding. This binding compares favorably to other short polycations, such as spermine (19% binding).

**2.4.2. DNA Binding of CD-Polymer.** Although CD monomer **2** is not able to bind to DNA in the presence of salt, polymer **4** is able to completely bind DNA above polymer/DNA charge ratios of 1.5, as shown by DNA gel retardation (Figure 2.4). Binding is observed for complex formation in dH<sub>2</sub>O, 150 mM NaCl, and complete media (data not shown). Polymer **3** does not bind to DNA even at polymer/DNA charge ratios as high as 50 (data not shown) and is likely due to the same reasons as mentioned previously with compound **1**.

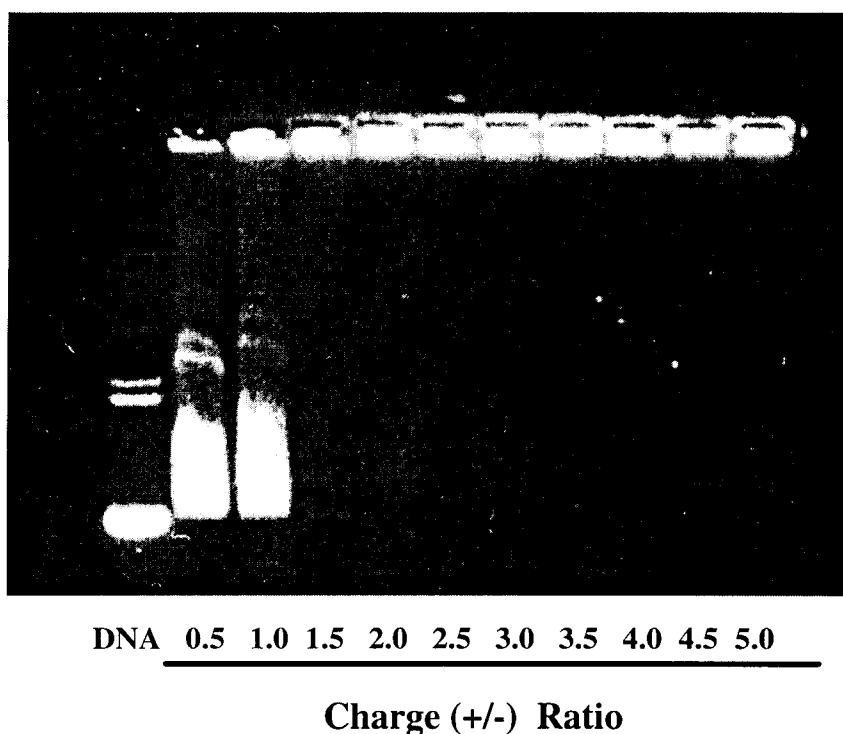


**Figure 2.4.  $\beta$ -CD polymer 4/DNA binding.**

Determination of  $\beta$ -CD polymer 4/DNA charge ratio necessary for complex formation by DNA retardation. DNA is visualized by ethidium bromide.

**2.4.3. In Vitro Transfection and Toxicity of DNA Complexes.** One microgram of pGL3-CV, encoding for the luciferase gene under the control of the SV40 promoter, was complexed with **4** at various charge ratios in 10% serum and serum-free conditions and added to BHK-21 and CHO-K1 cells plated in 24-well plates. Transfection efficiencies of these complexes were determined by assaying for luciferase protein activity and reported in relative light units (RLU) per milligram of total cell protein. Luciferase protein activity in BHK-21 cells transfected in serum-free conditions reached a stable maximum at 30 +/- with  $\sim 1 \times 10^9$  RLU/mg of protein. The presence of 10% serum in the transfection media decreased luciferase activity at all charge ratios (Figure 2.5a). With CHO-K1 cells, increasing charge ratio also enhanced the transfection for all conditions tested. Additionally, transfection in serum decreased light units by an order of magnitude (Figure 2.5b). The toxicity of the  $\beta$ -CD polymer to cells was measured by determining total cellular protein in the wells 48 h after transfection. Polymer **4** showed toxicity only to BHK-21 cells for transfections in the absence of serum. Toxicity was minimized with the presence of 10% serum during transfection (Figure 2.5a). No noticeable toxicity was observed from transfections to CHO-K1 cells (Figure 2.5b).

pGL3-CV was complexed with various commercially available transfection agents and exposed to BHK-21 and CHO-K1 cells under the same protocol as used with **4** for comparison. The transfection and toxicity results for PEI (branched 25 kDa) are shown in Figure 2.6. Maximum transfection was obtained at a charge ratio of 3 +/- for BHK-21 cells and 6 +/- for CHO-K1 cells, and decreased slightly at high charge ratios (probably as a result of increased toxicity at those ratios). The presence of 10% serum decreased transfection efficiencies in both cell lines, although more dramatically for BHK-21 cells. Concentration-dependent toxicity was observed for both cell lines regardless of serum conditions.

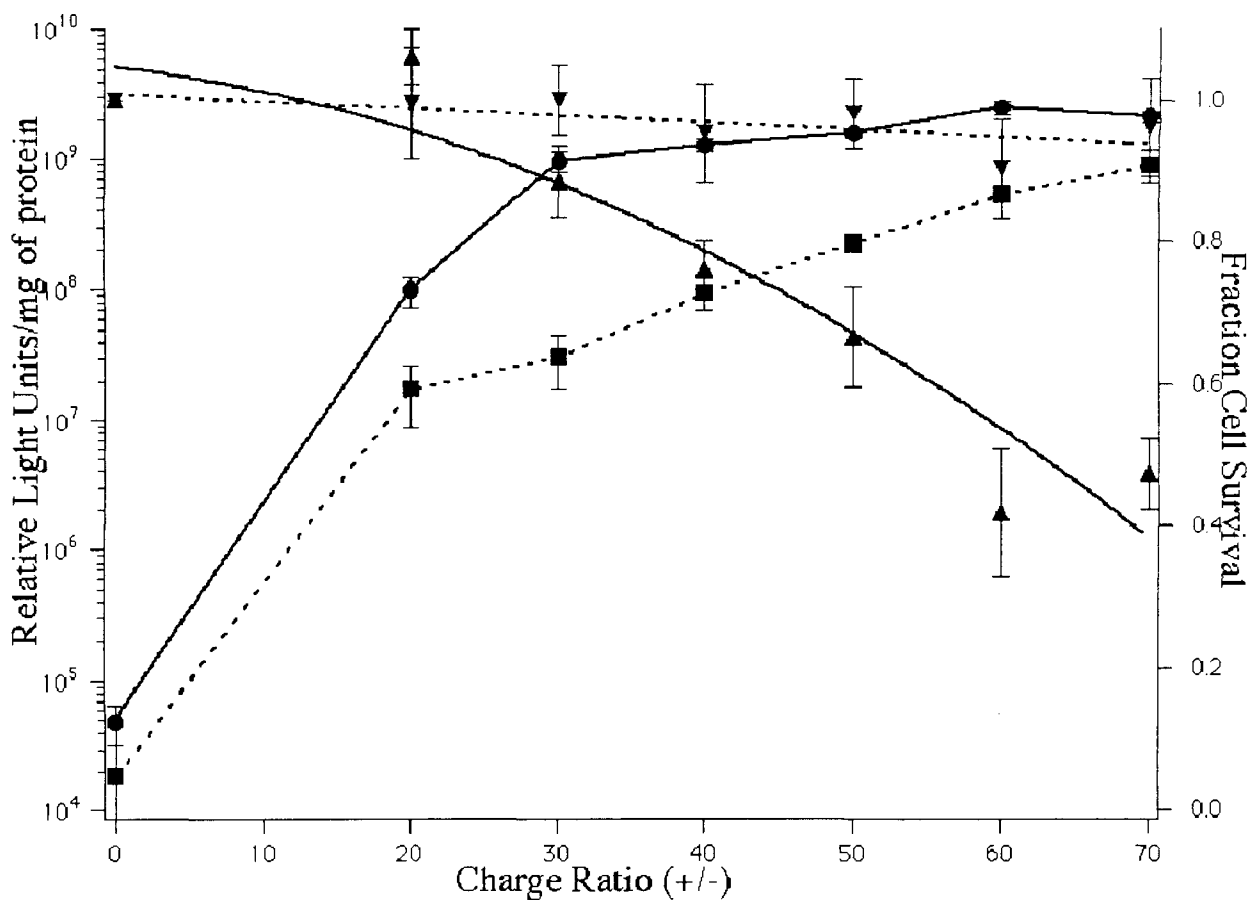


**Figure 2.5a.**

**Figure 2.5.  $\beta$ -CD polymer 4-mediated transfection to BHK-21 and CHO-K1.**

The effect of  $\beta$ -CD polymer 4/DNA charge ratio and serum conditions on transfection efficiency (● and ■) and cell survival (▼ and ▲) in BHK-21 (a) and CHO-K1 (b) cells. Results from transfections in 10% serum and serum-free media are shown with the dotted and solid lines, respectively. Data are reported as the mean  $\pm$  S.D. of three samples. Toxicity data are presented as best fit lines.

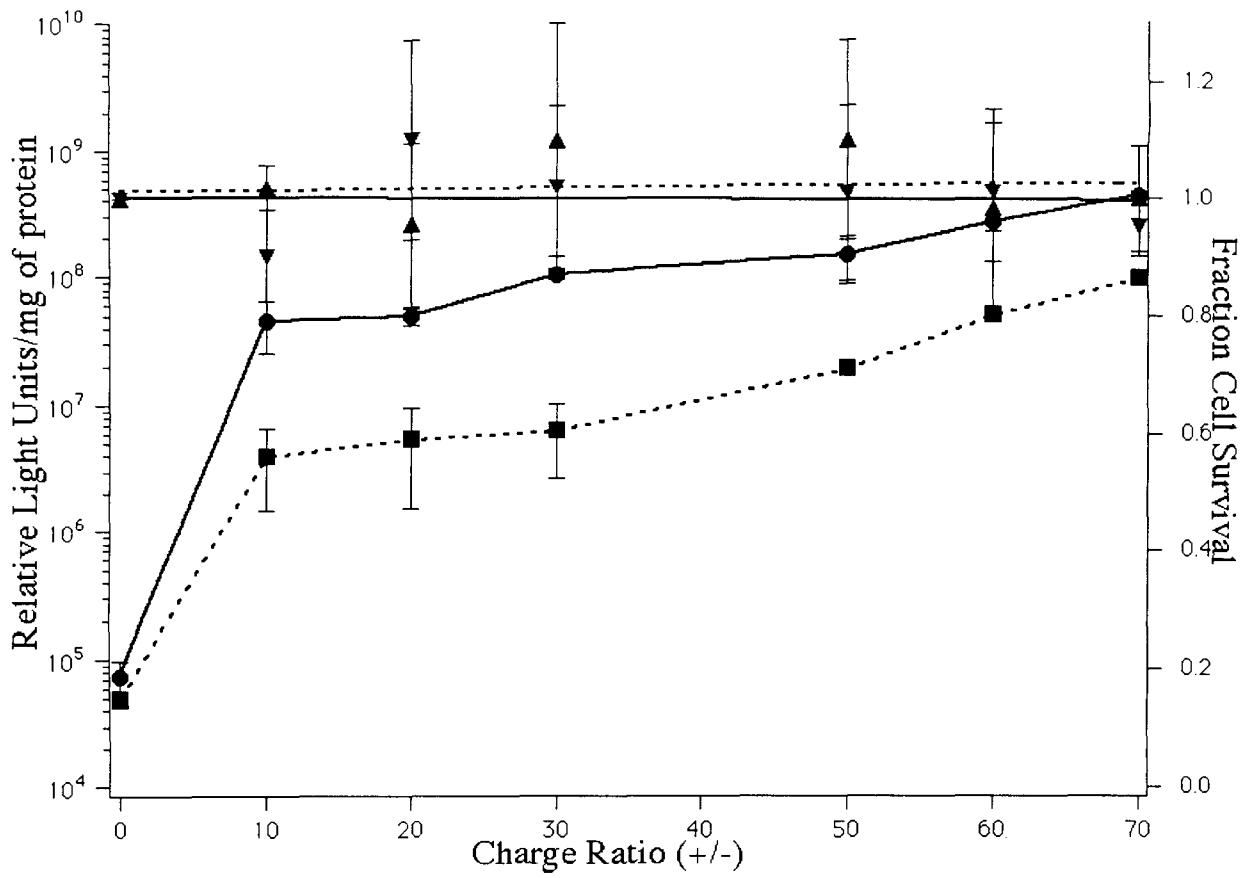
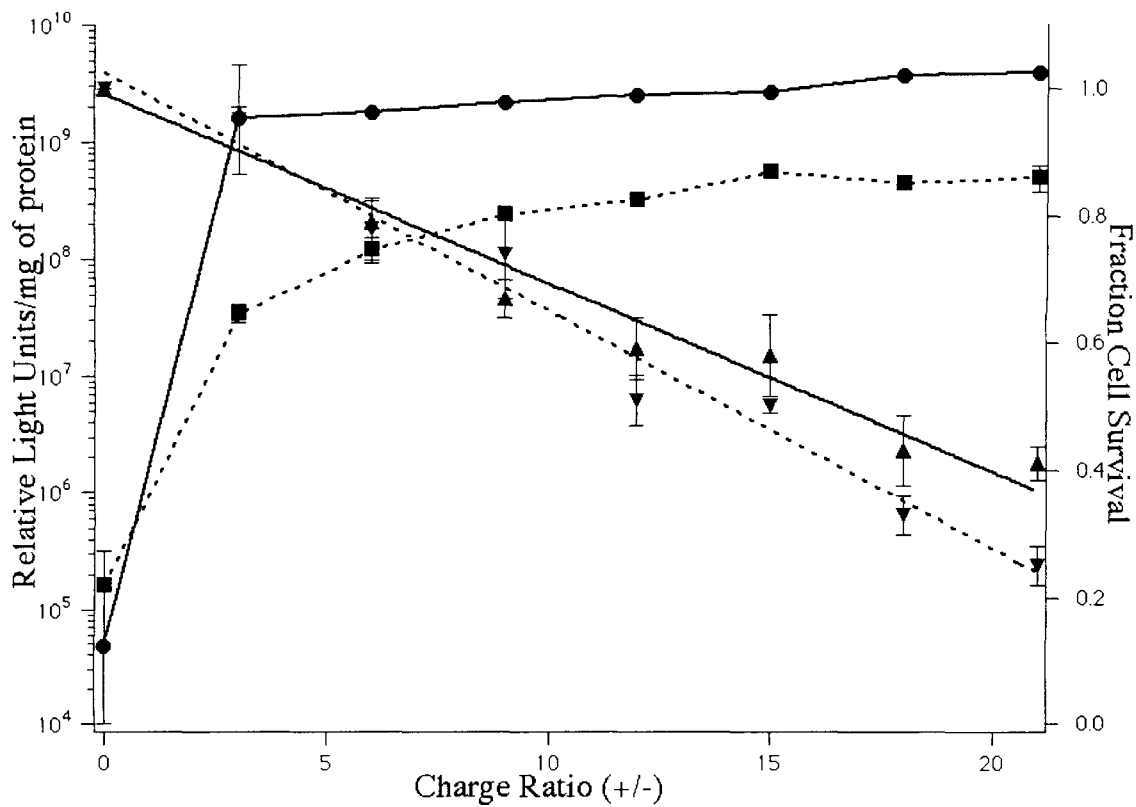


Figure 2.5b.



**Figure 2.6a.**

**Figure 2.6. PEI-mediated transfection to BHK-21 and CHO-K1.**

The effect of PEI/DNA charge ratio and serum conditions on transfection efficiency (● and ■) and cell survival (▼ and ▲) in BHK-21 (a) and CHO-K1 (b) cells. Results from transfections in 10% serum and serum-free media are shown with the dotted and solid lines, respectively. Data are reported as the mean +/- S.D. of three samples. Toxicity data are presented as best fit lines.

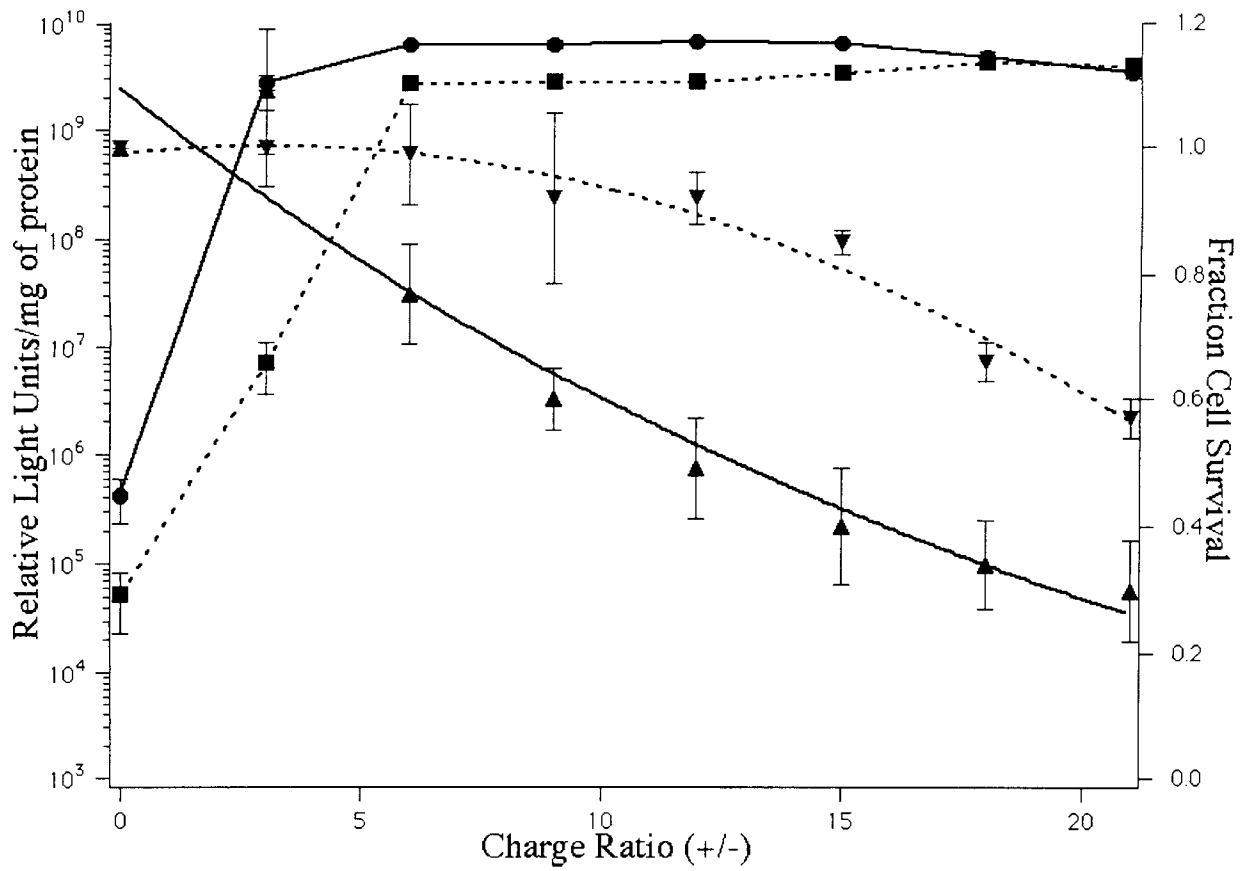
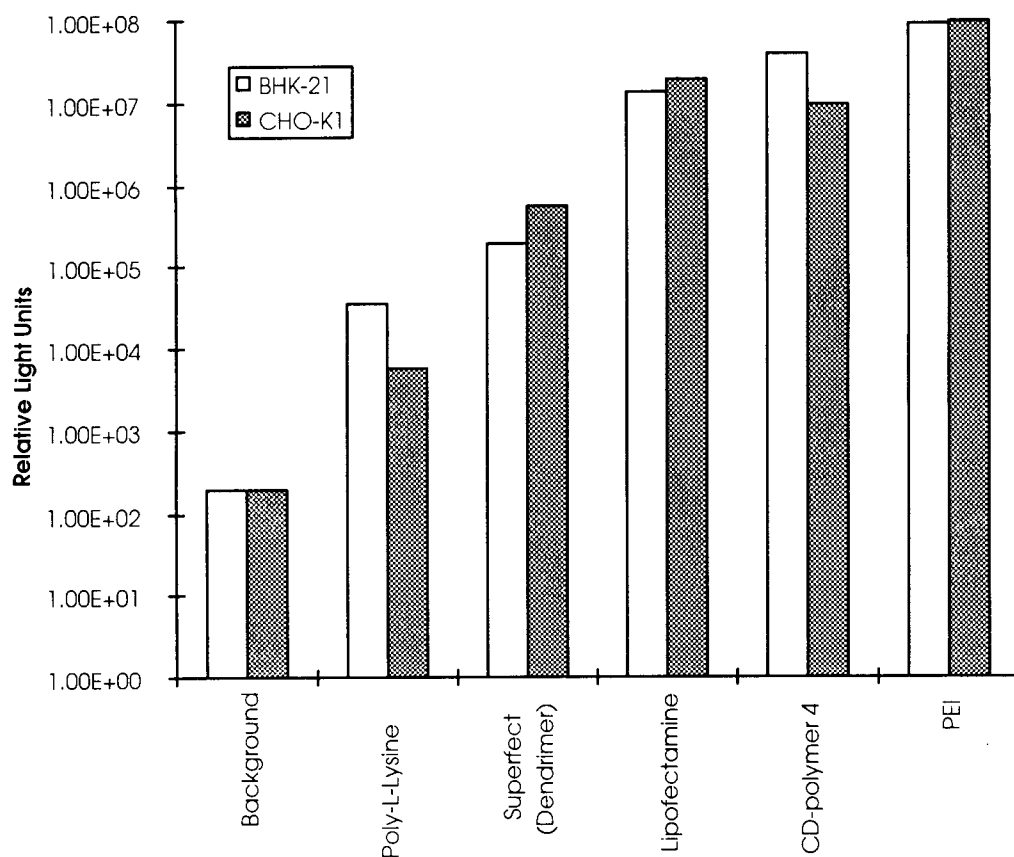
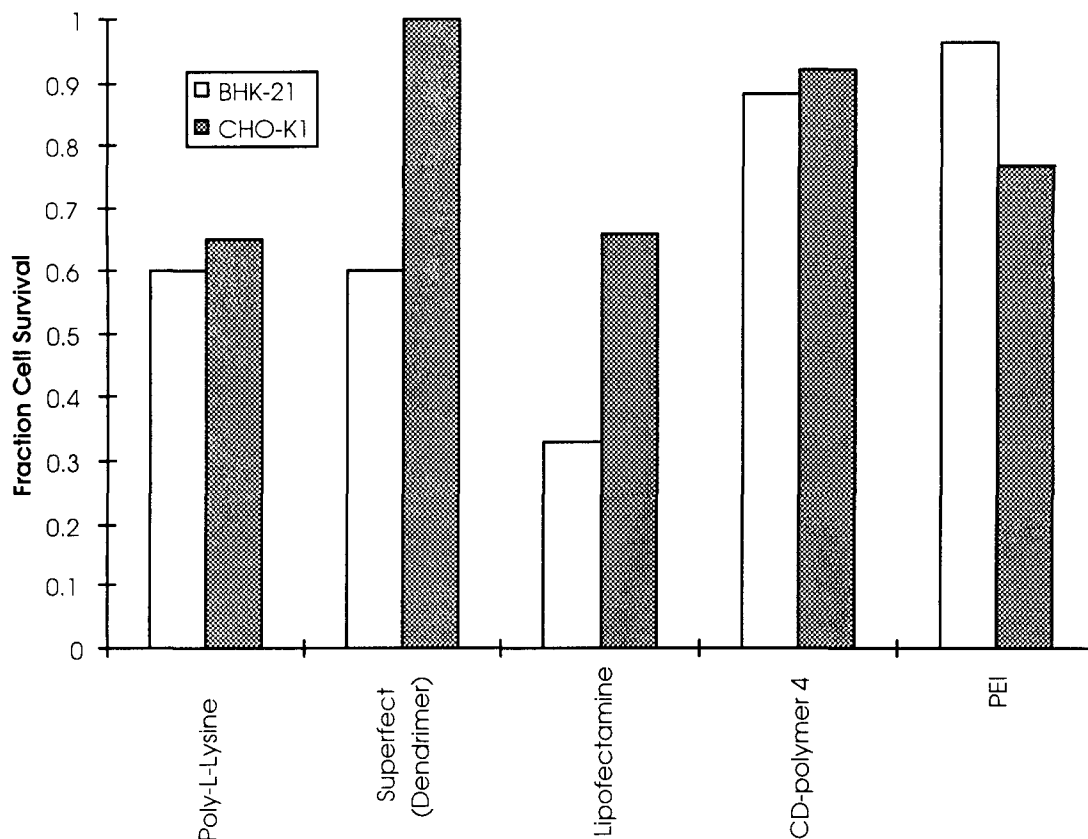


Figure 2.6b.

pGL3-CV transfected with **4** gave RLU's that are two orders of magnitude higher than transfection with Superfect and on of the same order of magnitude as transfection with PEI and Lipofectamine (Figure 2.7a). The toxicity of the vectors at conditions for maximum transfection are shown in Figure 2.7b. While transfection with some of the vectors resulted in less than 60% cell survival in one or both of the cell lines tested, transfection with **4** showed low toxicity.



**Figure 2.7a. Comparison of transfection efficiency of various non-viral vectors.** BHK-21 cells were transfected with a range of vector/DNA charge ratios and starting cell densities for all vectors in serum-free media. The value reported here is obtained from the optimum transfection conditions found for each vector.



**Figure 2.7b. Comparison of the toxicities of various non-viral vectors.** BHK-21 and CHO-K1 cells were transfected with  $\beta$ -CD polymer 4. Percent survival was determined by a modified Lowry protein assay at serum-free conditions giving the maximum transfection for each non-viral vector.

**2.4.4. Particle Characterization.** Previously, it has been reported that negative staining with uranyl acetate may affect DNA condensation (7,8). Here, samples for electron microscopy were prepared by both rotary shadowing and negative staining. Electron microscopy of rotary-shadowed 4/DNA samples showed discrete particles around 100-150 nm in diameter; however, these samples did not appear focused due to low electron density. Negatively-stained samples revealed uniform structures at charge ratios of 5+/- and above (Figure 2.8), as observed by Tang, et al. (7), that were not present in samples without polymer addition.

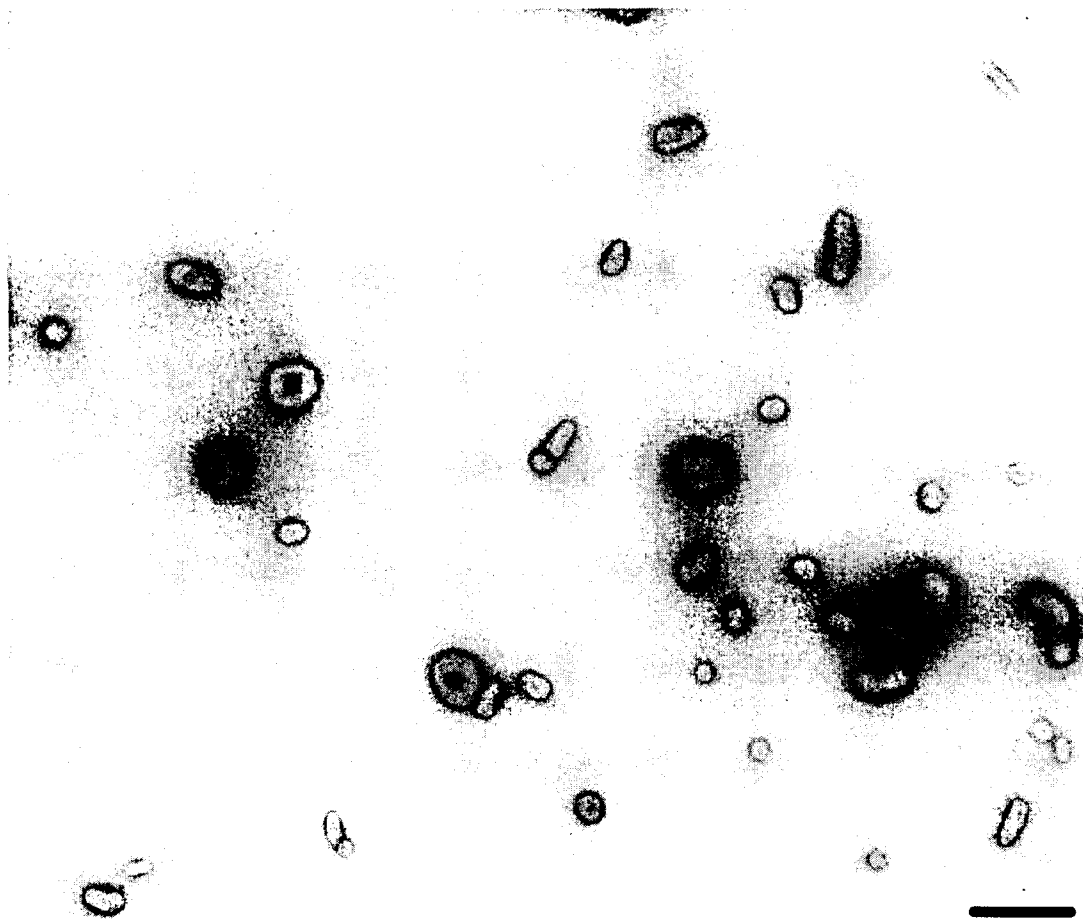


**Figure 2.8. TEM of polymer 4/DNA complexes.**

Electron micrographs of negatively-stained complexes of polymer 4 complexed with DNA at 30 +/- charge ratio in distilled water. Bar represents 200 nm.

Particle size was also confirmed by dynamic light scattering and surface charge of the particles was determined by zeta potential measurements (Figure 2.9a). Particle charge increased with increasing polymer addition, reaching neutrality between polymer/DNA charge ratios of 1 and 2. Zeta potential of the particles approached +32 mV as charge ratios increased. Polymer 4 begins to condense DNA at a charge ratio of 1+/-, although the particles have a net negative charge. When the charge ratio is increased to 2 +/-, the particles are near neutrality (zeta potential = 5.8 mV) and particle aggregation occurs. The 4/DNA particle diameter remains relatively constant at 150-180

nm above charge ratios of 10+/- . The particle size measured by DLS is slightly higher than that observed by TEM because the DLS measures the hydrodynamic diameter. Particles formed in water remained stable for several hours. Addition of 150 mM salt to the particles results in extensive aggregation that begins almost immediately. These results are consistent with those observed for peptide/DNA complexes (9).

A similar zeta potential and particle diameter profile is observed for PEI/DNA complexes (Figure 2.9b). PEI begins to condense DNA at 1+/- . Neutral particles are formed around a charge ratio of 1.5+/- (1.5mV) as demonstrated by the aggregation of particles at this charge ratio. PEI also forms particles with pDNA of ca. 150 nm in diameter above charge ratios of 3. The zeta potential of the particles increases with charge ratio, reaching +40 mV at 21+/- .

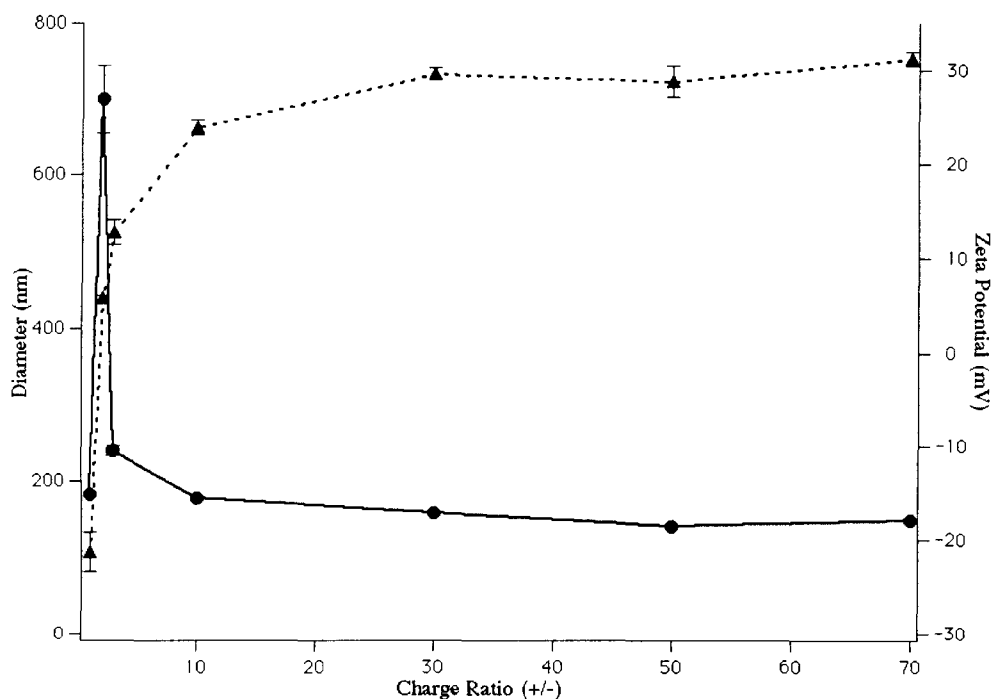


**Figure 2.9a**

**Figure 2.9. Particle size and zeta potential.**

The effect of polymer 4/DNA (a) and PEI/DNA (b) charge ratio on particle size (●), as determined by dynamic light scattering, and particle charge (▲), as estimated by zeta potential measurements.

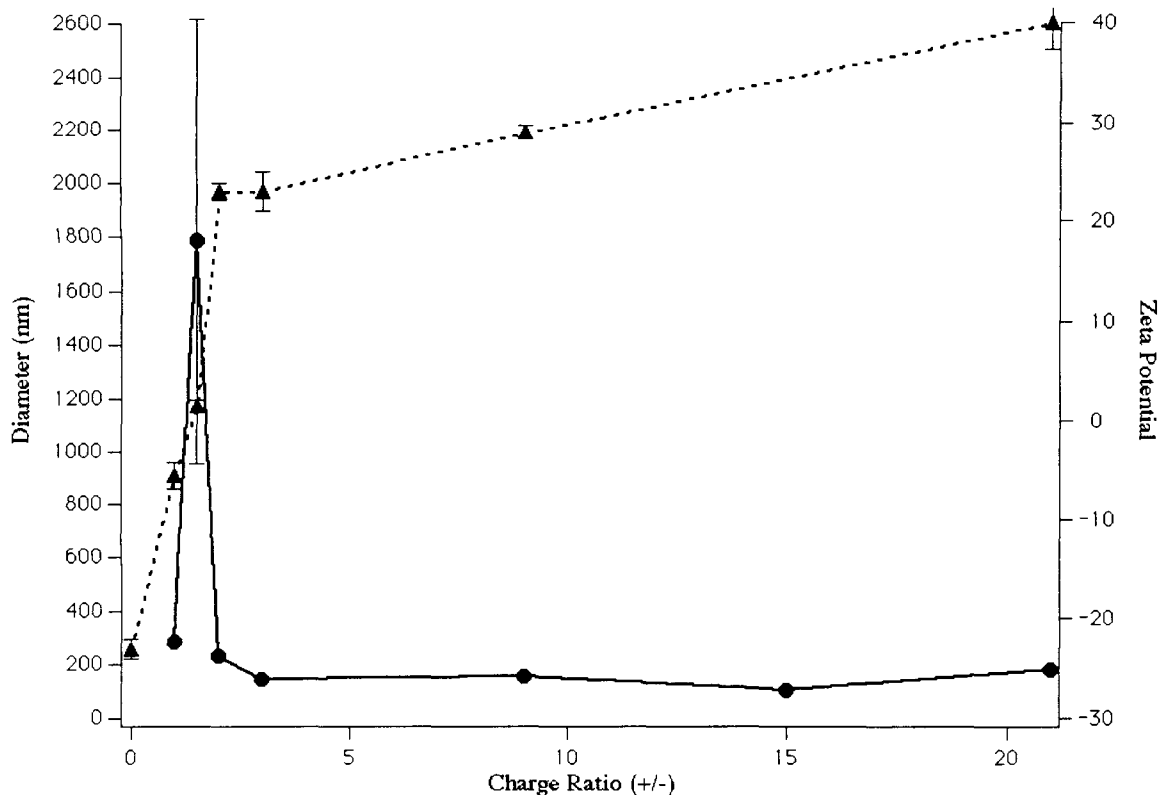


**Figure 2.9b.**

## 2.5 DISCUSSION

The polyamidine-CD copolymer **4** prepared here is obtained with an overall yield of 24%. This yield is comparable to other synthetic, sugar-containing cationic polymers that are prepared via an AABB-type polymerization(10). The molecular weight, as determined by light scattering, was ca. 8,800. This molecular weight corresponds to a degree of polymerization of 6, and an end-group analysis by  $^{13}\text{C}$  NMR spectroscopy is consistent with this degree of polymerization. Polymers with pendent cyclodextrins of equivalent molecular weight have been prepared (11), but those reported here are the first to have the cyclodextrin as a part of the polymer backbone. Polymer **4** is found to be

highly water soluble; solutions of at least 0.4 M concentration can be prepared. Thus, we were able to successfully incorporate a rather insoluble  $\beta$ -cyclodextrin moiety (1.6 mM) in a water-soluble polymer formulation.

The cationic nature of **4** allows for complexation to DNA. Plank, et al. report that a minimum chain length of six to eight cationic amino acids is required to compact DNA into structures active in receptor-mediated gene delivery (9). Polymer **4** contains an average of twelve cationic charges and is able to condense plasmid DNA into discrete particles of 150 nm size in dH<sub>2</sub>O. Although **4**/DNA particles aggregate under physiological salt conditions, there are methods of inhibiting particle aggregation by PEGylation (12) and we are currently exploring these and other techniques for preparing particle formulations that would be stable at physiological conditions.

The **4**/DNA complexes are also able to efficiently transfect cells *in vitro*. Transfection is observed for particles formed at and above +/- ratios of 10, which corresponds to an average zeta potential of at least +24mV. Increasing +/- ratios also increases transfection efficiency. Thus, particles are probably transfecting cells by proteoglycan-mediated entry (13). The presence of 10% serum during transfection decreases transfection efficiency in both BHK-21 and CHO-K1 cell lines.

Although positively-charged **4**/DNA complexes of 150 nm diameter are formed by charge ratios of 5+/- (Figure 2.9a), transfection efficiencies continue to improve with increasing charge ratios despite little change in particle size and charge (Figure 2.5). It is possible that increasing the polymer/DNA ratio only serves to increase the concentration of free polymer in solution, which may in turn aid transfection by affecting the integrity of the cell membrane. To test this possibility, plasmid DNA was complexed with PEI under low charge ratio conditions which allow for complete DNA binding, but negligible transfection. Polymer **4** was then added to the transfection mixture at charge ratios up to 50+/- . Because PEI essentially binds irreversibly to pDNA, increases in transfection efficiency could be attributed to the effects of free **4** in the media. Instead, transfection

efficiencies remained slightly above baseline at all concentrations of **4**. These results indicate that the increasing ratios of **4**/DNA aid transfection by affecting the properties of the **4**/DNA complexes. The nature of these phenomena are currently under investigation.

Initial trafficking studies with fluorescently-labeled DNA (Gene Therapy Systems, San Diego, CA) show successful penetration of nearly 100% of cells; however, most of the complexes appear trapped in intracellular vesicles, even 24 hours after initial cell contact. The high percentage of cell transfection followed by subsequent vesicular entrapment has also been reported in lipid-based systems (14). Transfections at various charge ratios were therefore conducted in the presence of 25  $\mu$ M chloroquine, an agent which delays lysosomal degradation of the pDNA by buffering the endosomal pH (15). The addition of chloroquine enhanced transfection efficiencies by over two orders of magnitude (an increase from  $1 \times 10^8$  RLU/mg of protein to  $7 \times 10^{10}$  RLU/mg of protein at 20+/-). The transfection efficiency in the presence of chloroquine was also dependent on the polymer to DNA charge ratio; as seen before, increasing the polymer concentration also increases transfection efficiency. The transfection enhancement due to chloroquine addition confirms particle entry by endocytosis and the lack of efficient endosomal release. Nevertheless, the **4**/DNA complexes show transfection efficiencies comparable to vectors with endosome-escape mechanisms: PEI, that is speculated to act as a "proton sponge" to release complexes from endosomes by osmotic pressure (16, 17) and lipofectamine, which supposedly releases DNA by destabilizing endosomal membranes (18).

The cyclodextrin-based polymer **4** provides for efficient *in vitro* transfection of cells while remaining non-toxic under most conditions. Most cationic materials, such as lipid-based vectors and dendrimers have revealed some toxicity in *in vitro* studies (17). Polymer **4** showed toxicity to BHK-21 cells at increasing charge ratios in serum-free media (Figure 2.5a). However, no toxicity is observed with 10% serum for BHK-21 and CHO-K1 cell lines (Figure 2.5b), and in serum-free conditions for CHO-K1 cells, even up to charge ratios of 200 +/- (data not shown).

Cytotoxicity of individual cyclodextrins is dependent upon type, e.g.,  $\alpha$ ,  $\beta$ ,  $\gamma$ , and functionalization, e.g., native vs. hydroxypropylated (19). Cyclodextrins can produce cell membrane solubilization by complexation with membrane components such as cholesterol (19). In order to test whether observed toxicity with **4** is from the polycationic nature of the polymer or from the cyclodextrin itself, BHK-21 and CHO-K1 cells were contacted with polymer **5** (no cationic charge),  $\beta$ -CD, and comonomer **2**. No toxicity was observed at  $\beta$ -CD monomer concentrations or monomer concentrations of **5** up to 700  $\mu$ M, which is equivalent to the monomer concentration of **4** used for transfections at 200 $\pm$ . Finally, the cells were contacted with difunctionalized monomer DMS at concentrations up to 700  $\mu$ M. Because DMS is a membrane permeable molecule, it is possible that the cell toxicity noted at high polymer concentrations is caused by the DMS end groups of the polymers. However, no cell toxicity was seen at the tested concentrations. These results indicate that the toxicity of **4** in BHK-21 cells is likely due to the polycationic nature of the polymer.

Preliminary *in vivo* toxicity studies have also been consistent with the *in vitro* findings. Single intravenous and intraperitoneal injections in mice of a cyclodextrin polymer similar to **4** at concentrations up to 200 mg/kg showed no mortalities. Macroscopic examinations at necropsy revealed no evidence of damage 5 days after polymer administration. For comparison, 22 kDa linear PEI has a LD<sub>50</sub> of approximately 30 mg/kg in the presence of 5 mg/kg pDNA in mice (20) and a PEG-terminated copolymer of d-lysine/d-serine is lethal to mice within 30 minutes of i.v. administration at 200 mg/kg (21).

$\beta$ -Cyclodextrin containing cationic polymers were synthesized in an effort to develop a delivery vehicle that would be non-toxic and would condense DNA to particles sufficiently small to enable efficient transfection. The polyamidine polymer **4** satisfies these criteria.

## 2.6. ACKNOWLEDGMENTS

This work was partially supported by the Colvin Foundation and S.J.H. thanks the Whitaker Foundation for a doctoral fellowship. We also thank Pat Koen for his assistance with the transmission electron microscope.

## 2.7. LITERATURE CITED

1. Zhu, J., Grace, M., Casale, J., Chang, A.T.I., Musco, M.L., Bordens, R., Greenberg, R., Schaefer, E. and Indelicato, S.R. (1999) Characterization of Replication-Competent Adenovirus Isolates from Large-Scale Production of a Recombinant Adenoviral Vector *Hum. Gene Ther.* 10, 113-121.
2. Rolland, A.P. (1998) From Genes to Gene Medicines: Recent Advances in Nonviral Gene Delivery *Crit. Rev. Ther. Drug Carr. Sys.* 15, 143-198.
3. Szejtli, J. and Osa, T. eds. (1996) Cyclodextrins. *Comp. Supramolecular Chem.* 3, Pergamon, UK.
4. Gonzalez, H., Hwang, S.J., and Davis, M.E. (1998) U.S. Pat. Appl.
5. Tabushi, I., Shimokawa, K., and Fujita, K. (1977) Specific Bifunctionalization on Cyclodextrin *Tetrahedron Lett.* 18, 1527-1530.
6. Hermanson, G. T. (1996) *Bioconjugate Techniques* Academic Press, San Diego.

7. Tang, M.X. and Szoka, F.C. (1997) The Influence of Polymer Structure on the Interactions of Cationic Polymers with DNA and Morphology of the Resulting Complexes. *Gene Therapy* 4, 823-832.
8. Böttcher, C. Endisch, C., Fuhrhop, J.-H., Catterall, C. and Eaton, M. (1998) High-Yield Preparation of Oligomeric C-Type DNA Toroids and Their Characterization by Cryoelectron Microscopy. *J. Am. Chem. Soc.* 120, 12-17.
9. Plank, C., Tang, M.X., Wolfe, A.R., and Szoka, F.C. (1999) Branched Cationic Peptides for Gene Delivery: Role of Type and Number of Cationic Residues in Formation and *in Vitro* Activity of DNA Polyplexes. *Hum. Gene Ther.* 10, 319-322.
10. Liu, X.C. and Dordick, J.S. (1999) Sugar-Containing Polyamines Prepared Using Galactose Oxidase Coupled with Chemical Reduction *J. Am. Chem. Soc.* 121, 466-467.
11. Harada, A., Furue, M., Nozakura, S. (1976) Cyclodextrin-Containing Polymers. 1. Preparation of Polymers *Macromolecules* 9, 701-704.
12. Ogris, M., Brunner, S., Schüller, S., Kircheis, R. and Wagner, E. (1999) PEGylated DNA/transferrin-PEI complexes: reduced interaction with blood components, extended circulation in blood and potential for systemic gene delivery. *Gene Ther.* 6, 595-605.
13. Mislick, K.A. and Baldeschwieler, J.D. (1996) Evidence for the Role of Proteoglycans in Cation-Mediated Gene-Transfer. *Proc. Nat. Acad. Sci.* v93, 12349-12354.

14. Tseng, W.-C., Haselton, F.R., and Giorgio, T.D. (1997) Transfection by Cationic Liposomes Using Simultaneous Single Cell Measurements of Plasmid Delivery and Transgene Expression. *J.Biol. Chem.* 272, 25641-25647.
15. Stenseth, K., and Thyberg, J. (1989) Monensin and chloroquine inhibit transfer to lysosomes of endocytosed macromolecules in cultured mouse peritoneal macrophages. *Eur. J. Cell Bio.* 49, 326-333.
16. Boussif, O. (1995) A Versatile Vector for Gene and Oligonucleotide Transfer into Cells in Culture and In-Vivo - Polyethylenimine. *Proc. Nat. Acad. Sci.* v92, 7297-7301.
17. Demeneix, B.A. and Behr, J.P. (1996) The Proton Sponge: A Trick the Viruses Did Not Exploit. In *Artificial Self-assembling Systems for Gene Delivery* (P. Felgner, Ed.) pp146-151, American Chemical Society, Washington D.C..
18. Felgner, J.H., Kumar, R., Sridhar, C.N., Wheeler, C.J., Tsai, Y.J., Border, R., Ramsey, P., Martin, M. and Felgner, P.L. (1994) Enhanced Gene Delivery and Mechanism Studies with a Novel Series of Cationic Formulations. *J. Biol. Chem.* 269, 2550-2561.
19. Irie, T. and Uekama, K. (1997) Pharmaceutical Applications of Cyclodextrins. III. Toxicological Issues and Safety Evaluation. *J. Pharm. Sci.* 86, 147-162.
20. Goula, D., Benoist, C., Mantero, S., Merlo, G., Levi, G., and Demeneix, B.A. (1998) Polyethylenimine-based intravenous delivery of transgenes to mouse lungs. *Gene Ther.* 5, 1291-1295.

21. Hisayasu, S., Miyauchi, M., Akiyama, K., Gotoh, T., Satoh, S., and Shimada, T. (1999) In vivo targeted gene transfer into liver cells mediated by a novel galactosyl-D-lysine/D-serine copolymer. *Gene Ther.* 6, 689-693.

## Chapter 3

### Effects of Structure of $\beta$ -Cyclodextrin-Containing Polymers on Gene Delivery

#### 3.1. ABSTRACT

Linear cationic  $\beta$ -cyclodextrin-based polymers ( $\beta$ CDPs) are capable of forming polyplexes with nucleic acids and transfecting cultured cells. The  $\beta$ CDPs are synthesized by the condensation of a diamino-cyclodextrin monomer A with a diimidate comonomer B. In this paper, the effects of polymer structure on polyplex formation, in vitro transfection efficiency and toxicity are elucidated. By comparison of the  $\beta$ CDPs to polyamidines lacking cyclodextrins, the inclusion of a cyclodextrin moiety in the comonomer A units reduces the  $IC_{50}$ s of the polymer by up to three orders of magnitude. The spacing between the cationic amidine groups is also important. Different polymers with 4, 5, 6, 7, 8 and 10 methylene units ( $\beta$ CDP4, 5, 6, 7, 8, 10) in the comonomer B molecule are synthesized. Transfection efficiency is dependent on comonomer B length with up to 20-fold difference between polymers. Optimum transfection is achieved with the  $\beta$ CDP6 polymer. In vitro toxicity varied by one order of magnitude and the lowest toxicity is observed with  $\beta$ CDP8. The  $LD_{40}$  of the  $\beta$ CDP6 to mice is 200 mg/kg, making this polymer a promising agent for in vivo gene delivery applications.

### 3.2. INTRODUCTION

The development of polyplexes (cationic polymer + nucleic acid (1)) for gene delivery has grown rapidly to include cationic polymers such as poly-L-lysine (PLL) (2), chitosan (3), pAMAM dendrimers (4), polyethylenimine (PEI) (5) and many other polycations. A recent review of cationic polymer based delivery systems is presented by De Smedt et al. (6). Cationic polymers are able to deliver plasmid DNA into cells by self-assembling with the anionic DNA via electrostatic interactions with subsequent condensation into small particles that are readily endocytosed.

While cationic polymers share a similar mechanism of delivery, their transfection efficiencies differ greatly from polymer to polymer. Indeed, significant transfection and toxicity variations have been noted with the use of various molecular weight fractions of the same polymer. Ziady et al. observed both in vitro and in vivo behavioral differences with the use of short (36-mer) and long (256-mer)-chain PLL (7). Additionally, polyplexes formed with these polymers had different physicochemical characteristics. The transfection efficiency of PEI is also highly dependent on molecular weight and structure (8,9). Remy et al. compared in vitro gene delivery for various branched and linear PEIs and found significant variations with PEI structure (10). Malik et al. also found that the dendrimer generation influences the efficacy of pAMAM dendrimers (11).

Plank et al. studied peptide derivatives within a low molecular weight range by synthesizing branched cationic peptides with variations in number and type of amino acids within the peptides (12). They found DNA binding affinity to be mainly a function of the number of cationic residues, and the transfection efficiency to be influenced by the type of cationic residues used. It is evident from these reports that polycation structure impacts delivery efficiency. Additionally, it is clear that further investigation into the features of polycations that influence their behavior in gene delivery is merited. Here, we perform a structure-property study of this type.

We have reported the synthesis of a new family of  $\beta$ -cyclodextrin-based polymers ( $\beta$ CDPs) that are prepared by the condensation of difunctionalized CD monomers (comonomer A) with other difunctionalized comonomers (comonomer B) (13). The modular synthesis of the  $\beta$ CDPs allows for the systematic study of the effects of polymer structure on polyplex formation and polyfection. Previously, the importance of a spacer between the cyclodextrin and amine functional groups in the comonomer A units has been discussed (13). The spacer was shown to be required for DNA binding of comonomer A, most likely by relieving the steric hindrance of the bulky cyclodextrin cups. Here, we study the effect of comonomer B structure on DNA delivery and toxicity, since variations in comonomer B result in changes in polymer charge density and hydrophobicity. In order to better understand the origin of the functional differences, the polyplexes are characterized by comparing particle size, DNase protection ability, and relative DNA binding constants.

### 3.3. MATERIALS AND METHODS

#### 3.3.1. $\beta$ -Cyclodextrin-Polymers.

$\beta$ -cyclodextrin polymers ( $\beta$ CDPs) were prepared by the polymerization of a difunctionalized  $\beta$ -CD monomer (A) with a difunctionalized comonomer (B) to give an ABAB product as described previously (13). The synthesis procedure involves the preparation of the difunctionalized  $\beta$ -CD (6A, 6D-dideoxy-6A, 6D-di(2-aminoethanethio)- $\beta$ -cyclodextrin; denoted dicysteamine- $\beta$ -cyclodextrin) and the synthesis of the difunctionalized comonomer B.

*Synthesis of the comonomer A (3, Fig. 3.1).*

$\beta$ -CD (Wacker Biochem Corp, Adrian, MI) was dried in vacuo ( $< 0.1$  mTorr) at 120 °C for 14 h before use. Biphenyl-4,4'-disulfonyl chloride (Aldrich, Milwaukee, WI) was recrystallized from chloroform/hexane. Potassium iodide was powdered with a mortar and

pestle and dried in an oven at 200 °C. Cysteamine (Fluka, Milwaukee, WI) was sublimed at 40 °C under vacuo before use. All other reagents were obtained from commercial suppliers and were used as received without further purification.

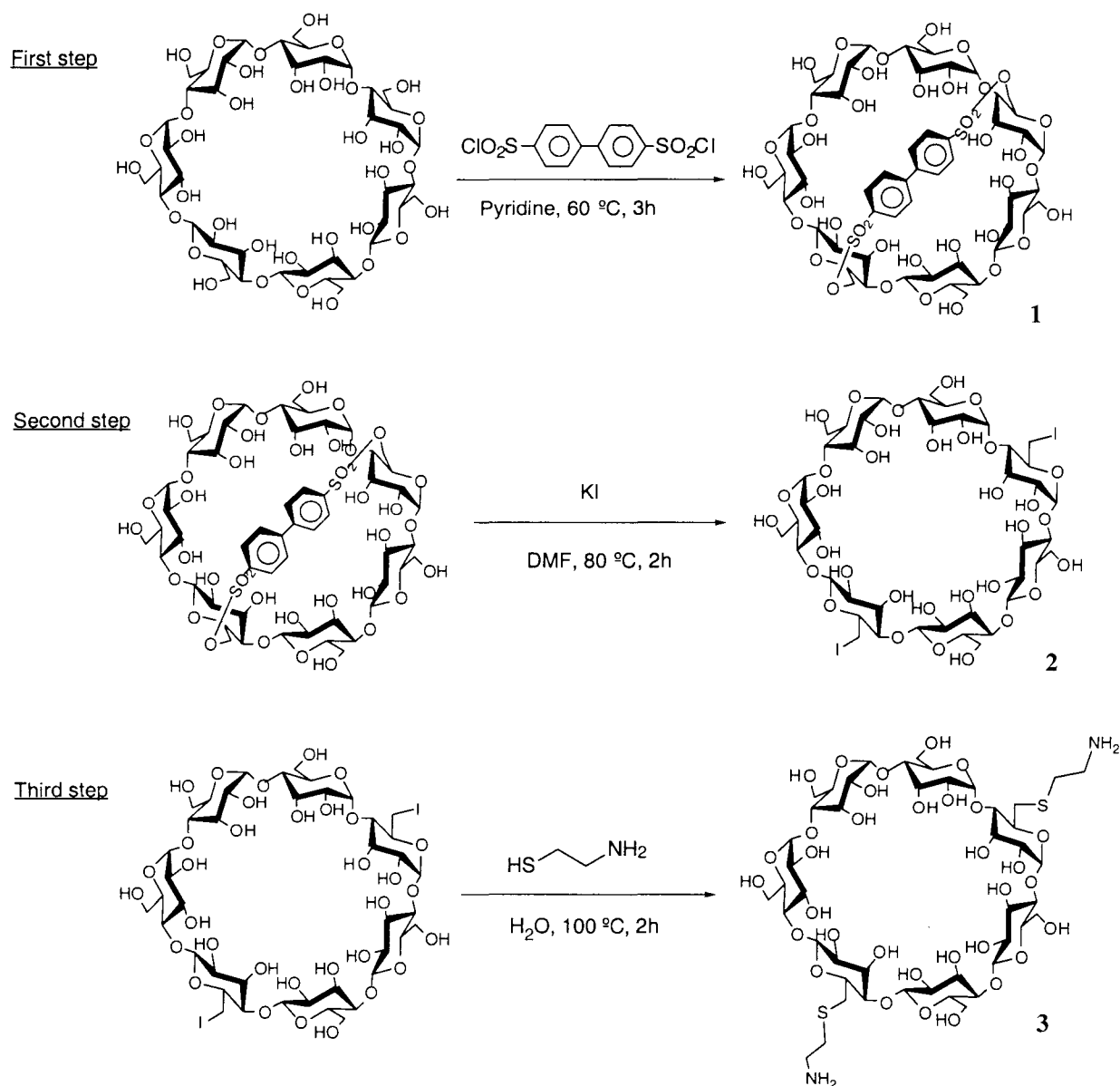


**Figure 3.1.** Synthesis of the comonomer A (dicysteamine- $\beta$ -cyclodextrin).

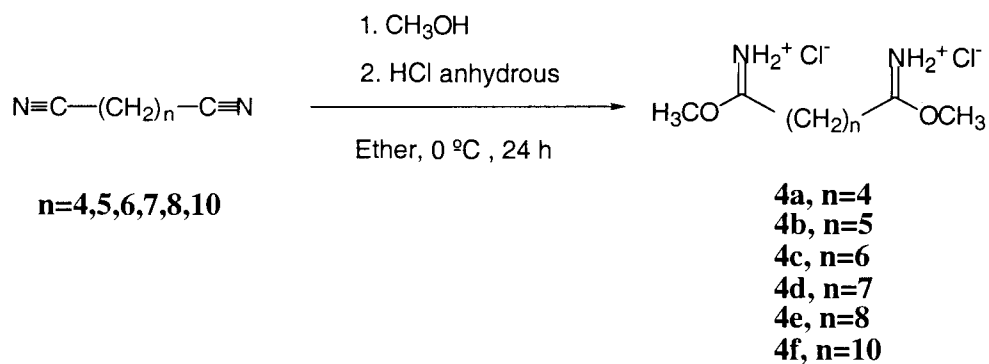
First step: Synthesis of biphenyl-4,4'-disulfonate-capped  $\beta$ -CD **1**. The capped  $\beta$ -CD was synthesized according to a modified procedure of Tabushi et al. (14). To a solution of dried  $\beta$ -CD (10g, 8.81 mmol) in 250 mL of freshly distilled anhydrous pyridine (Aldrich) was added 2.78g (7.93 mmol) of biphenyl-4,4'-disulfonyl chloride in four equal portions at 15 min intervals. The resulting solution was stirred at 60 °C under nitrogen for an additional 3 h and the solvent was removed to dryness in vacuo at room temperature. The residue was subjected to C8 reversed-phase column chromatography using a gradient elution of 0-40% acetonitrile in water. Fractions were analyzed by HPLC and the appropriate fractions were combined. After removing the acetonitrile on a rotary evaporator, the resulting aqueous suspension was lyophilized to dryness. This procedure gave 5.42g (40% yield) of **1**.  $^{13}\text{C}$  NMR (Bruker 500 MHz,  $\text{Me}_2\text{SO}-d_6$ )  $\delta$  ppm: 60.3 (C6), 70.9, 71.6, 72.7 (C2, C3, C5), 82.4 (C4), 102.0 (C1), 128.4-143.2 (phenyl).

Second step: Synthesis of diiodo  $\beta$ -CD **2** (15). To a solution of 5.42g (3.52 mmol) of **1** in 100 mL of anhydrous DMF (Aldrich) was added 17.53g (0.106 mol) of dry powdered potassium iodide. The solution was kept at 80 °C for 2 h with stirring. After the mixture cooled to room temperature, insoluble materials were removed by filtration and the solution was evaporated to dryness in vacuo. The residue was then dissolved in 60 mL of water and 6 mL of tetrachloroethylene was added at 0 °C with vigorous stirring. The precipitate formed was collected and dried in vacuo to give 4.69g (90% yield) of a slightly yellow colored solid.  $^{13}\text{C}$  NMR (Bruker 500 MHz,  $\text{Me}_2\text{SO}-d_6$ )  $\delta$  ppm: 10.4 (C6 adjacent to I), 60.3 (C6 adjacent to OH), 70.9, 71.6, 72.7 (C2, C3, C5), 82.4 (C4), 102.0 (C1).

Third step: Synthesis of dicysteamine  $\beta$ -CD **3**. To a solution of 4.69g (3.17 mmol) of **2** in 100 mL of degassed water was added 0.489g (6.34 mmol) of freshly sublimed cysteamine. The solution was stirred under reflux for 2 h. After cooling to room temperature and acidifying with 1N HCl, the solution was applied to a Toyopearl SP-650M ion-exchange column ( $\text{NH}_4^+$  form) and the product was eluted with a 0 to 0.2M ammonium bicarbonate gradient. Appropriate fractions were combined and lyophilized to dryness. This

procedure gave 1.87g (39% yield) of a white solid. The solid was characterized by TLC (silica gel, *n*-PrOH-AcOEt-H<sub>2</sub>O-NH<sub>3</sub>aq 5/3/3/1, detection by ninhydrin) and exhibited a major spot corresponding to **3** and a minor spot corresponding to free cysteamine. This unreacted cysteamine was eliminated on a rotary evaporator after dissolution of the solid in water with monitoring by Ellman's reagent (16). Matrix-assisted laser desorption/ionization (MALDI) time-of flight (TOF) mass spectrum was recorded on 2 meter ELITE instrument supplied by PerSeptive Biosystems, Inc. MALDI-TOF *m/z* calcd for **3**: 1252, found: 1253.5 [M+H]<sup>+</sup>, 1275.5 [M+Na]<sup>+</sup>, 1291.4 [M+K]<sup>+</sup>. <sup>13</sup>C NMR (Bruker 500 MHz, D<sub>2</sub>O) δ ppm: 32.1 (S-CH<sub>2</sub>) and 38.8 (CH<sub>2</sub>-NH<sub>2</sub>), 32.9 (C6 adjacent to S), 60.2 (C6 adjacent to OH), 70.8, 71.4, 72.5 (C2, C3, C5), 81.8 (C4), 101.7 (C1).

*Synthesis of the comonomer B (4a-f, (17)).*



Dimethyladipimidate.2HCl **4a**, dimethylpimelimidate.2HCl **4b**, and dimethylsuberimidate.2HCl **4c** (DMS) were purchased from Pierce Chemical Co. and were used as received.

Synthesis of dimethylazelimidate.2HCl **4d**. Azelanitrile (1.08g, 7.2 mmol) (Aldrich) was dissolved in an ice-cold mixture of anhydrous methanol (4 mL) and anhydrous diethylether (30 mL). Anhydrous hydrogen chloride was passed through the solution for 60 min and the reaction mixture was left at 0 °C for 24 h. Dry diethyl ether (50 mL) was added to precipitate the product that was washed twice with 100 mL of dry methanol/diethylether

(mixture (volume ratio 1:3)) under anhydrous conditions. The solid was dried under vacuum for 2 h. This procedure gave 1.64g (79% yield) of **4d**. Calcd for  $C_{11}H_{24}O_2N_2Cl_2$ : C, 45.96; H, 8.36; N, 9.75. Found: C, 45.48; H, 8.30; N, 9.71.  $^{13}C$  NMR (Bruker 500 MHz,  $CD_3OD$ )  $\delta$  ppm: 26.1, 29.4, 29.5, 33.9 (4  $CH_2$ ), 59.9 ( $OCH_3$ ), 183.2 ( $C=NH$ ).

Synthesis of dimethylsebacimidate.2HCl **4e**. This compound was obtained from 1.16g (7.1 mmol) of sebaconitrile (Aldrich) by the same procedure used to prepare **4d** and gave 2.04g (96% yield). Calcd. for  $C_{12}H_{26}O_2N_2Cl_2$ : C, 47.81; H, 8.63; N, 9.30. Found: C, 47.68; H, 8.51; N, 9.23.  $^{13}C$  NMR (Bruker 500 MHz,  $CD_3OD$ )  $\delta$  ppm: 26.2, 29.6, 29.7, 33.9 (4  $CH_2$ ), 59.9 ( $OCH_3$ ), 183.2 ( $C=NH$ ).

Synthesis of dodecanediimidate.2HCl **4f**. This compound was obtained from 1.35g (7.0 mmol) of dodecanedinitrile (TCI America Organic Chemicals, Portland, OR) by the same procedure used to prepare **4d** and gave 1.85g (80% yield). Calcd for  $C_{14}H_{30}O_2N_2Cl_2$ : C, 51.03; H, 9.11; N, 8.51. Found: C, 50.96; H, 9.08; N, 8.44.  $^{13}C$  NMR (Bruker 500 MHz,  $CD_3OD$ )  $\delta$  ppm: 26.3, 29.8, 30.0, 30.3, 33.9 (5  $CH_2$ ), 60.0 ( $OCH_3$ ), 183.4 ( $C=NH$ ).

#### *Polymerization (Fig. 3.2).*

$\beta$ CDPs were synthesized as described previously (13). In a typical experiment, a 25 mL vial was charged with a solution of the bis(hydrogen carbonate) salt of dicysteamine  $\beta$ -CD **3** (399.6 mg, 0.269 mmol) dissolved in 500  $\mu$ L of 0.5M  $Na_2CO_3$ . The comonomer B, e.g., **4c** (73.5 mg, 0.269 mmol) was added and the solution was centrifuged briefly to dissolve the components. The resulting mixture was stirred at 25 °C for 15 h. The mixture was then diluted with 10 mL of water and the pH brought below 4 with the addition of 1N HCl. This solution was then dialyzed against a Spectra/Por 7 MWCO 3500 dialysis membrane (Spectrum) in  $dH_2O$  for 24 h. The dialyzed solution was lyophilized to dryness.  $^{13}C$  NMR (Bruker 500 MHz,  $D_2O$ )  $\delta$  ppm: 25.8, 26.0, 27.0, 28.7, 29.9, 32.2, 37.5, 38.1, 41.1, 60.0, 71.6, 72.3, 72.6, 80.8, 101.4, 167.9.

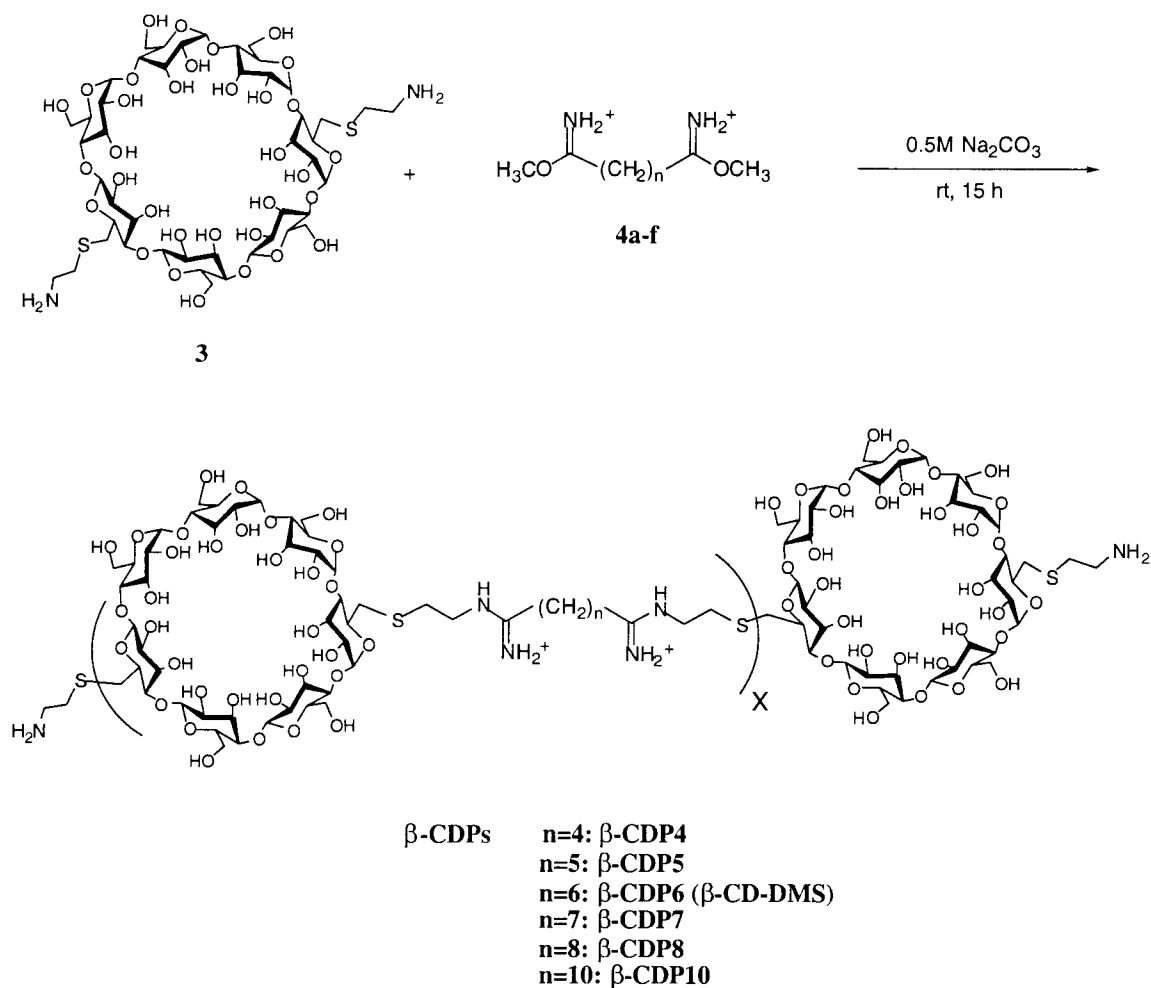


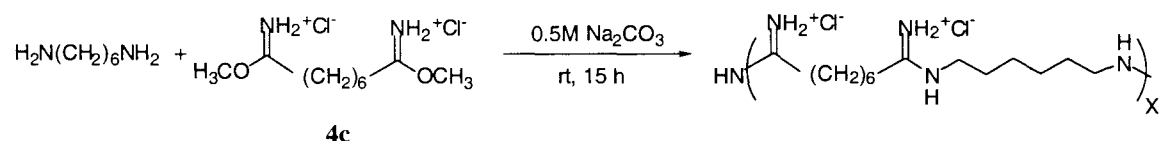
**Figure 3.2.** Polymerization scheme for  $\beta$ -cyclodextrin polymers.

### 3.3.2. Polyamidine Polymers

Polyamidine polymers were synthesized as described for  $\beta$ CDPs except methylene diamines were used as the comonomer A instead of dicysteamine  $\beta$ -CD. These non- $\beta$ -CD-containing polymers were prepared for comparison to the  $\beta$ CDPs in order to ascertain the influence of the  $\beta$ -CD in the polymer backbone upon gene delivery.

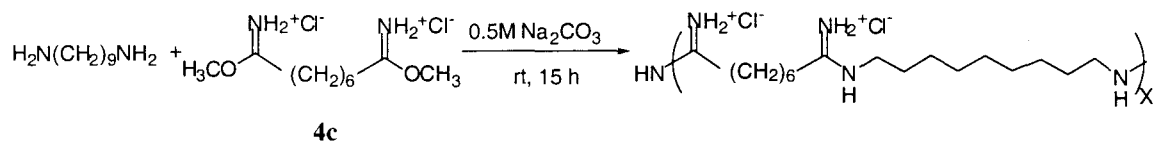
*C6-C6 polyamidine*: A 8 mL glass vial was charged with 80 mg of hexamethylenediamine (comonomer A, 0.690 mmol, Aldrich) and 195 mg of dimethylsuberimidate.2HCl (comonomer B, 0.714 mmol, Pierce). The solids were dissolved by the addition of 0.25 mL of 0.5M Na<sub>2</sub>CO<sub>3</sub>. The mixture was stirred at 25 °C for 15 h, yielding a viscous, clear solution. The mixture was diluted with water and pH brought below 4 with the addition of 1N HCl. The solution was transferred to a Spectra/Por 7 MWCO 1000 dialysis membrane and dialyzed for 24 h in dH<sub>2</sub>O. The dialyzed material was lyophilized to dryness, yielding 30 mg of a white, fluffy solid (13% yield).

### C6-C6 Polyamidine:



*C9-C6 polyamidine*. The C9-C6 polyamidine polymer was synthesized as described above for the C6-C6 polyamidine polymer except 1, 9 diamnonane (comonomer A, Aldrich) was reacted with dimethylsuberimidate.2HCl (comonomer B) to result in a 21% yield of a white, fluffy solid. The C9 distance is a reasonable approximation to that of the β-CD.

### C9-C6 Polyamidine:



### 3.3.3. Polymer Characterization.

*Light Scattering and Molecular Weight Determination.* βCDPs were analyzed on a Hitachi D6000 HPLC system equipped with a ERC-7512 RI detector, a Precision Detectors PD2020/SLS light scattering detector and a Progel-TSK G2000 SW<sub>XL</sub> column using 0.3M NaCl as eluant at a 0.7 mL/min flow rate as described previously (13).

*End Group Analysis by Amine Quantification.*  $\beta$ CDPs were dissolved in 0.1M NaHCO<sub>3</sub> at a concentration of 0.25 mg/mL, and the amine concentration of these solutions was determined by reaction with TNBS (16). In brief, 250  $\mu$ L of 0.01% TNBS in 0.1M NaHCO<sub>3</sub> were added to 500  $\mu$ L of polymer solutions and resulting mixture placed in a 37 °C water bath. After 2 h, 250  $\mu$ L of 10% sodium dodecyl sulfate and 125  $\mu$ L of 1N HCl was added to each sample. The absorbance at 335 nm was determined and compared to a dicysteamine- $\beta$ CD standard curve.

### 3.3.4. Polyplexes

*Plasmids.* Plasmid pGL3-CV (Promega, Madison, WI), that contains the luciferase gene under the control of the SV40 promoter, and plasmid pCA-EGFP (generously donated by Dr. Rusty Lansford and Prof. Scott Fraser at the California Institute of Technology), that contains the EGFP gene under a chick actin promoter, were amplified by *Escherichia Coli* strain DH5 $\alpha$  and were purified using Qiagen's Endotoxin-free Megaprep kit (Valencia, CA).

*Complex Formation.* An equal volume of cationic polymer dissolved in dH<sub>2</sub>O was added to plasmid DNA (0.1 mg/mL in dH<sub>2</sub>O) at the appropriate charge ratios (cationic to anionic, denoted as "+/-").

*Dynamic Light Scattering.* For particle sizing by dynamic light scattering (DLS), 2  $\mu$ g of pCA-EGFP was complexed with polymers at 50 +/- and allowed to stand for 10 min before diluting with 1.2 mL of dH<sub>2</sub>O. Particle size was measured using a ZetaPals dynamic light scattering instrument (Brookhaven Instruments Corporation, Holtsville, NY).

*Transmission Electron Microscopy.* One microgram of DNA was complexed with cationic polymer at 50 +/- charge ratio and applied to formvar carbon-coated grids for 45 seconds

before removing excess liquid. Samples were then stained with 2% uranyl acetate for 45s before blotting. Images were recorded using a Philips 201 Electron Microscope operated at 80V.

*DNase Protection Assay.* The DNase protection assay was modified from a procedure by Gao et al. (18). One microgram of DNA (pCA-EGFP) was complexed with cationic polymer at 5 +/- . The complexes were then incubated with 20  $\mu$ L of fetal bovine serum (FBS, Gibco BRL, Gaithersburg, MD) for 30 min. Five microliters of 10% SDS were added to the complexes to displace the polymers from the DNA. Twenty microliters of FBS were added to "control" complexes followed by immediate addition of SDS for the "0 minute" timepoint. The samples were then applied to a 0.8% agarose gel containing 6  $\mu$ g ethidium bromide/100 mL TAE buffer (40 mM Tris-Acetate, 1 mM EDTA) after the addition of 1  $\mu$ L loading buffer and electrophoresed.

*Competitive Displacement by Heparan Sulfate.* Cationic polymer was complexed with 0.5  $\mu$ g of pGL3-CV at a 20 +/- charge ratio. Heparan sulfate (5 mg/mL in water, Sigma, from porcine intestinal mucosa, St. Louis, MO) was then added to the complexes. After a 5 min incubation, 1  $\mu$ L of loading buffer was added and samples were electrophoresed in an agarose gel as described for the DNase protection assay.

**3.3.5. Cell Culture and Polyfections.** BHK-21 cells were purchased from ATCC (Rockville, MD) and maintained in Dulbecco's Modified Eagle Medium supplemented with 10% FBS, 100 units/mL penicillin, 100  $\mu$ g/mL streptomycin, and 0.25  $\mu$ g/mL amphotericin at 37° C and 5% CO<sub>2</sub>. Media and supplements were purchased from Gibco BRL (Gaithersburg, MD). For transfections, BHK-21 cells were plated at 50,000 cells/well in 24-well plates. Cells were transfected with 1  $\mu$ g of pGL3-CV complexed with  $\beta$ CDPs at various charge ratios in serum-free media and lysates analyzed for luciferase activity as

described previously (13). The toxicities associated with the transfections were assessed by the Lowry protein assay, also described previously (13).

**3.3.6. IC<sub>50</sub> Determination.** BHK-21 cells were plated at 5000 cells/0.1 mL/well in 96 well plates and incubated at 37° C for 24 h.  $\beta$ CDPs (16 mg/mL in complete media) were then added to the third column of cells and diluted serially across the rows. The cells were incubated with the polymers for 24 h at 37° C. The media was then removed from the cells and cells were washed once with PBS. Fifty microliters of MTT (2 mg/mL in PBS) were added to each well followed by 150  $\mu$ L of complete media. The cells were incubated for an additional 24 h before the media was removed and blue formazan crystals formed were dissolved in 150  $\mu$ L of DMSO. The absorbances were read at 562 nm in a microplate reader (EL-312e Biokinetics Reader, Biotek Instruments, Winooski, VT).

**3.3.7. Intravenous Toxicity of  $\beta$ CDP6 in Mice.** Groupings of five outbred mice were injected intravenously with a single dose of  $\beta$ CDP6 (8.33  $\mu$ L/g mouse). Stock dosing solutions of  $\beta$ CDP6 were prepared in 0.9% sodium chloride, sterilized by passing through a 0.2  $\mu$ m filter, and diluted with 0.9% sodium chloride as needed. Mice were observed for 3 days post-injection.

## 3.4. RESULTS

**3.4.1.  $\beta$ CDPs Synthesis and Characterization.**  $\beta$ CDPs were synthesized using comonomer B's with 4, 5, 6, 7, 8 and 10 methylene units. The length of the comonomer B was found to influence the polymerization as shown by the data given in Table 3.1. The molecular weight  $M_w$  and the polydispersity index  $M_w/M_n$  as determined by light scattering are provided in Table 1 for each polymer. Molecular weight  $M_n$  was also estimated by end group analysis. The two possible terminal functional groups for the  $\beta$ CDPs are carboxylic acids or amines. Attempts to conjugate a fluorescent tag to the polymer assuming

carboxylic end groups resulted in no observed reaction. However, the conjugation of TNBS (reacts with primary amines) resulted in the detection of molecular weights  $M_n$  very similar to those detected by SLS (Table 3.1). These molecular weights give a degree of polymerization of 4 to 5 for all  $\beta$ CDPs studied. The yield of polymer increased with the number of methylene groups within comonomer B. The yield of  $\beta$ CDP10 was 56%; however, this polymer was synthesized from a different batch of comonomer A than all the other polymers. Therefore, direct comparison to the other  $\beta$ CDPs may not be appropriate.

Polymer	Yield (%)	$M_w$ (kDa) <sup>a</sup>	$M_w/M_n$	Degree of polymerization	$M_w$ (kDa) <sup>b</sup>
$\beta$ CDP4	18	6.1	1.13	4	5.7
$\beta$ CDP5	21	5.8	1.12	4	5.2
$\beta$ CDP6	20	5.8	1.12	4	5.5
$\beta$ CDP7	29	6.9	1.14	4	4.9
$\beta$ CDP8	37	7.6	1.16	5	6.7

<sup>a</sup> Determined by static light scattering. <sup>b</sup> Estimated by end group analysis.

**Table 3.1. Effect of the length of comonomer B on the polymerization**

**3.4.2. Polyplex Characterization.**  $\beta$ CDPs were complexed with plasmids at various charge ratios and polyplex size was measured by dynamic light scattering (DLS) and TEM. Particle size depended on polymer and DNA concentrations during polyplex formulations. However, above 3+/-, polyplex size remained largely independent of charge ratio. When measured by DLS, particle sizes of polyplexes formulated at DNA concentrations of 50  $\mu$ g/mL ranged from 124-152 nm (Fig. 3.3).  $\beta$ CDP4,  $\beta$ CDP5 and  $\beta$ CDP10-based polyplexes gave the largest particles, with diameters of 148, 141, and 144 nm respectively.

$\beta$ CDP6,  $\beta$ CDP7, and  $\beta$ CDP8-based particles had smaller diameters of 127, 128, and 124 nm respectively. Electron micrographs of all  $\beta$ CDP-polyplexes prepared in water showed uniform particles that appeared spherical in shape.  $\beta$ CDP6-based polyplexes are shown in Fig. 3.4 as an example.

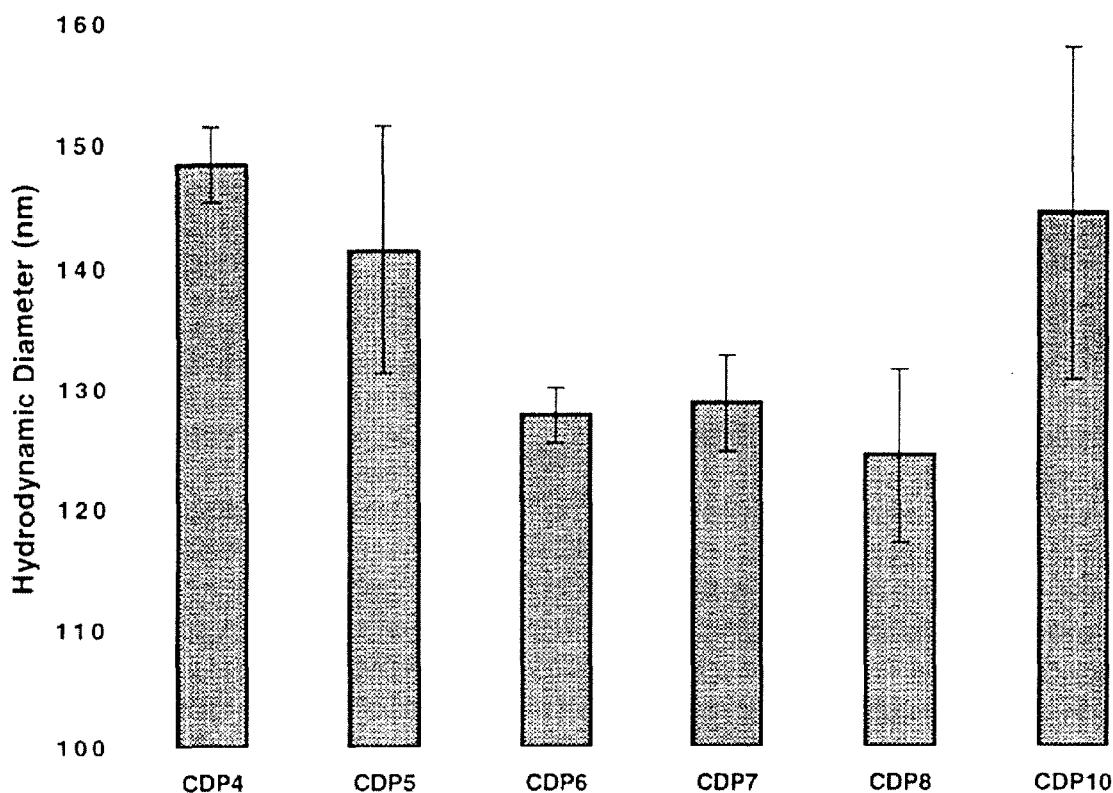
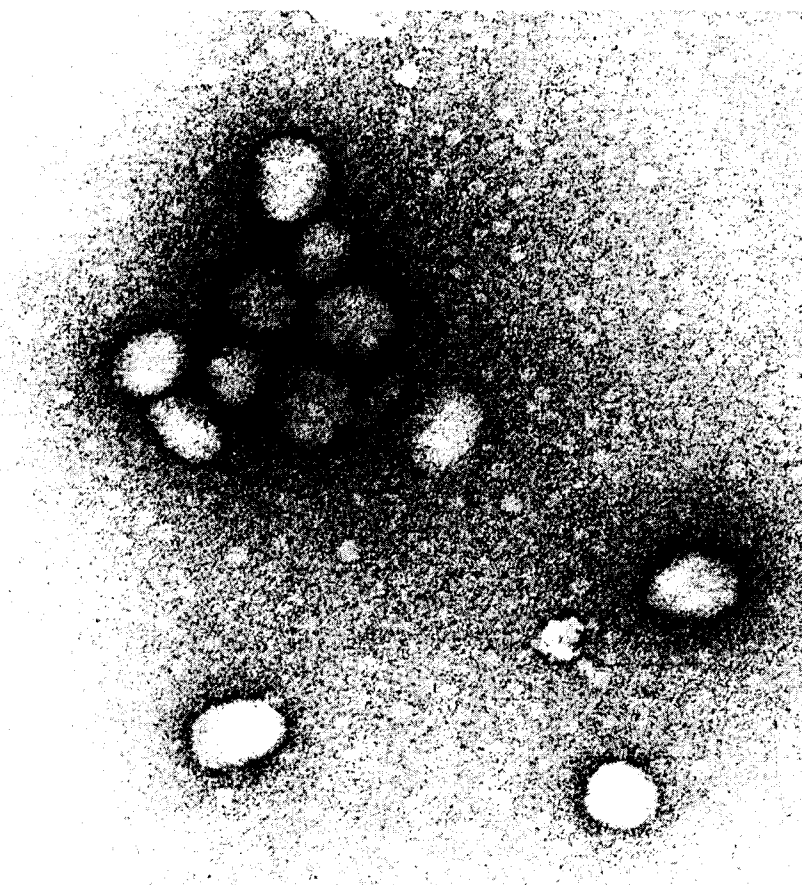


**Figure 3.3. Hydrodynamic diameter of  $\beta$ CDP-based polyplexes.**

Polyplexes were prepared with 2  $\mu$ g of plasmid DNA at a DNA concentration of 0.05 mg/mL and then diluted with dH<sub>2</sub>O to 1.2 mL final volume for hydrodynamic measurements by dynamic light scattering. The results shown are mean  $\pm$  S.D. for three experiments, each measured in triplicate.



100 nm

**Figure 3.4. Electron micrograph depicting polyplexes of  $\beta$ CDP6 and pGL3-CV at a 50+/- charge ratio.**

**3.4.3. DNase Protection.** The ability of the  $\beta$ CDPs to protect plasmid DNA from DNase degradation was assessed. Plasmid DNA was complexed with  $\beta$ CDPs and incubated with an equal volume of fetal bovine serum for 30 min at 37° C. The DNA was released from the complexes by the addition of sodium dodecyl sulfate and run on an agarose gel (Fig. 3.5).  $\beta$ CDPs with 4, 6, 8, and 10 methylene units completely protected DNA, while  $\beta$ CDP5 and  $\beta$ CDP7 offered only partial protection.

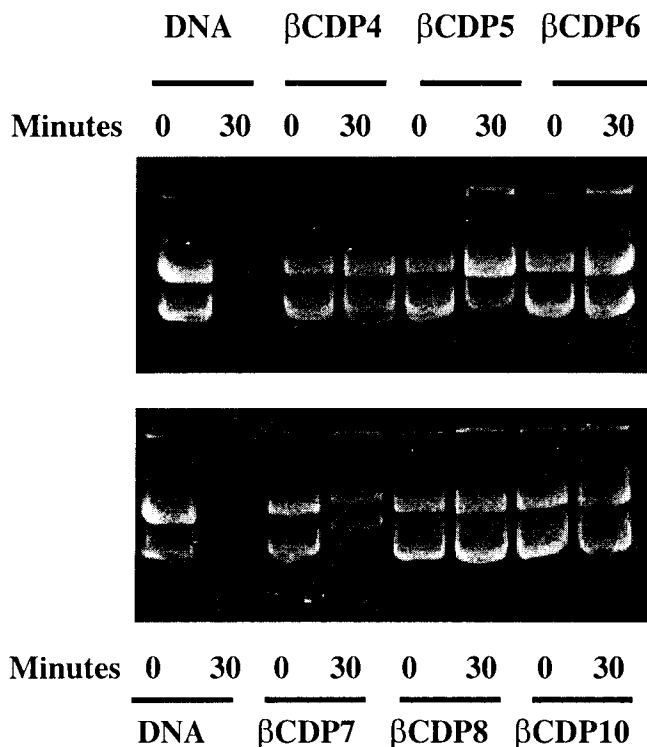


**Figure 3.5. DNase protection of plasmid DNA by  $\beta$ CDP complexation.**

Polyplexes of DNA complexed with the various  $\beta$ CDPs were incubated with an equal volume of fetal bovine serum for zero or thirty min.  $\beta$ CDPs were then displaced by SDS and DNA visualized by electrophoresis in an agarose gel.

**3.4.4. In Vitro Transfection and Toxicity of  $\beta$ CDP Polyplexes.** BHK-21 cells were plated in 24-well plates and transfected under serum-free conditions with 1  $\mu$ g of pGL3-CV complexed with the  $\beta$ CDPs at various charge ratios. Transfection efficiencies were determined by assaying for luciferase protein activity, with results reported in relative light units (RLUs). Several polymer to DNA charge ratios were tested (Fig. 3.6) and a

comparison of relative transfection efficiencies and cell survival are reported here for 50 +/- (Fig. 3.7). At this charge ratio, the transfection efficiencies have reached their maximum and the toxicity differences between the polymers become evident. The  $\beta$ CDP with six methylene units,  $\beta$ CDP6, gives the highest transfection efficiency:  $2.5 \times 10^{10}$  RLU/mg protein. The transfection efficiencies of all the polymers are normalized to the  $\beta$ CDP6 transfection achieved at 50 +/- and reported as a fraction of  $\beta$ CDP6 transfection (Fig. 3.7).  $\beta$ CDP7 and  $\beta$ CDP8 transfected at 50% and 64%, respectively, of the  $\beta$ CDP6 levels while  $\beta$ CDP4,  $\beta$ CDP5, and  $\beta$ CDP10 compared even less favorably at 22%, 6%, and 10%, respectively.

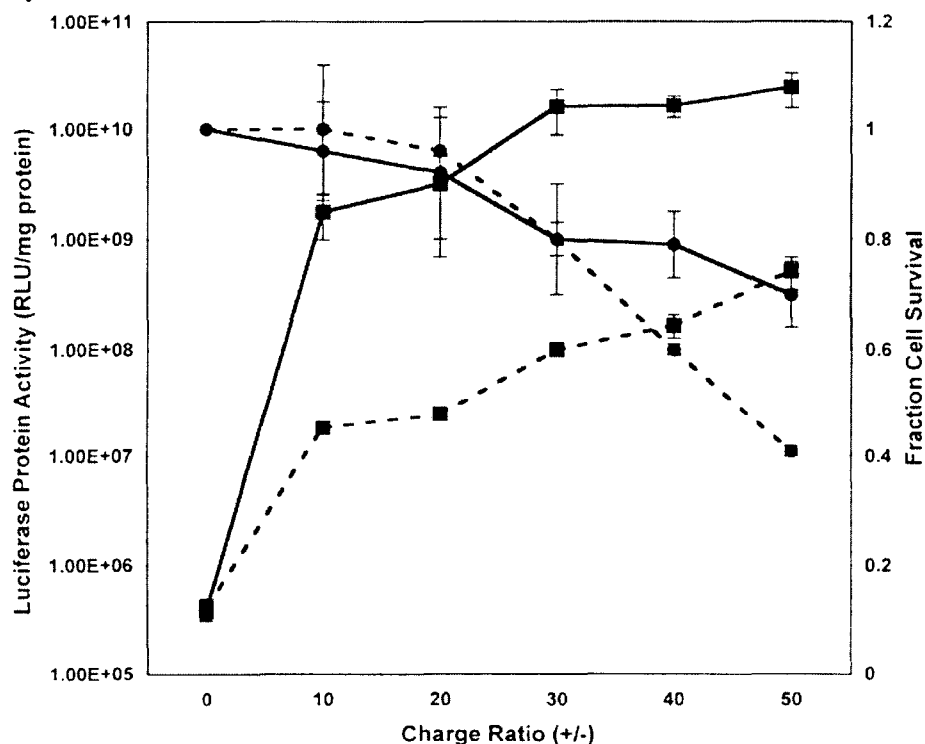


**Figure 3.6. Transfection and toxicity of  $\beta$ CDP5 and  $\beta$ CDP6 to BHK-21** Transfection efficiencies (■) and cell survival (●) for BHK-21 cells transfected with 1  $\mu$ g of pGL3-CV complexed with  $\beta$ CDP5 (dashed lines) and  $\beta$ CDP6 (solid lines) at charge ratios ranging from 10 to 50 +/- . Luciferase protein activity is reported as relative light units (RLU) per mg of total cellular protein, as determined by Lowry protein assay. Cell survival was calculated by dividing cellular protein levels of transfected cells by untransfected cells. Data are reported as the mean  $\pm$ SD of three samples.

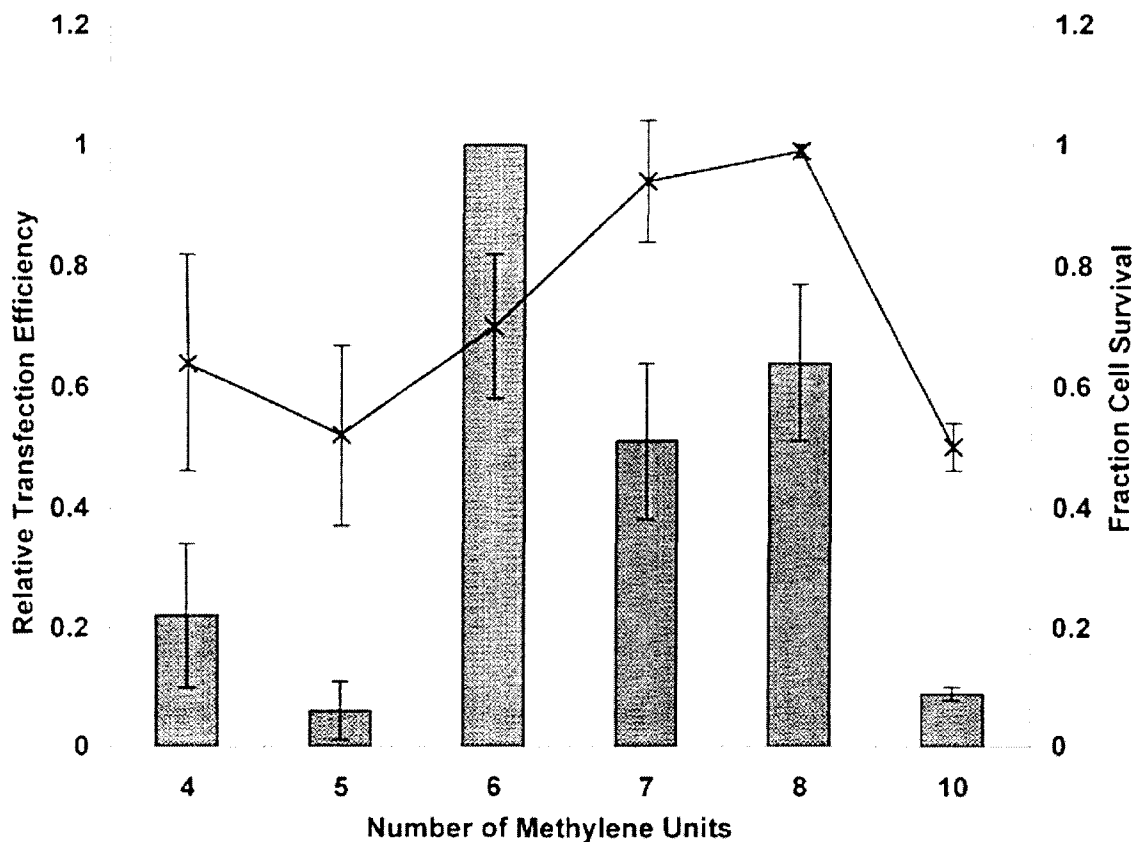


**Figure 3.7. Comparison of transfection and toxicity of various  $\beta$ CDP-based polyplexes.**

A comparison of luciferase transfection and cell survival for  $\beta$ CDP-based polyplexes at 50 +/- charge ratios. The data reported are the mean  $\pm$  S.D. of three experiments, each performed in triplicate. Transfection results for the different polymers are normalized with the average transfection achieved by  $\beta$ CDP6-based polyplexes for each experiment. Cell survival (X) was determined by assaying for total protein concentrations and normalizing each sample with protein levels for untransfected cells.

The toxicity of the  $\beta$ CDPs associated with the transfections at 50 +/- was measured by determining the total protein concentration in cell lysates 48 h after transfection and comparing with protein levels of untransfected cells. The fraction cell survival in the presence of the polyfection mixture was also dependent on comonomer B length (Fig. 3.7). No toxicity was observed for  $\beta$ CDP8. However, toxicity in general increased for all comonomer B lengths differing from that used in  $\beta$ CDP8.

The  $IC_{50}$ s of the  $\beta$ CDPs to BHK-21 cells were determined by plating the cells in 96-well plates, exposing the polymers to the cells in serial dilutions for 24 h and monitoring

cell viability by the MTT assay. The polymer  $IC_{50}$ s show the same trend as the toxicities associated with polyplex transfection (Fig. 3.8).  $\beta$ CDP8 had the highest  $IC_{50}$  (2200  $\mu$ M, reported as cyclodextrin concentration), followed in order of decreasing  $IC_{50}$ s by  $\beta$ CDP7 (1800  $\mu$ M),  $\beta$ CDP6 (1100  $\mu$ M),  $\beta$ CDP4 (380  $\mu$ M),  $\beta$ CDP5 (350  $\mu$ M) and  $\beta$ CDP10 (330  $\mu$ M).

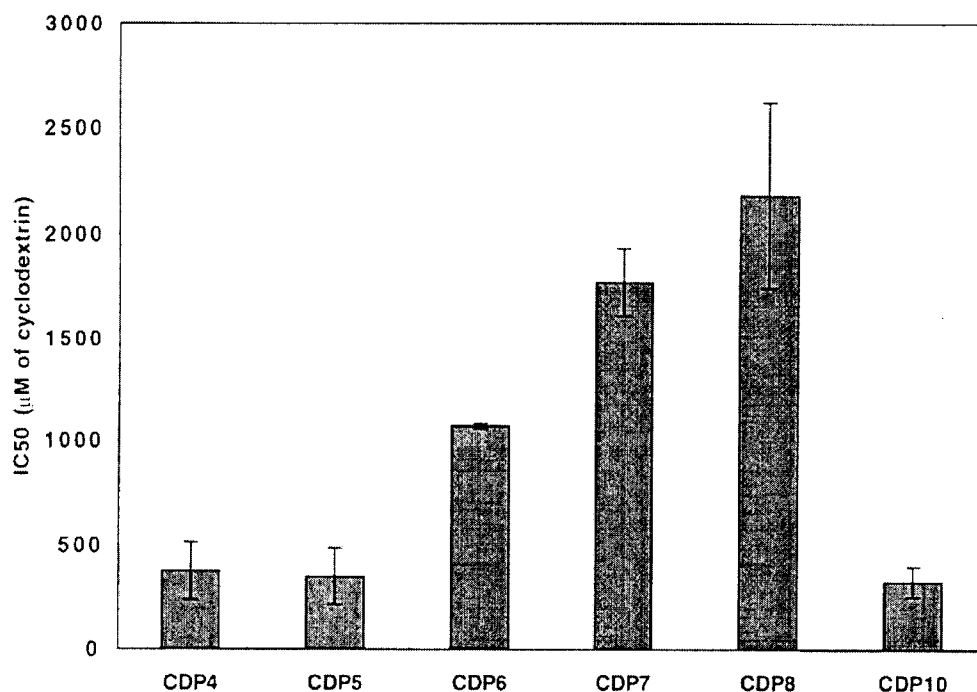


**Figure 3.8.**  $IC_{50}$ s of  $\beta$ CDPs to BHK-21 cells.

$\beta$ CDPs were added in serial dilutions to BHK-21 cells plated in 96-well plates. Cell viability was determined 24 h after polymer exposure by MTT assay. The  $IC_{50}$ s, reported as cyclodextrin concentration, were determined by interpolation on a best-fit line and are reported as the mean  $\pm$  S.D. for three replicates.

Polyamide polymers were synthesized by the condensation of dimethylsuberimidate (DMS, comonomer B with 6 methylene units) with hexylmethyldiamine or 1,9 diamnononane to give C6-C6 polyamide and C9-C6 polyamide, respectively. The  $IC_{50}$ s of the polyamide polymers to BHK-21 cells were

determined to be 4.6  $\mu\text{M}$  (reported per repeat unit) for C6-C6 polyamidine and 34.0  $\mu\text{M}$  for C9-C6 polyamidine.

**3.4.5. Polymer Displacement by Heparan Sulfate.** Polyplexes can be unpackaged by the addition of an anionic competitor such as heparan sulfate to bind to the cationic polymer and release the DNA (19). The relative binding constants of the  $\beta\text{CDPs}$  were determined by complexing the polymers with plasmid DNA at a 20 +/- charge ratio and then adding increasing amounts of heparan sulfate. The solutions were loaded onto an ethidium bromide-containing agarose gel and electrophoresed. Complexed DNA remained in the loading well. Successful polymer displacement by heparan sulfate released the DNA, that migrated in the electric field and was visualized by ethidium bromide intercalation. A comparison of the amount of heparan sulfate required to release the DNA from the  $\beta\text{CDPs}$  reflected the relative binding constants.  $\beta\text{CDP6}$  demonstrated the highest DNA binding constant, requiring the addition of 22  $\mu\text{g}$  of heparan sulfate before any DNA release could be observed (Fig. 3.9). 14  $\mu\text{g}$  of heparan sulfate were necessary to displace  $\beta\text{CDP4}$  while 16  $\mu\text{g}$  were required to displace  $\beta\text{CDP5}$ . The polymers with comonomer B longer than 6 methylene units showed a different behavior. For  $\beta\text{CDP7}$ ,  $\beta\text{CDP8}$  and  $\beta\text{CDP10}$ , the addition of heparan sulfate, even as low as 6  $\mu\text{g}$ , resulted in the visualization of some uncomplexed DNA. For  $\beta\text{CDP8}$  and  $\beta\text{CDP10}$ , the DNA release remains only partial, even with the addition of 32  $\mu\text{g}$  of heparan sulfate.

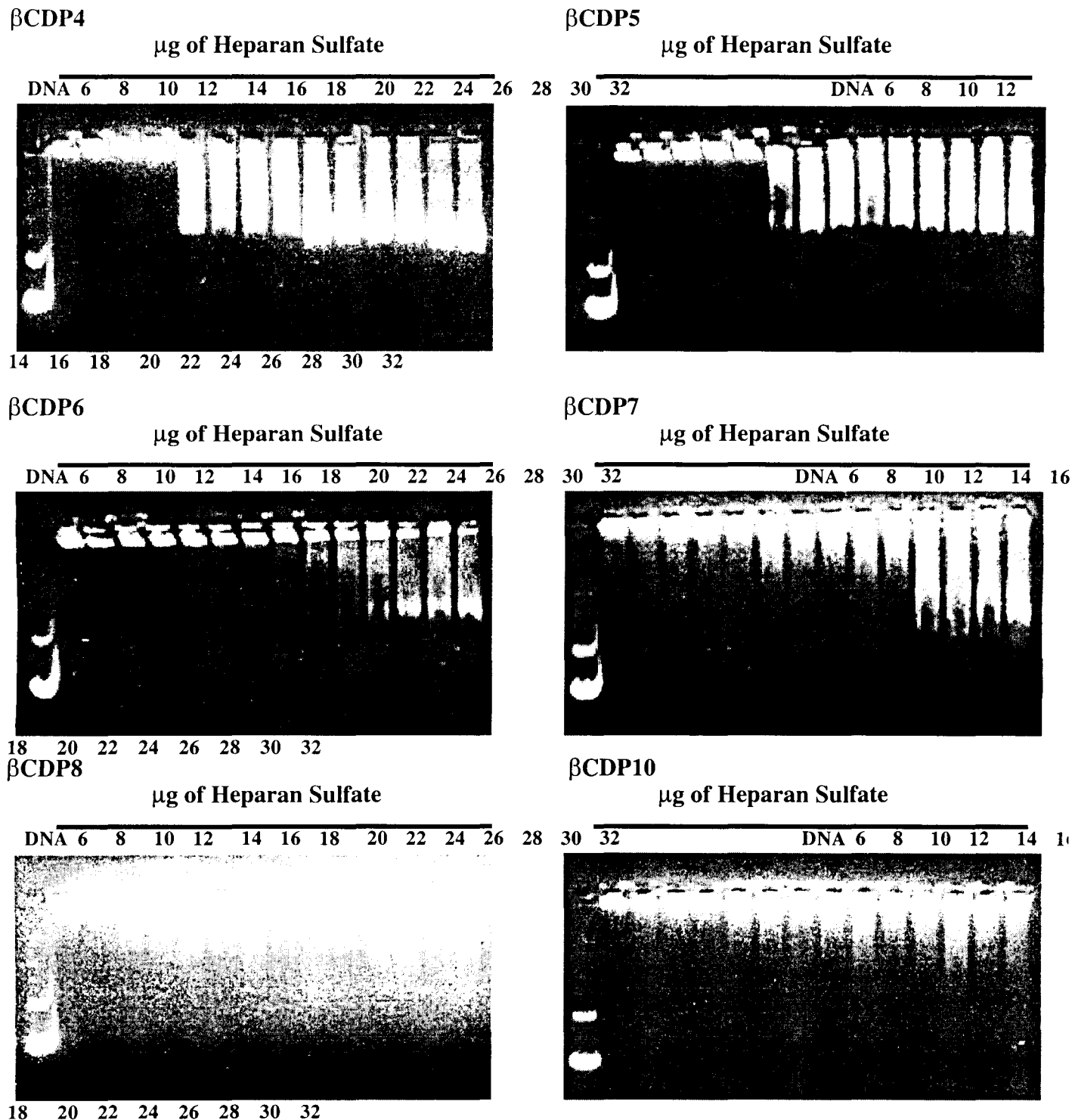


**Figure 3.9. Determination of relative binding constants by heparan sulfate displacement.**

The amount of heparan sulfate (in  $\mu$ g) required to free DNA from  $\beta$ CDP-based polyplexes (prepared with 1  $\mu$ g of DNA at 20 +/-). The uncomplexed and freed DNA was visualized by ethidium bromide in an agarose gel.

### 3.5. DISCUSSION

The objective of this study is to investigate the structure-property relationships between a family of  $\beta$ -cyclodextrin containing, cationic polymers and their interaction with and ability to deliver to cells plasmid DNA. In order to accomplish these goals a series of  $\beta$ CDPs were prepared using comonomer Bs with 4,5,6,7,8, and 10 methylene units. The polymer yields were proportional to the comonomer B length with  $\beta$ CDP10 $\approx$   $\beta$ CDP8 >  $\beta$ CDP7 >  $\beta$ CDP6 >  $\beta$ CDP5 >  $\beta$ CDP4. Higher reaction yield with longer diimidate **4a-f** linkers was also noted by Denkinger et al. (17) who crosslinked poly(allylamine) with esters of diimidic acids such as those used here (**4a-f**) to form hydrogels. The  $\beta$ CDP molecular weights, detected by both static light scattering and end group analysis, ranged from 5800 to 7600, corresponding to a degree of polymerization of 4 to 5 and giving 8 to 10 cationic charges per chain. Therefore, differences in polymer performance should be a result of polymer structure and not molecular weight since they all have similar molecular weights and polydispersities.

The  $\beta$ CDPs form polyplexes with DNA by rapid self-assembly in aqueous solutions. Polyplexes formed in water are relatively monodisperse and uniform in size, as evidenced by DLS and TEM. The size of the polyplexes depends on the formulation conditions, as has been described previously by Duguid et al. (20). Particles formed with  $\beta$ CDP6 have an average diameter of 60 nm at 2  $\mu$ g/mL final DNA concentration but an average diameter of 130 nm at 50  $\mu$ g/mL as measured by DLS. The latter particles were used for the DLS, TEM and transfection studies presented here. Electron micrographs of  $\beta$ CDP6-based polyplexes show particles smaller than 100 nm in diameter. DLS measurements, due to calculations that are based on weighting by particle light scattering intensity, are biased toward larger particles. DLS also determines the hydrodynamic diameter and hence DLS size measurements of particles are larger than the sizes of the polyplexes pictured by electron micrographs.

Polyplexes formed from  $\beta$ CDP4,  $\beta$ CDP5 and  $\beta$ CDP10 are larger in diameter than polyplexes formed from the other  $\beta$ CDPs (Fig. 3.3). These larger particles transfected cultured cells less efficiently (Figs. 3.6,3.7). A correlation between particle size and transfection efficiency has been described for other systems (6), although it is normally observed that the larger the particle size, the greater the transfection. Here, the differences in the particle size are not large and likely not the reason for the large differences in transfection. In addition, the cationic polyplexes are prone to aggregation under physiological salt conditions. Thus, the variations in particle size may be indicative of differences in the polymer-DNA binding interactions rather than having direct effects on particle uptake.

For effective gene delivery, the polycation must protect the DNA from nuclease activity. While  $\beta$ CDP4,  $\beta$ CDP6,  $\beta$ CDP8, and  $\beta$ CDP10 completely protected plasmid DNA from DNase degradation,  $\beta$ CDP5 and  $\beta$ CDP7 offered only partial protection (Fig. 3.5). Yoshikawa et al. observed a difference in binding of various methylene diamines to DNA; however, they noticed greater DNA condensation with odd numbers of methylene units and larger particles with even numbers of methylene units (21). Thus, small differences in charge separation can produce dramatic effects. It is interesting to note that the two  $\beta$ CDPs with odd numbers of methylenes are the only ones to not completely protect the DNA.

All of the synthesized  $\beta$ CDPs are able to transfect BHK-21 cells, although with varying efficiencies. Transfection increases with charge ratios up to 50 +/- (Fig. 3.6). This high optimal charge ratio is probably due to the short nature of the polymers, a phenomenon also noticed by Plank et al. (12) for short peptides. The transfection profiles as a function of polymer to DNA charge ratio are similar for all of the polymers; however, the magnitudes of the profiles differ greatly between polymers. In order to illustrate differences in transfection and toxicity, we chose to compare delivery performance between the polymers at 50 +/-, as displayed in Fig. 3.7. The highest transfection efficiency, as determined by luciferase protein activity, is consistently achieved by the  $\beta$ CDP6-based polyplexes. The

transfection efficiency is found to be dependent on the comonomer B length. For example, when compared to  $\beta$ CDP6, luciferase transfections with  $\beta$ CDP5 result in a 20-fold reduction of luciferase protein activity, while the difference between the two comonomer B lengths is only 1.8 Å. Therefore, a few Å change in comonomer B length reduces the transfection by up to one order of magnitude (Fig. 3.7).

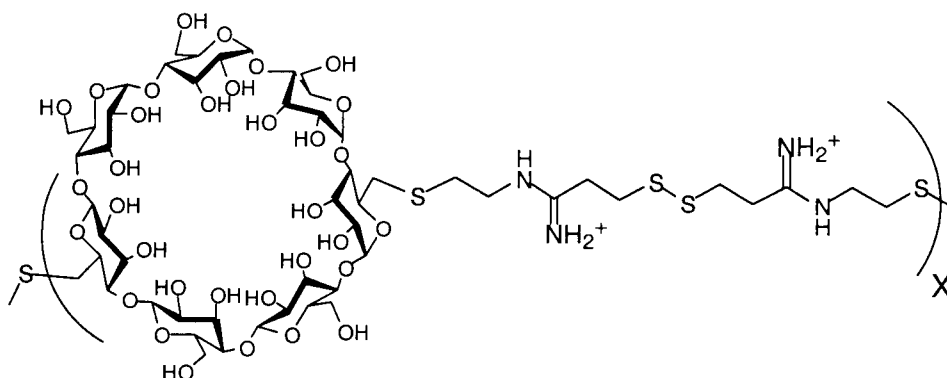
A possible rationalization for the large decrease in transfection is that the spacing between the cationic amidine groups in  $\beta$ CDP6 is optimal for DNA binding. In an attempt to study  $\beta$ CDP-DNA interactions, polymer binding kinetics were monitored via a quartz crystal microbalance and DNA condensation kinetics by DLS. It was found that binding and condensation were complete within one second for all the polymers. Because of the speed of these processes, the procedures used here were unable to provide useful information. Thus, only relative binding constants were determined by heparan sulfate displacement. The amount of heparan sulfate required to release DNA from the polyplexes should be related to the DNA binding constant of the displaced polymer. The heparan sulfate displacement studies (Fig. 3.9) reveal that  $\beta$ CDP6 has a significantly higher binding constant than the other  $\beta$ CDPs. The polymers synthesized from shorter comonomer Bs ( $\beta$ CDP4,  $\beta$ CDP5, and  $\beta$ CDP6) also seem to bind differently from  $\beta$ CDP7,  $\beta$ CDP8, and  $\beta$ CDP10. The former set of polymers bound tightly to the DNA at low heparan sulfate concentrations but are mostly displaced from the DNA at a critical heparan sulfate concentration that increases with increasing distance between the charges. The latter polymers are slightly displaced from the DNA even at low heparan sulfate concentrations, with a higher intensity of free DNA visualized with increased heparan sulfate concentration. Therefore, the DNA binding characteristic of  $\beta$ CDP6 likely contributes to its gene delivery properties.

The toxicity of the  $\beta$ CDPs also depends on comonomer B length.  $\beta$ CDP8 reveals no cell death under the tested transfection conditions while  $\beta$ CDP7 is only slightly toxic. Because the comonomer Bs for these polymers were synthesized in our lab while

comonomer Bs for  $\beta$ CDP4,  $\beta$ CDP5, and  $\beta$ CDP6 were purchased from commercial sources, it is possible that an impurity in the commercial samples could be the origin of toxicity. The  $\beta$ CDP6 was therefore synthesized from three different comonomer Bs: (i) purchased DMS, (ii) purchased and recrystallized DMS, and (iii) freshly synthesized in our labs DMS. The transfection and toxicity of the three  $\beta$ CDP6s were very similar, thus confirming cell toxicity to be caused by the  $\beta$ CDPs and not reaction impurities.

Although no toxicity was detected for  $\beta$ CDP8 at a charge ratio of 50 +/-, cell death was observed for the other  $\beta$ CDPs at charge ratios above 20 +/- with the toxicity differences between the polymers becoming evident by 50 +/- (Fig. 3.7). At this high charge ratio, most of the polymer is free in solution and not bound to DNA. The noted toxicity is therefore probably due mostly to the free polymer in solution. The  $IC_{50}$ s of  $\beta$ CDPs alone to BHK-21 cells were determined by the MTT assay. The trends in the  $IC_{50}$ s for the  $\beta$ CDPs correlated nicely with the toxicities detected at the 50 +/- transfection conditions (Fig. 3.8). Again, the  $IC_{50}$ s cover nearly an order of magnitude range. The  $IC_{50}$ s increase as the charge density decreases in going from  $\beta$ CDP4 to  $\beta$ CDP8. Additionally, as the comonomer B lengthens, the corresponding polymer becomes less soluble. Therefore, it is possible that the lower solubilities may contribute to the toxicity observed for  $\beta$ CDP10. If such is the case, then there is a trade-off between charge density and solubility and for the polymers investigated here, the  $\beta$ CDP8 appears to be the optimal material with regard to toxicity.

Wadhwa et al. (22) and Fisher et al. (8) reported reduced cytotoxicity for low molecular weight fractions of PLL and PEI, respectively. Although the  $\beta$ CDPs presented here are low molecular weight polymers, we tested the cytotoxicity of a  $\beta$ CDP capable of being further degraded in the cell. To this end, we synthesized a disulfide-containing  $\beta$ CDP ( $\beta$ CDP-Disulfide), as reported previously (13).



**$\beta$ CDP-Disulfide**

The disulfide was incorporated in a comonomer of length 11.9 Å between the charges; that is, 0.9Å longer than  $\beta$ CDP6 but shorter than  $\beta$ CDP7.  $\beta$ CDP-Disulfide should be reduced to monomeric units in the cellular environment. The  $\beta$ CDP-Disulfide polymer was able to bind to DNA at the same charge ratio as the  $\beta$ CDP6 and transfect cells with efficiencies between those observed for  $\beta$ CDP6 and  $\beta$ CDP7. However, the toxicity of  $\beta$ CDP-Disulfide associated with these transfections was higher than  $\beta$ CDP6 toxicity (62% cell survival versus 70%). These results indicate that the  $\beta$ CDP toxicity will not be decreased further with a polymer that can be reduced to molecules within the cell.

The idea behind the synthesis of the  $\beta$ CDPs was to ascertain whether polymers incorporating relatively nontoxic building units, i.e., cyclodextrins, could maintain the low toxicity of the cyclodextrin while simultaneously providing the properties necessary for gene delivery (13). The influence of cyclodextrin incorporation in the polymer backbone was tested by comparing  $\beta$ CDP polymer behavior to those having methylene diamines as comonomer As rather than CD-dicysteamine. Because the non-cyclodextrin polymers were also synthesized by an A-B condensation, the degree of polymerization was comparable to those achieved for  $\beta$ CDPs (degree of polymerization of 5 for C6-C6 polyamidine and 8 for C9-C6 polyamidine). These polyamidine polymers are able to bind to plasmid DNA by

charge ratios of 1.5 +/-, form polyplexes with hydrodynamic diameters of ~140 nm, and transfect cultured cells as well as the  $\beta$ CDPs. However, their  $IC_{50}$ s are 2-3 orders of magnitude lower than the  $IC_{50}$ s for  $\beta$ CDP8. These results indicate that cyclodextrin incorporation into the backbone of the cationic polymers greatly reduces the polymer toxicity.

Based on the in vitro results, the  $\beta$ CDP6 polymer was chosen for in vivo toxicity testing. This polymer gives the highest transfection efficiency with a reasonably high  $IC_{50}$ . Groupings of five mice were injected intravenously with a single dose of  $\beta$ CDP6 ranging from 2-200 mg/kg. No toxicity was observed at 100 mg/kg and the  $LD_{40}$  was found to be 200 mg/kg. Previously, we have tested a disulfide-containing  $\beta$ CDP for in vivo toxicity, and determined it to be well tolerated at 200 mg/kg (13). However, the previous disulfide-containing  $\beta$ CDP displayed lower DNA binding affinity and transfection efficiency than the  $\beta$ CDP6. The in vivo toxicity parallels the in vitro studies in that increased charge density appears to yield higher toxicities. Thus, the in vivo toxicity limit should increase when the  $\beta$ CDP are complexed with DNA.

Here, it is demonstrated that the structure of the  $\beta$ CDPs critically determines performance in DNA delivery and cell toxicity. The difference of a few Å in comonomer B length can affect transfection and polymer  $IC_{50}$  values by orders of magnitude. In addition, the incorporation of  $\beta$ -cyclodextrin in the polymer backbone is shown to significantly decrease polymer toxicity. The low in vitro and in vivo toxicity of these  $\beta$ CDPs make them promising and attractive agents for in vivo gene delivery applications.

### 3.6. LITERATURE CITED

- (1) Felgner, P. L., Barenholz, Y., Behr, J. P., Cheng, S. H., Cullis, P., Huang, L., Jessee, J. A., Seymour, L., Szoka, F., Thierry, A. R., Wagner, E. Wu, G. (1997) Nomenclature for synthetic gene delivery systems. *Hum. Gene Ther.* 8, 511-512.
- (2) Wu, G. Y. Wu, C. H. (1987) Receptor-mediated in vitro gene transformation by a soluble DNA carrier system. *J. Biol. Chem.* 262, 4429-4432.
- (3) Leong, K. W., Mao, H.-Q., Truong-Le, V. L., Roy, K., Walsh, S. M. August, J. T. (1998) DNA-Polycation Nanospheres as Non-viral Gene Delivery Vehicles. *J. Controlled Release* 53, 183-193.
- (4) Haensler, J. Szoka, F. C. (1993) Polyamidoamine cascade polymers mediate efficient transfection of cells in culture. *Bioconjugate Chem.* 4, 372-379.
- (5) Boussif, O., Lezoualch, F., Zanta, M. A., Mergny, M. D., Scherman, D., Demeneix, B. Behr, J.-P. (1995) A versatile vector for gene and oligonucleotide transfer into cells in culture and in vivo: Polyethylenimine. *Proc. Natl. Acad. Sci. U.S.A.* 92, 7297-7301.
- (6) Smedt, S. C. D., Demeester, J. Hennink, W. E. (2000) Cationic Polymer Based Gene Delivery Systems. *Pharm. Res.* 17, 113-126.
- (7) Ziady, A., Ferkol, T., Dawson, D., Perlmutter, D. Davis, P. (1999) Chain length of the polylysine in receptor-targeted gene transfer complexes affects duration of reporter gene expression both in vitro and in vivo. *J. Biol. Chem.* 274, 4908-4916.
- (8) Fisher, D., Bieber, T., Li, Y., Elsasser, H. Kissel, T. (1999) A novel non-viral vector for DNA delivery based on low molecular weight, branched polyethylenimine: Effect of molecular weight on transfection efficiency and cytotoxicity. *Pharm. Res.* 16, 1273-1279.
- (9) Godbey, W., Wu, K. Mikos, A. (1999) Size matters: Molecular weight affects the efficiency of poly(ethylenimine) as a gene delivery vehicle. *J. Biomed. Mat. Res.* 45, 268-275.

- (10) Remy, J.-S., Abdallah, P., Zanta, M. A., Boussif, O., Behr, J.-P. Demeneix, B. (1998) Gene transfer with lipospermines and polyethylenimines. *Adv. Drug Deliv. Rev.* 30, 85-95.
- (11) Malik, N., Wiwattanapatapee, R., Klopsch, R., Lorenz, K., Frey, H., Weener, J., Meijer, E., Paulus, W. Duncan, R. (2000) Dendrimers: Relationship between structure and biocompatibility in vitro, and preliminary studies on the biodistribution of I-125-labelled polyamidoamine dendrimers in vivo. *J. Controlled Release* 65, 133-148.
- (12) Plank, C., Tang, M. X., Wolfe, A. R. Szoka, F. C. (1999) Branched Cationic Peptides for Gene Delivery: Role of Type and Number of Cationic Residues in Formation and in Vitro Activity of DNA Polyplexes. *Hum. Gene Ther.* 10, 319-332.
- (13) Gonzalez, H., Hwang, S. J. Davis, M. E. (1999) New class of polymers for the delivery of macromolecular therapeutics. *Bioconjugate Chem.* 10, 1068-1074.
- (14) Tabushi, I., Yamamura, K. Nabeshima, T. (1984) Characterization of regiospecific A,C-and A,D-disulfonate capping of  $\beta$ -Cyclodextrin. Capping as an Efficient Production Technique. *J. Am. Chem. Soc.* 106, 5267-5270.
- (15) Tabushi, I. Kuroda, Y. (1984) Bis(histamino)cyclodextrin-Zn-imidazole complex as an artificial carbonic anhydrase. *J. Am. Chem. Soc.* 106, 4580-4584.
- (16) Hermanson, G. T. *Bioconjugate Techniques* Academic Press: Rockford, Illinois, 1996.
- (17) Denkinger, P., Rey, A. W, B. (1989) Crosslinking of Poly(allylamine) with esters of diimidic acids in aqueous-media. *Makromol. Chem., Rapid Commun.* 10, 675-681.
- (18) Gao, X. Huang, L. (1996) Potentiation of Cationic Liposome-Mediated Gene Delivery by Polycations. *Biochem.* 35, 1027-1036.
- (19) Ruponen, M., Yla-Herttuala, S. Urtti, A. (1999) Interactions of polymeric and liposomal gene delivery systems with extracellular glycosaminoglycans: physicochemical and transfection studies. *Biochem. Biophys. Acta* 1415, 331-341.

- (20) Duguid, J., Li, C., Shi, M., Logan, M., Alila, H., Rolland, A., Tomlinson, E., Sparrow, J. Smith, L. (1998) A physicochemical approach for predicting the effectiveness of peptide-based gene delivery systems for use in plasmid-based gene therapy. *Biophys. J.* 74, 2802-2814.
- (21) Yoshikawa, Y. Yoshikawa, K. (1995) Diaminoalkanes with an odd number of carbon atoms induce compaction of a single double-stranded DNA chain. *FEBS Lett.* 361, 277-281.
- (22) Wadhwa, M. S., Collard, W. T., Adami, R. C., McKenzie, D. L. Rice, K. G. (1997) Peptide-mediated gene delivery: Influence of peptide structure on gene expression. *Bioconjugate Chem.* 8, 81-88.

## Chapter 4

### Increased Transfection by Histidylation of a Cationic Cyclodextrin-based Polymer

#### 4.1. ABSTRACT

Cationic, cyclodextrin-based polymers (CDPs) are capable of efficient DNA delivery to cells but remain largely trapped in endosomal vesicles. The goal of this work is to synthesize a pH-sensitive CDP capable of enhancing endosomal escape. One approach to this problem is to attach a weak base to the polymer that has a sufficient pKa to allow for protonation under acidic conditions of the endosome in order to buffer the pH, thereby delaying the transition to lysosomes (subsequent degradation of endocytosed material). Histidine contains an imidazole group that is protonated below pH 6.0, and was conjugated to the amine endgroups of a CDP,  $\beta$ CDP6, to form histidylated  $\beta$ CDP6 (Hist-CDP6). This polymer is capable of self-assembling with and condensing DNA, to form uniform, positively-charged particles above charge ratios of 2 +/- . The transfection efficiency of CDP6 is increased 20-fold by histidylation with no increase in cell toxicity. Visualization by confocal microscopy revealed greater intracellular accumulation of Hist-CDP6-delivered DNA than CDP6-delivered DNA. Hist-CDP6 transfection in the presence of chloroquine revealed no synergistic effect. Therefore, Hist-CDP6 is capable of increasing transfection efficiency in cultured cells most likely by buffering the endosomal pH and delaying DNA degradation in lysosomes.

## 4.2. INTRODUCTION

The potential of synthetic gene delivery systems to bypass the major limitations of viral vectors has spawned a rapidly growing field of research. In order to have efficient delivery ability, lipoplexes and polyplexes must be able to overcome cellular barriers: cell, endosome, and nuclear membranes. When formulated with a net positive charge, lipoplexes and polyplexes are readily taken into cells by interaction with cell surface glycoproteins and endocytosis (1, 2). The attachment of a targeting ligand such as galactose or folate results in receptor-mediated uptake of complexes (3-7). Both methods result in internalization and accumulation of complexes into cellular vesicles. Unless released, these complexes are shuttled to lysosomes and rapidly degraded.

Felgner et al. quantitated the uptake of fluorescently labeled plasmids into cultured cells by cationic lipofection and found that only 2% of intracellular plasmids are found in the nucleus (8). In our lab, microscopy studies of fluorescently-labeled plasmids transfected by cationic cyclodextrin-based polymers (CDPs) reveal punctate staining indicative of endosomal trapping. Curiel et al. noted a 3 order of magnitude increase in reporter gene activity by including adenovirus in transferrin/poly(L)lysine (PLL) transfection media. Adenovirus mediate endosomal disruption and polyplex release (9). Clearly, endosomal release is a major limitation in non-viral delivery.

Most polyplexes and lipoplexes are internalized by cells into vesicles that fuse with endosomes. As the endosomes mature from early endosomes to late endosomes, the pH of the vesicles rapidly drops due to ATP-dependent proton pumps in the membrane. Most endosomal material is then transferred to lysosomes and degraded by nucleases and proteases (10). Viruses escape from the endosome by taking advantage of this pH drop. For example, the adenovirus capsid undergoes a change in conformation at the acidic conditions, allowing escape of the virus into the cytoplasm (11). Some lipoplexes include in their formulation a pH-sensitive lipid such as DOPE, that causes the lipoplexes

to undergo a phase transition to hexagonal arrays at the low pH, and thus destabilizing the endosomal membrane for releasing DNA into the cytosol (12). Amphiphilic peptides that become fusogenic at acid conditions have been used to increase transfection efficiencies of cationic polymers (13-16). Cationic polymers such as polyethylenimine and pAMAM dendrimers contain multiple secondary amines with  $pK_a \sim 6$  (17,18). These secondary amines protonate as the endosomal pH drops, thus buffering the pH and protecting endosome material from lysosomal degradation. In addition, it is hypothesized that influx of water into the endosome results in osmotic swelling and eventually rupture.

The imidazole group in histidine also has a  $pK_a$  around 6.0 and has been studied for its endosomal buffering abilities. Poly(L)histidine (PLH) initiates fusion of negatively-charge liposomes at acidic conditions (19,20). However, PLH is neutral at pH 7.4 and does not bind to DNA at physiological conditions. Investigations with histidylated PLL reveal substantial increase in transfections over PLL (21,22).

In this work, conjugation of histidine to a previously described cationic cyclodextrin-based polymer ( $\beta$ CDP6, (23)) to produce a pH-sensitive derivative polymer is carried out. Here, it is shown that (i) the resulting polymer remains water soluble, (ii) it is able to bind and condense DNA, and (iii) the formed polyplexes transfect cultured cells more effectively than those made with the parent polymer. It is also demonstrated that the histidine moieties act as a buffer in the endosome to increase transfection efficiencies.

### **4.3. MATERIALS AND METHODS**

#### **4.3.1. Polymer Synthesis.**

*$\beta$ -cyclodextrin-DMS.*  $\beta$ -cyclodextrin-DMS ( $\beta$ CDP6) was prepared by the polymerization of a difunctionalized  $\beta$ -CD monomer (A) with a difunctionalized comonomer (B) to give an ABAB product as described previously (23). In brief,  $\beta$ -CD dicysteamine (1.193 g, 866  $\mu$ mol) and dimethyl suberimidate (DMS, 866  $\mu$ mol, Pierce, Rockford, Illinois) were

dissolved in 2.3 mL of 0.5 M Na<sub>2</sub>CO<sub>3</sub> and stirred overnight at room temperature. The pH of the resulting solution was brought below 5.0 by the addition of 1 M HCl and dialyzed extensively against dH<sub>2</sub>O in a MWCO 3500 dialysis membrane (Pierce) for 24 hours. The dialyzed solution was lyophilized to dryness to give 530 mg (38.4% yield).

*Synthesis of Histidylated βCDP6 (Hist-CDP6).* βCDP6 (57.2 mg, 9.9 μmol) was dissolved in 1.0 mL of 50 mM NaHCO<sub>3</sub> and reacted for 12 hours with a solution of Fmoc-His(trt)-OH (123 mg, 200 μmol, Novabiochem), DCC (40 mg, 200 μmol, Aldrich) and 1-HOBt (2.5 mg, 20 μmol, Aldrich) dissolved in 4.0 mL THF. The solvent was removed in vacuo and the trityl protecting groups were cleaved by adding trifluoroacetic acid/water/triisopropylsilane (95:2.5:2.5) and mixing for one hour at room temperature. The solvent was removed in vacuo and the residue was washed several times with ether before lyophilizing. The histidine conjugation was 70% (determined by TNBS assay to quantify the amount of unreacted polymer endgroups). The Fmoc protecting groups were removed by adding 20% piperidine in DMF and stirring for 20 minutes before removing the solvent under reduced pressure. The remaining solid was redissolved in water, centrifuged to remove the precipitated Fmoc, dialyzed extensively, and lyophilized to yield 23.2 mg (40%).

#### **4.3.2. Polyplexes.**

*Plasmids and oligonucleotides.* Plasmid pGL3-CV (Promega, Madison, WI), containing the luciferase gene under the control of the SV40 promoter, was amplified by *Esheria coli* and purified using Qiagen's Endotoxin-free Megaprep kit (Valencia, CA). Fluorescein-labeled oligonucleotides (FITC-oligos) of approximately 50 bases were used. Rhodamine-labeled plasmids were purchased from Gene Therapy Systems (San Diego, CA) and used as received.

*Polyplex formation and characterization.* Polyplexes were prepared by mixing an equal volume of  $\beta$ CDP dissolved in dH<sub>2</sub>O with DNA (0.1 mg/mL in dH<sub>2</sub>O) at the appropriate charge ratios. The size and charge of particles were determined by dynamic light scattering and zeta potential measurements, respectively. Two  $\mu$ g of plasmid DNA were complexed with polymer at various charge ratios and diluted with the addition of 1.2 mL dH<sub>2</sub>O. Particle size and zeta potential were measured using a ZetaPals dynamic light scattering detector (Brookhaven Instruments Corporation, Holtsville, NY).

#### **4.3.3. Cells and Transfections.**

*Cells and cell culture.* BHK-21 cells were purchased from ATCC (Rockville, MD) and cultured in DMEM supplemented with 10% fetal bovine serum, 100 units/mL penicillin, 100  $\mu$ g/mL streptomycin, and 0.25  $\mu$ g/mL amphotericin in a humidified incubator operated at 37 °C and 5% CO<sub>2</sub>. Media and supplements were purchased from Gibco BRL (Gaithersburg, MD).

*Luciferase transfections.* BHK-21 cells were plated in 24-well plates at 50,000 cells/well and incubated for 24 hours at 37 °C. Media was removed from the cells prior to transfection and cells washed with PBS. Optimem (200  $\mu$ L per well, Gibco BRL) was added to the polyplexes, which were prepared as described above, and the entire transfection solution was added to the cells for four hours. After four hours, 800  $\mu$ L of complete media was added to each well. Media was changed 24 hours after transfection and cells were lysed 48 hours after transfection to assay for luciferase activity and cell survival as described previously (23).

*Flow cytometry analysis.* BHK-21 cells were plated in 6-well plates at 200,000 cells/well and incubated for 24 hours at 37 °C. 3  $\mu$ g of rhodamine-labeled EGFP plasmid were

complexed with  $\beta$ CDP6 or Hist-CDP6 at a 5 +/- charge ratio. Media was removed from the cells and cells washed with PBS. For transfection, one mL of Optimem was added to each polyplex solution and the entire solution transferred to the cells. The cells were incubated with the transfection mixture for four hours before another four mL of complete media was added to each well. 24 hours after transfection, the cells were collected by trypsinization and prepared for FACS analysis. Cells were washed twice in wash buffer (Hank's Balanced Salt Solution containing DNase and  $MgCl_2$ ) and resuspended in 500  $\mu$ L FACS buffer (Hank's Balanced Salt Solution, 2.5 mg/mL bovine serum albumin, 10  $\mu$ g/mL propidium iodide). FACS analysis was performed using a FACSCalibur flow cytometer (Becton Dickinson, San Jose, CA) and CellQuest software.

*Confocal Microscopy.* BHK-21 cells were plated on 22 mm glass coverslips in 6-well plates at  $2 \times 10^5$  cells/well. Cells were maintained at 37 °C for 24 hours before transfection. Transfection solutions were prepared by complexing 5  $\mu$ g of FITC-oligos with  $\beta$ CDP6 and Hist-CDP6 at charge ratios of 6, 8, and 10 +/- . To prepare the cells for transfection, media was removed from the cells and the cells were washed once with PBS. Serum-free media (Optimem, 1 mL,) was added to each transfection solution and the entire solution transferred to each well. The cells were incubated at 37 °C for another four hours before adding 4 mL of complete media to each well and incubating for another 20 hours at 37 °C. After the incubation, the cells were rinsed twice with PBS and fixed with 4% p-formaldehyde for 10 minutes. The cells were washed three times with PBS and then stained with 20  $\mu$ M DiI (Molecular Probes, Eugene, Oregon) in 0.32 M sucrose for 10 minutes. The cells were washed twice with 0.32 M sucrose and once with PBS. Coverslips were then removed from the wells and mounted on glass slides with Prolong Antifade reagent (Molecular Probes). After drying, the slides were analyzed with a Zeiss 310 Axiophot Upright confocal microscope (Caltech Biological Imaging Center) with 488 nm fluorescein excitation and 543 nm DiI excitation.

#### 4.4. RESULTS

**4.4.1. Histidylated  $\beta$ -cyclodextrin-DMS.** The amine endgroups of  $\beta$ CDP6 were substituted with protected histidine residues by DCC coupling with (Fmoc)-His(Trt)-OH. The trityl groups were removed after coupling and TNBS (reacts with primary amines) monitoring of the polymer endgroups revealed 70.0% conjugation. The  $\alpha$ -amino groups of the histidine residues were then deprotected to obtain histidylated  $\beta$ CDP6 (Hist-CDP6, Fig 4.1).

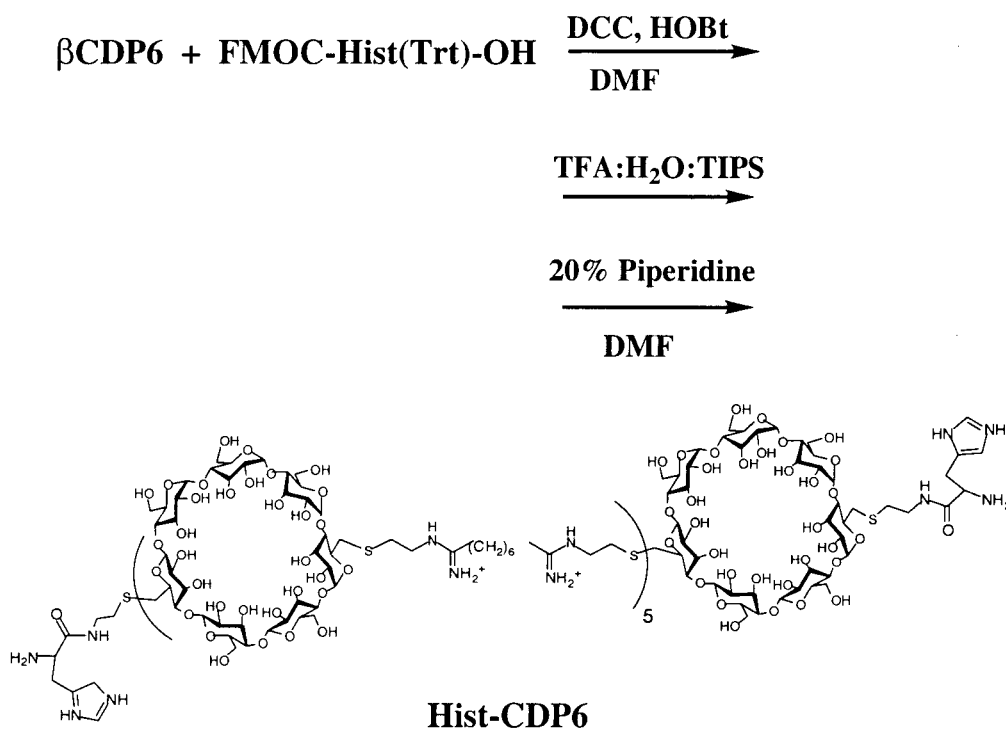


**Figure 4.1. Synthesis of Hist-CDP6.**

**4.4.2. Polyplex Formation.** The ability of Hist-CDP6 to bind to and condense plasmid DNA was determined by monitoring particle size and charge. 2  $\mu$ g of DNA in 20  $\mu$ L was mixed with an equal volume of solution containing Hist-CDP6 at various charge ratios.

The resulting solution was diluted for measurements. The hydrodynamic diameter was determined by dynamic light scattering and the particle mobility and charge assessed by zeta potential measurements (Fig 4.2). Neutral particles are formed at 2 +/- charge ratios, with corresponding diameters of 730 nm. These particles are not very stable and have gradually increasing diameters (evidenced by the larger S.D.). Stable particle sizes of around 200 nm in diameter were achieved above charge ratios of 4+/- . At this charge ratio, the particles have an average zeta potential of 27.3 mV.

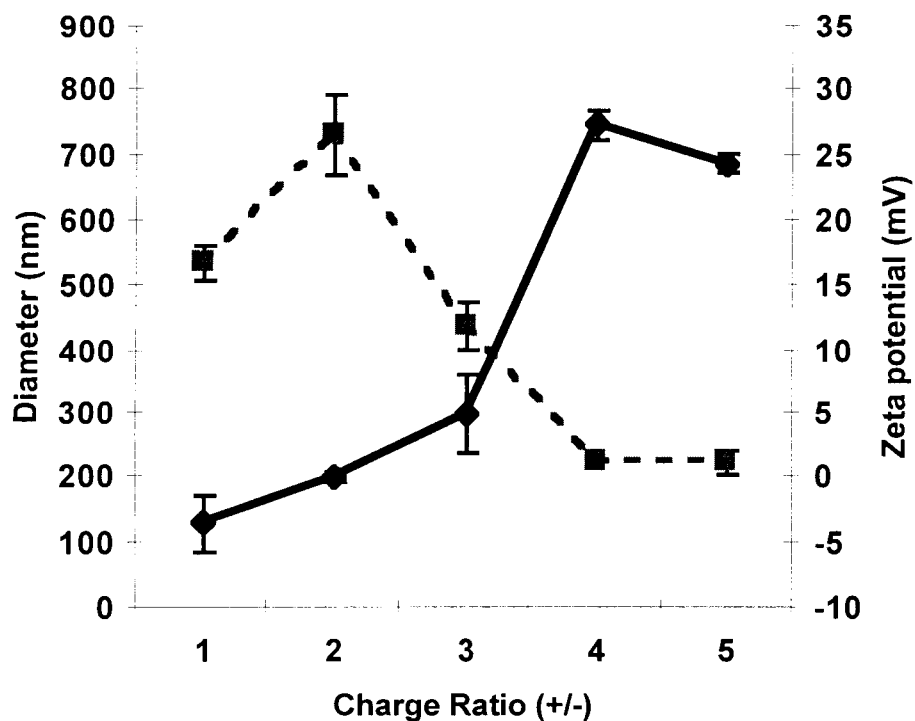


**Figure 4.2. Zeta potential and hydrodynamic diameter of Hist-CDP6 polyplexes.**

2  $\mu\text{g}$  of plasmid DNA in 20  $\mu\text{L}$  was mixed with an equal volume of Hist-CDP6 at various charge ratios. Zeta potential (solid line) and hydrodynamic diameter (dashed line) were determined by light scattering measurements. Results are presented as mean  $\pm$  standard deviation of three measurements.

**4.4.3. Transfection Ability of Hist-CDP6.** The ability of polyplexes formed from Hist-CDP6 to transfect cultured cells was determined by delivery of a luciferase reporter gene. BHK-21 cells were plated in 24-well plates and transfected with 1  $\mu$ g of pGL-CV3 (plasmid containing the luciferase gene under the control of the SV40 promoter) complexed with  $\beta$ CDP6 or Hist-CDP6 at various charge ratios. The cells were lysed 48 hours after transfection and analyzed for luciferase activity (results are reported in relative light units (RLUs) (Fig 4.3)).

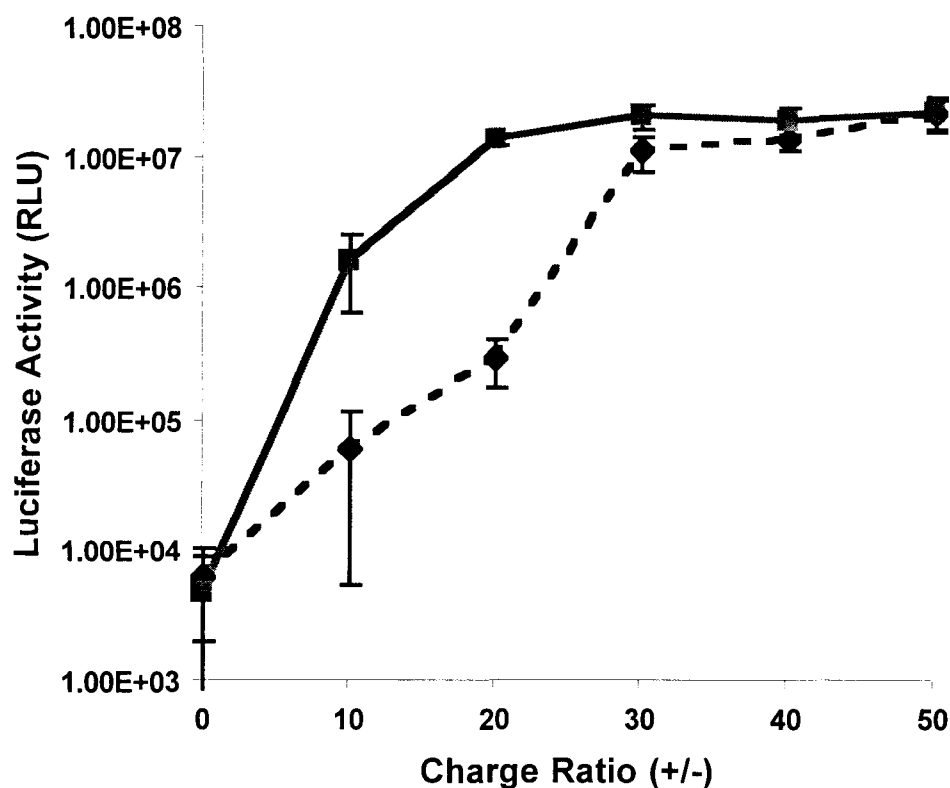


**Figure 4.3. Comparison of  $\beta$ CDP6 and Hist-CDP6-mediated luciferase transfection to BHK-21 cells.**

1  $\mu$ g of polymer was complexed with  $\beta$ CDP (dashed line) or Hist-CDP6 (solid line) at various charge ratios and exposed to BHK-21 cells seeded in 24-well plates. Transfection efficiency was determined by assaying for luciferase protein activity and presented as relative light units. Results are presented as mean  $\pm$  standard deviation of three assays. Background RLU=6 x 10<sup>3</sup>.

While both polymers successfully deliver plasmid DNA to cells, Hist-CDP6 is able to transfect BHK-21 cells with higher efficiencies than the unmodified  $\beta$ CDP6 at all charge ratios up to 50 +/- . The relative transfection efficiency between the two polymers is shown in Fig 4.4. Histidylation of  $\beta$ CDP6 enhances transfection by over 20-fold below charge ratios of 30 +/- and by 2-fold at 30 and 40 +/-.

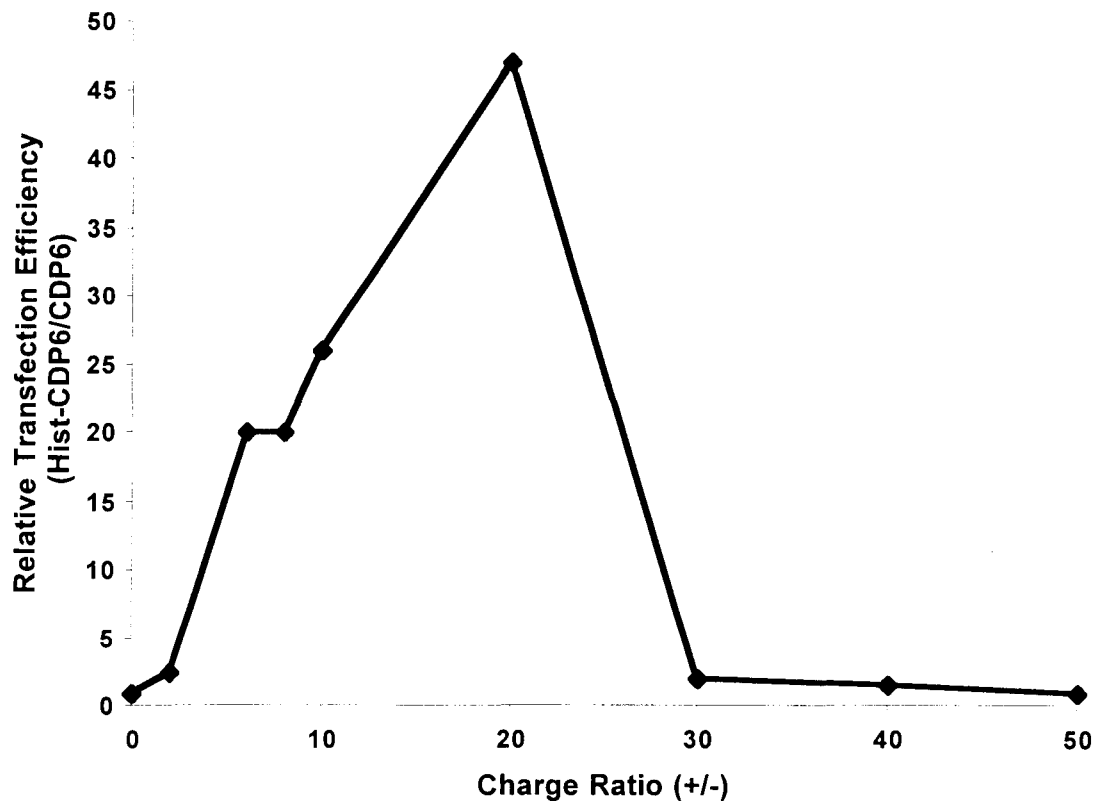


**Figure 4.4. Relative transfection efficiencies of Hist-CDP6 to  $\beta$ CDP6 at various charge ratios.**

BHk-21 cells were transfected with the luciferase plasmid complexed with Hist-CDP6 or  $\beta$ CDP6 at various charge ratios. Luciferase protein activity was measured in relative light units in triplicate assays. Relative transfection efficiency was calculated by dividing average Hist-CDP6 RLU by average  $\beta$ CDP6 RLU measured at each charge ratio.

**4.4.4. Plasmid Delivery by Hist-CDP6.** The plasmid cellular uptake by Hist-CDP6-based polyplexes was determined by flow cytometry. BHK-21 cells were exposed for 24 hours to rhodamine-labeled plasmids complexed with Hist-CDP6 or  $\beta$ CDP6 at a charge ratios of 5+/. DNA uptake levels for individual cells were then determined by recording the rhodamine fluorescence intensity in each cell. The rhodamine fluorescence profiles are presented in Fig 4.5. The instrument parameters were set such that the background rhodamine fluorescence of all BHK-21 cells resides in the first decile (Fig 4.5a) The fluorescence profiles of  $\beta$ CDP6 (Fig 4.5b) and Hist-CDP6 (Fig 4.5c) transfected cells are nearly identical; only 35.6% of the  $\beta$ CDP6-transfected cells and 36.1% of the Hist-CDP6 transfected cells remain in the first decile, indicating ~65% plasmid uptake (lower bound estimate due to the low rhodamine fluorescence intensity and conservative gate setting during flow cytometry analysis).

**4.4.5. Intracellular Distribution of Hist-CDP6-delivered Oligos.** The intracellular distribution of DNA due to Hist-CDP6-mediated delivery was visualized by confocal microscopy. BHK-21 cells were plated onto glass coverslips in 6-well plates and transfected with 5  $\mu$ g of FITC-Oligo complexed with  $\beta$ CDP6 or Hist-CDP6. The cells were incubated with polyplexes for 24 hours before fixing and staining with DiI. Transfected cells showed punctate fluorescein fluorescence indicative of vesicular staining (Fig 4.6). FITC-Oligo complexed with Hist-CDP6 was delivered to over 95% of BHK-21 cells, even at the 6 +/- charge ratio. Cells transfected with Hist-CDP6 polyplexes exhibited stronger fluorescence than CDP6-transfected cells at all charge ratios tested, indicating either higher polyplex uptake or reduced fluorescence quenching at the lower late endosomal pH. Images recorded at higher magnification confirmed stronger punctate fluorescence in Hist-CDP6 transfected cells (Fig 4.7). In addition, these cells showed cytosolic delivery, as indicated by the orange color due to the overlay

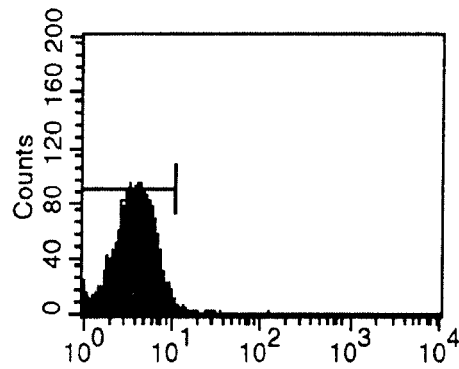


**Fig 4.5a. Untransfected BHK-21 cells**

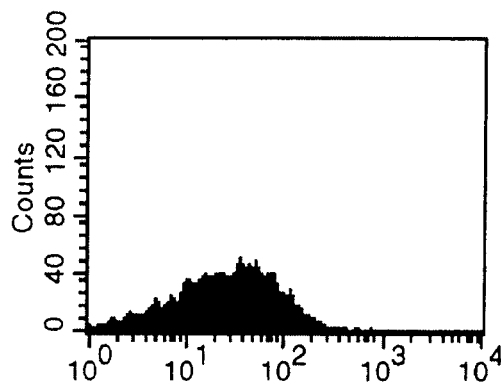


**Fig 4.5b.  $\beta$ CDP6 Transfection**

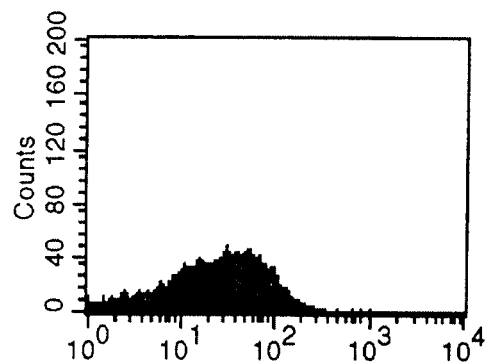


**Fig 4.5c. Hist-CDP6 Transfection**

**Figure 4.5. Rhodamine-labeled plasmid uptake mediated by  $\beta$ CDP6 and Hist-CDP6.** Rhodamine labeled plasmids complexed with  $\beta$ CDP6 (Fig 5b) or Hist-CDP6 (Fig 5c) at 5+/- were delivered to BHK-21 cells. The amount of DNA uptake was determined by FACS. The fluorescence distribution is plotted with number of cell counts on the y-axis and fluorescence intensity on the x-axis.

$\beta$ CDP6

Hist-CDP6

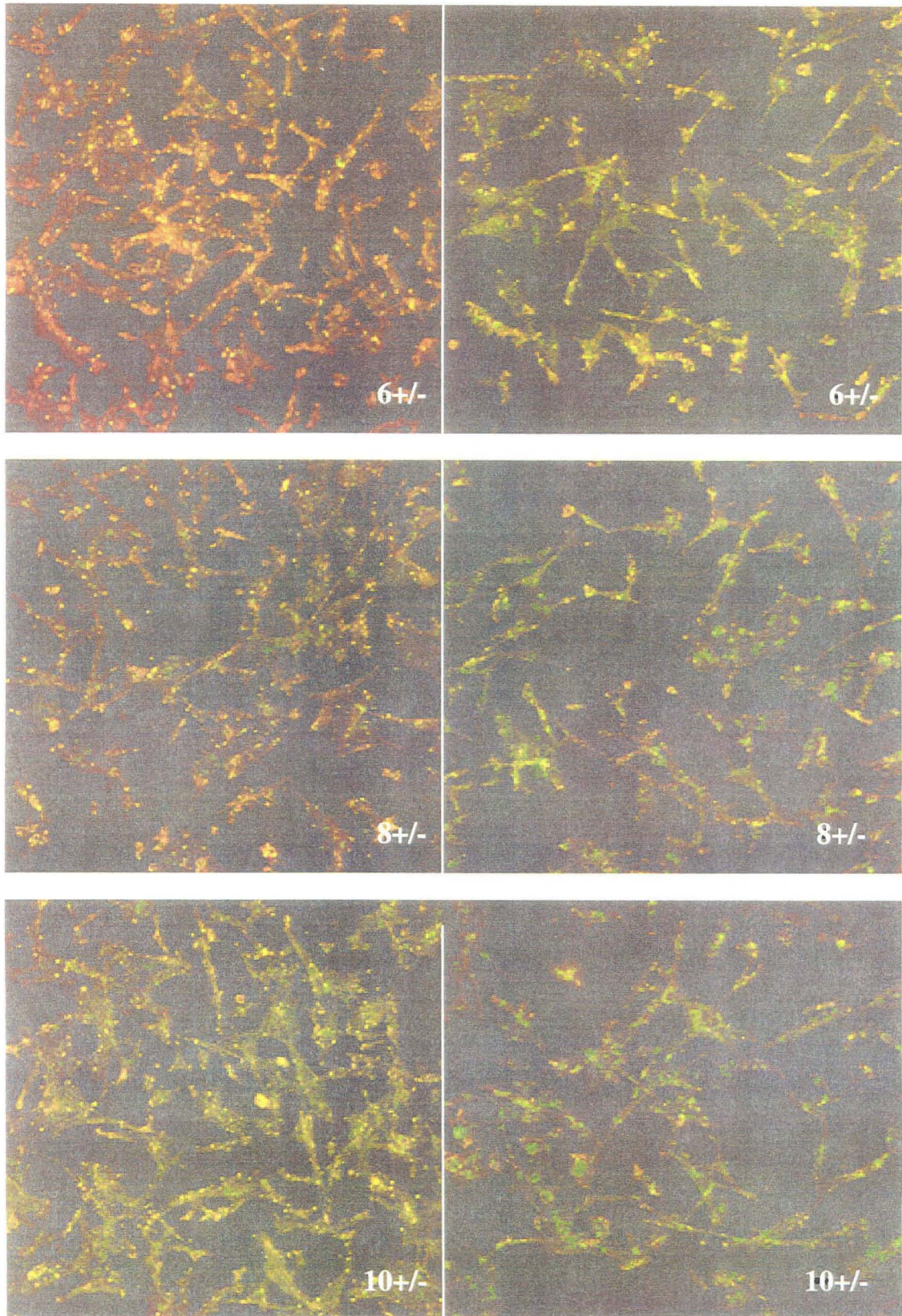


**Figure 4. 6. Transfection of fluorescein-labeled oligos to BHK-21 cells with  $\beta$ CDP6 and Hist-CDP6**  
BHK-21 cells were transfected with FITC-Oligos complexed with  $\beta$ CDP6 and Hist-CDP6 at various charge ratios and visualized by confocal microscopy. Cells on the left were transfected with  $\beta$ CDP6 and cells on the right with Hist-CDP6.

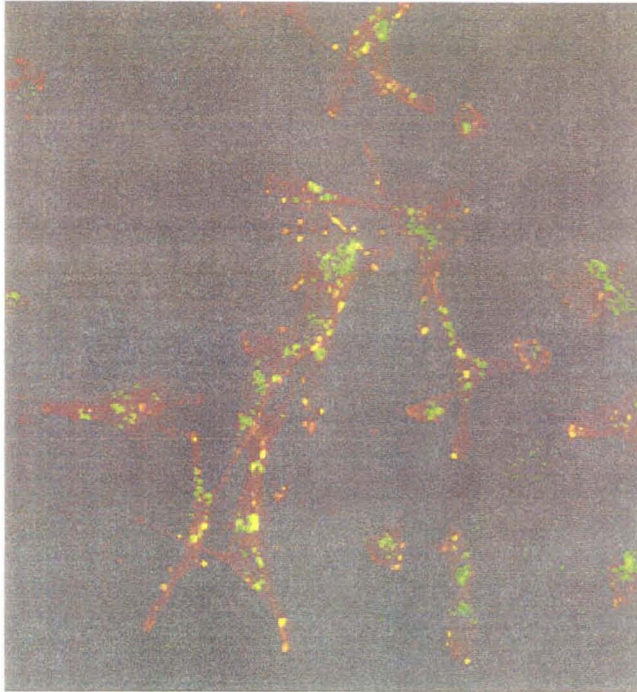


**Figure 7a.  $\beta$ CDP6-transfected cells**

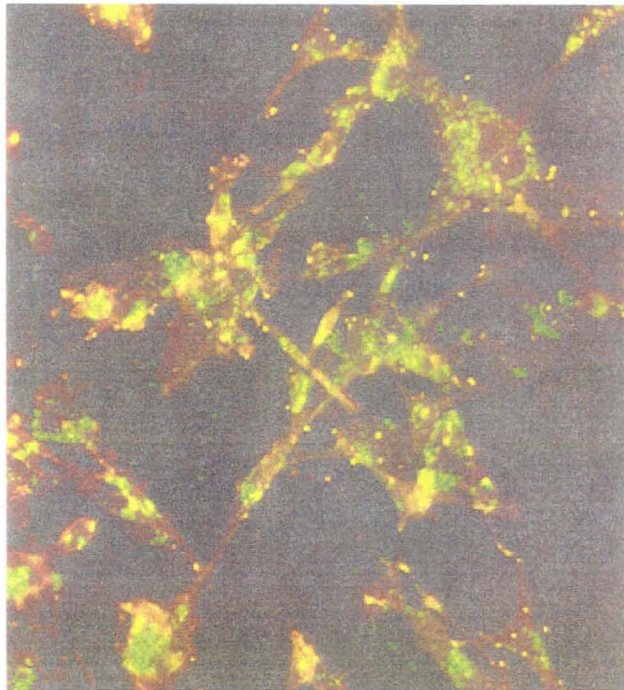


**Figure 7b. Hist-CDP6-transfected cells**

**Figure 4.7. Confocal images of BHK-21 cells transfected with fluorescently labeled oligos complexed with  $\beta$ CDP6 and Hist-CDP6 at 10 +/-.**

of cellular staining in red with the FITC Oligo staining in green. No cytosolic delivery was observed for cells transfected with CDP6 polyplexes. Nuclear localization was not observed for transfection with either polymer.

**4.4.6. Transfections in the Presence of Chloroquine.** BHK-21 cells were transfected with a plasmid containing the luciferase gene complexed with  $\beta$ CDP6 or Hist-CDP6 in the presence of 25  $\mu$ M chloroquine, an endosomal buffering agent. Because chloroquine is toxic to cells (35% cell survival in the presence of chloroquine), luciferase protein activity, typically measured in RLU, was normalized with total cellular protein levels. The relative transfection efficiencies were calculated by dividing the normalized RLU of each sample by the normalized RLU measured for  $\beta$ CDP6-based transfections in the absence of chloroquine. The effect of chloroquine on transfections is reported in Fig 4.8. Chloroquine addition increases transfection efficiency by nearly two orders of magnitude over  $\beta$ CDP6-mediated transfections. The presence of chloroquine further increases Hist-CDP6 transfection efficiencies by 3-fold. However, the combination of Hist-CDP6 transfection and chloroquine does not enhance transfection efficiencies over the use of chloroquine alone.

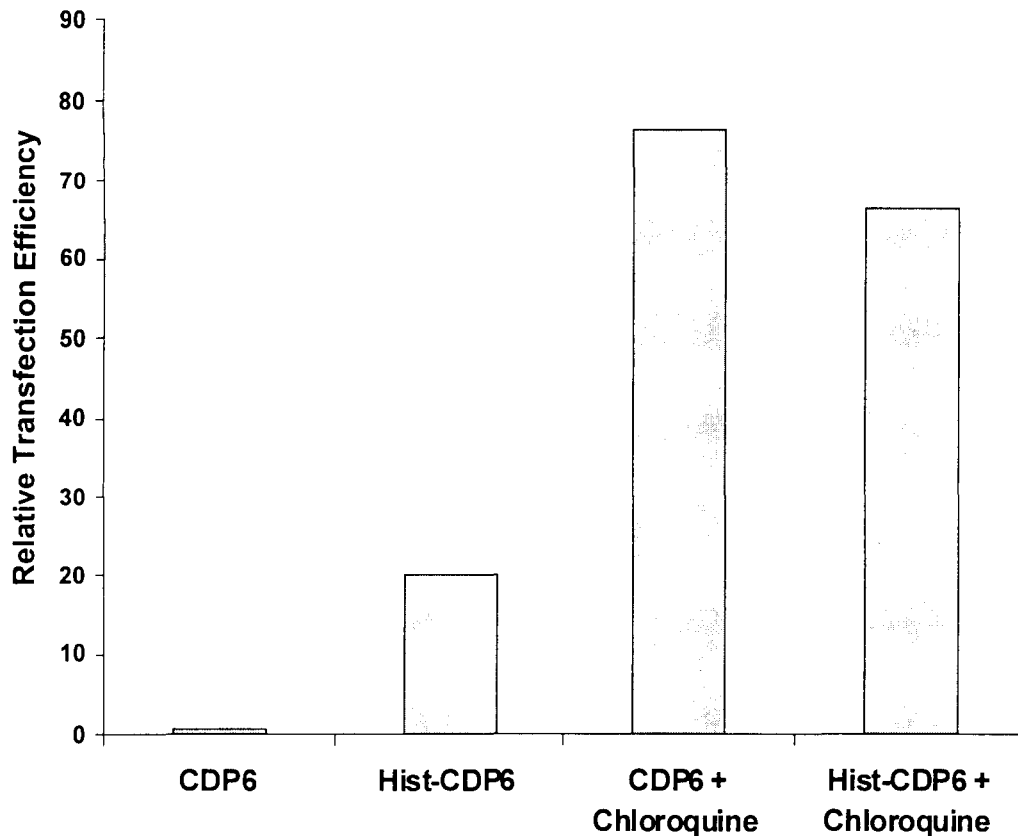


**Figure 4.8. Effect of chloroquine on  $\beta$ CDP6 and Hist-CDP6-mediated transfections.** BHK-21 cells were transfected with  $\beta$ CDP6 and Hist-CDP6 in the presence of 25  $\mu$ M chloroquine. Transfection efficiency was determined in RLU/mg total protein with luciferase protein activity measured in RLU and total cellular protein determined by Lowry's protein assay. Results are normalized with RLU/mg of  $\beta$ CDP6 transfections and presented as the average of two assays.

#### 4.5. DISCUSSION

The desired endpoint for therapeutic plasmid delivery is the cell nucleus. Cationic CDP-based polyplexes are efficiently endocytosed into acidic compartments by cells but remain largely trapped there. Here, Hist-CDP6 was prepared in an attempt to overcome this problem. Histidine, a pH-sensitive moiety, was conjugated to the amine termini of  $\beta$ CDP6 by peptide-bond formation chemistry. 70% of polymer endgroups were reacted, corresponding to a polymer charge increase of 15% below pH 6.0 due to histidine protonation. At pH 7.4, most of the histidine groups are neutral. Therefore,

while  $\beta$ CDP6 is completely soluble even at 50 mg/mL, Hist-CDP6 precipitates from solutions prepared at 10 mg/mL.

Benns et al. (24) report that polyhistidylated PLL binds DNA less effectively than PLL, requiring 20 times as much polymer to condense DNA to the same particle size. However, Hist-CDP6 is able to bind and condense plasmid DNA as with the same particle diameter profile as  $\beta$ CDP6 (Fig 4.2). Stable particles are formed above 3 +/- charge ratios and exhibit the same physicochemical characteristics as  $\beta$ CDP6 polyplexes. These particles are positively charged (zeta potential  $\sim +25$  mV), uniform in size ( $\sim 200$  nm in diameter) and are able to transfect cultured cells.

Hist-CDP6 polyplexes are able to transfect cells more efficiently than  $\beta$ CDP6 polyplexes without showing any difference in toxicity. Free histidine in solution does not improve transfection efficiency, probably because it is not taken into the endosome at sufficient concentrations. Hist-CDP6-mediated transfection of a luciferase plasmid results in 20-fold higher luciferase activity than transfection with  $\beta$ CDP6 (Fig 4.3). It should be noted that Midoux et al. report a four orders of magnitude increase in luciferase activity with histidylated PLL over PLL (21). However,  $\beta$ CDP6 itself is able to deliver the luciferase plasmid to cultured cells with higher efficiency than PLL. Luciferase activity of BHK-21 cells transfected with  $\beta$ CDP6/pGL-CV3 polyplexes is three orders of magnitude higher than activity of PLL/pGL-CV3 transfected cells (data not shown).

There are several possible explanations for increased transfection efficiency with Hist-CDP6: (i) cells may uptake Hist-CDP6 particles more readily than CDP6 particles. (ii) Hist-CDP6 may offer pH-buffering abilities in the endosomes (because the imidazole in the histidine has a  $pK_a$  of 6.0, thereby reducing DNA degradation and delivery to lysosomes, (iii) Hist-CDP6 may aid in membrane destabilization and endosomal release, and (iv) Hist-CDP6 may assist in nuclear trafficking of the delivered DNA. In order to assess these possibilities, transfections were conducted with fluorescently labeled DNA and in the presence of chloroquine.

Delivery of rhodamine labeled plasmid revealed no difference in DNA uptake between Hist-CDP6 and  $\beta$ CDP6 polyplexes (Fig 4.5). Plasmids were delivered to ~65% of cells with both polymers. Therefore, Hist-CDP6 does not improve transfection efficiency by increasing DNA uptake. Next, the intracellular localization of  $\beta$ CDP6 and Hist-CDP6-delivered oligos (labeled with fluorescein) was visualized by confocal microscopy (Figs 4.6 and 4.7). Cells transfected with Hist-CDP6 show much stronger fluorescence in larger vesicles. Because there is no difference in DNA uptake between the two polymers, the increase in fluorescence is likely due to greater DNA accumulation and lack of fluorescein quenching at low pH as a result of endosomal buffering. Polyplexes are taken up into vesicles that fuse with early endosomes. These endosomes acidify and mature into late endosomes and finally fuse with lysosomes. Histidine, with its imidazole pK of 6.0, is likely to affect the acidification of endosomes. Endosomal buffering is known to delay the transition of endosomes to lysosomes and allows for greater polyplex accumulation.

In addition, fluorescein fluorescence is strongly quenched below pH 6.5. Buffering the endosomal pH prevents the fluorescence quenching that occurs with  $\beta$ CDP6 delivery. The overlaying fluorescence intensity profiles (as determined by flow cytometry, Fig 4.5) of BHK-21 cells transfected with  $\beta$ CDP6/Rhod-DNA and Hist-CDP6/Rhod-DNA indicates that polyplex uptake is the same for  $\beta$ CDP6 and Hist-CDP6. Therefore, the lower fluorescence observed by confocal microscopy in  $\beta$ CDP6/FITC-Oligo transfected cells (Fig 4.6 and 4.7) is likely due to fluorescence quenching of FITC-Oligo in the endosomes. In contrast, Hist-CDP6, with its buffering capacity, may prevent endosomal acidification and subsequent fluorescence quenching. Thus, because polyplex uptake is the same for both polymers, the higher fluorescence intensity in Hist-CDP6 transfected cells suggests successful endosomal buffering by the histidine imidazole groups. In addition, Pichon et al. (22) also noticed a large difference in fluorescence

intensity for fluorescein-labeled oligos delivered with histidylated-oligolysines versus histidine-free oligolysine.

Despite the greater accumulation of oligos in Hist-CDP6-transfected cells, neither polymer appears to assist significantly in endosomal escape. Hist-CDP6-transfected cells demonstrate slightly increased cytosolic delivery, as evidenced directly by the low intensity of fluorescein fluorescence in cell cytosol and indirectly by the higher luciferase expression described previously. However, because fluorescence is mostly observed in punctate vesicular areas, endosomal escape is likely a sporadic event that occurs in higher incidence in Hist-CDP6-transfected cells due to the large accumulation of material in the endosome. In addition, neither  $\beta$ CDP6 nor Hist-CDP6-transfected cells show significant nuclear localization of oligos. Therefore, based on flow cytometry and confocal microscopy, Hist-CDP6 increases transfection efficiency by introducing a buffering capacity in the endosomal vesicles. Increased cellular uptake due to histidylation is not observed, nor is increased delivery to the nucleus. Although polyhistidine is known to destabilize membranes at  $\text{pH} < 6.5$  ((19,20)), the conjugation of monohistidine to  $\beta$ CDP6 is not enough to impart fusogenic properties to the polymer.

Luciferase transfections with the CDPs were also conducted in the presence of chloroquine. Chloroquine (a weakly basic molecule) is known to enhance transfection by raising the pH of endocytotic vesicles, reducing lysosomal degradation, protecting DNA from nuclease degradation, and aiding in the dissociation of DNA from cationic polymers ((25)). The presence of 25  $\mu\text{M}$  chloroquine in the transfection media increased the efficiency of both  $\beta$ CDP6 and Hist-CDP6 transfection by  $\sim 70$ -fold over the  $\beta$ CDP6 transfection alone. Hist-CDP6 transfection efficiency is further increased by over 3-fold in the presence of chloroquine. Therefore, the buffering capability of Hist-CDP6 is not optimal; further improvements are possible with chloroquine. Also, the use of histidine in conjunction with chloroquine results in no synergistic effects. Histidine and chloroquine are both able to prevent lysosomal degradation by endosomal buffering.

However, because chloroquine freely passes the cell membrane and accumulates in the endosome, it may be present at a higher concentration and have a stronger buffering effect that results in the higher transfection efficiencies.

In conclusion, the conjugation of histidine to  $\beta$ CDP6 results in a polymer with improved transfection abilities. Hist-CDP6 increases transfection by buffering the pH drop in the endosome that protects the DNA from degradation and allows for greater more opportunities for endosomal escape. Because Hist-CDP6 does not actively mediate endosomal escape, the possibility of incorporating fusogenic peptides into the CDP polyplexes is currently being pursued. Nonetheless, the ability of Hist-CDP6 to efficiently transfect cells at low charge ratios make it a promising *in vivo* delivery agent.

#### 4.6. LITERATURE CITED

- (1) Mislick, K. A., Baldeschwielder, J. D. *Proceedings of the National Academy of Sciences* Evidence for the role of proteoglycans in cation-mediated gene transfer **1996**, *93*, 12349-12354.
- (2) Labat-Moleur, F., Steffan, A.-M., Brisson, C., Perron, H., Feugeas, O., Furstenberger, P., Oberling, F., Brambilla, E., Behr, J.-P. *Gene Therapy* An electron microscopy study into the mechanism of gene transfer with lipopolyamines **1996**, *3*, 1010-1017.
- (3) Zanta, M.-A., Boussif, O., Adib, A., Behr, J.-P. *Bioconjugate Chemistry* In Vitro Gene Delivery of Hepatocytes with Galactosylated Polyethylenimine **1997**, *8*, 839-844.
- (4) Choi, Y. H., Liu, F., Park, J. S., Kim, S. W. *Bioconjugate Chemistry* Lactose-Poly(ethylene Glycol)-Grafted Poly-L-Lysine as Hepatoma Cell-Targeted Gene Carrier **1998**, *9*, 708-718.
- (5) Shinoda, T., Maeda, A., Kagatani, S., Konno, Y., Goto, M., Sonobe, T., Akaike, T. *Drug Delivery* Specific Interaction with Hepatocytes and Acute Toxicity of New Carrier Molecule Galactosyl-Polylysine **1999**, *6*, 127-133.
- (6) Lee, R. J., Huang, L. *Journal of Biological Chemistry* Folate-targeted, Anionic Liposome-entrapped Polylysine-condensed DNA for Tumor Cell-specific Gene Transfer **1996**, *271*, 8481-8487.
- (7) Lee, R. J., Low, P. S. *Journal of Biological Chemistry* Delivery of Liposomes into Cultured KB Cells via Folate Receptor-mediated Endocytosis **1994**, *269*, 3198-3204.
- (8) Felgner, P. L. In *The Development of Gene Therapy*; Friedman, T., Ed.; Cold Spring Harbor Press: Cold Spring Harbor, 1999; pp 241-260.
- (9) Wagner, E. In *Gene Therapeutics*; Wolff, J. A., Ed., 1997; pp 99-117.
- (10) Smythe, E., Warren, G. *European Journal of Biochemistry* The mechanism of receptor-mediated endocytosis **1991**, *202*, 689-699.

- (11) Leopold, P., Ferris, B., Grinberg, I., Worgall, S., Hachett, N., Crystal, R. *Human Gene Therapy* Fluorescent virions: dynamic tracking of the pathway of adenoviral gene transfer vectors in living cells **1998**, *9*, 367-378.
- (12) Lasic, D. D., Templeton, N. S. *Advanced Drug Delivery Reviews* Liposomes in gene therapy **1996**, *20*, 221-266.
- (13) Mechtler, K., Wagner, E. *New J. Chem* Influenza peptide enhanced gene transfer: The role of peptide sequences **1997**, *21*, 105-111.
- (14) Parente, R. A., Nir, S., Francis C. Szoka, J. *Biochemistry* Mechanism of Leakage of Phospholipid Vesicle Contents Induced by the Peptide GALA **1990**, *29*, 8720-8728.
- (15) Wagner, E. *Advanced Drug Delivery Reviews* Application of membrane-active peptides for non-viral gene delivery **1999**, *38*, 279-289.
- (16) Wagner, E.; Plank, C., Zatloukal, K., Cotten, M., Birnstiel, M. L. *Proc. Natl. Acad. of Sci.* Influenza-virus hemagglutinin-HA-2 N-terminal Fusogenic Peptides augment gene-transfer by transferrin polylysine DNA complexes-toward a synthetic virus-like gene-transfer vehicle **1992**, *89*, 7934-7938.
- (17) Boussif, O., Lezoualch, F., Zanta, M. A., Mergny, M. D., Scherman, D., Demeneix, B., Behr, J.-P. *Proceedings of the National Academy of Sciences* A versatile vector for gene and oligonucleotide transfer into cells in culture and in vivo: Polyethylenimine **1995**, *92*, 7297-7301.
- (18) Haensler, J., Szoka, F. C. *Bioconjugate Chemistry* Polyamidoamine cascade polymers mediate efficient transfection of cells in culture **1993**, *4*, 372-379.
- (19) Uster, P. S., Deamer, D. W. *Biochemistry* pH-dependent fusion of liposomes using titratable polycations **1985**, *24*, 1-8.
- (20) Wang, C.-Y., Huang, L. *Biochemistry* Polyhistidine mediates an acid-dependent fusion of negatively charged liposomes **1984**, *23*, 4409-4416.
- (21) Midoux, P., Monsigny, M. *Bioconjugate Chemistry* Efficient Gene Transfer by Histidylated Polylysine/pDNA Complexes **1999**, *10*, 406-411.

- (22) Pichon, C., Roufai, M. B., Monsigny, M., Midoux, P. *Nuc. Acids Res.* Histidylated oligolysines increase the transmembrane passage and the biological activity of antisense oligonucleotides **2000**, *28*, 504-512.
- (23) Gonzalez, H., Hwang, S. J., Davis, M. E. *Bioconjugate Chemistry* New class of polymers for the delivery of macromolecular therapeutics **1999**, *10*, 1068-1074.
- (24) Bennis, J. M., Choi, J.-S., Mahato, R. I., Park, J.-S., Kim, S. W. *Bioconj. Chem.* pH sensitive cationic polymer gene delivery vehicle: N-Ac-poly(L-histidine)-graft-poly(L-lysine) comb shaped polymer **2000**, *11*, 637-645.
- (25) Erbacher, P., Roche, A. C., Monsigny, M., Midoux, P. *Exp. Cell Res.* Putative role of chloroquine in gene transfer into a human hepatoma cell line by DNA/Lactosylated polylysine complexes **1996**, *225*, 186-194.

## Chapter 5

# Modification of $\beta$ -Cyclodextrin Polymer-based Polyplexes by Cyclodextrin-Adamantane Inclusion Complex Formation

### 5.1. ABSTRACT

Most polymeric gene delivery systems developed for in vitro applications require alterations before they can be applied in in vivo settings. Modification of polymers by direct grafting of secondary components may interfere with polymer/DNA binding interactions; this is a particular problem for short polymers such as linear,  $\beta$ -cyclodextrin polymers ( $\beta$ CDPs) that have intrinsically lower DNA binding constants. Here,  $\beta$ CDP-based polyplexes are modified by taking advantage of the ability of cyclodextrin molecules to form inclusion compounds with hydrophobic guest molecules. An anionic peptide (GALA) is conjugated to adamantane, a molecule that has a high cyclodextrin association constant. The resulting GALA-adamantane (GALA-Ad) peptide associates with the  $\beta$ CDP-based polyplexes without disrupting polymer/DNA interactions. While unmodified polyplex particles and 100% GALA-modified polyplexes prepared at 5 +/- have zeta potentials of +13 mV and -15 mV, respectively, 100% GALA-Ad modified polyplexes has a zeta potential of -43 mV. GALA-Ad modification of polyplexes inhibits DNA uptake in cultured cells and reporter gene expression, while GALA addition results in minimal changes in polyplex transfection. Modification of  $\beta$ CDP-based polyplexes by cyclodextrin/adamantane association provides a new method of grafting desired entities to preformed polyplexes without disruption of polymer/DNA interactions.

## 5.2 INTRODUCTION

Cationic polymers are routinely used as transfection reagents for DNA delivery to cultured cells (1-3). These polycations are able to self-assemble with and condense DNA to small particles called polyplexes (4). When formulated with a net positive charge, polyplexes bind to cell surfaces and are internalized (5). Despite laboratory success with polyplexes, there are to date no cationic polymers used in human trials for gene delivery. Cationic polymers are often highly toxic to cells. In addition, polyplex formulation optimized for in vitro delivery is typically not amenable for in vivo use as successful in vivo systemic delivery requires very different particle characteristics. First, cationic polyplexes interact with serum proteins and are quickly eliminated from the bloodstream by phagocytic cells after intravenous injection (6,7). Also, these polyplexes are unstable at physiological salt conditions, resulting in rapid aggregation. Finally, the polyplexes normally need to be directed to specific cells in the body and cationic polyplexes are known to be captured by the first tissue they encounter, e.g., with i.v. injection, the lungs. Therefore, cationic polyplexes need to be modified before they can be applied for in vivo gene delivery.

Most polymers investigated thus far are cationic in order to facilitate the binding to DNA. The charge normally is derived from amine groups on the polymer. Therefore, one possible way of modifying the polymers is to modify the polymer amine groups. This method has been used for pegylating polyethylenimine (PEI) and poly(L)lysine (PLL) to impart steric stabilization to particles formed with these polymers (8,9). In doing so, the charge density associated with the primary amines is reduced. This method does not work well for short polymers that have lower DNA binding constants, i.e., the polymer-DNA interactions are disrupted.

A family of  $\beta$ -cyclodextrin-containing polymers ( $\beta$ CDPs) suitable for DNA delivery has been described (10). These polymers contain  $\beta$ -cyclodextrin in the polymer backbone and are cationic due to repeating amidine groups.  $\beta$ CDP6-based polyplexes

show low in vitro toxicity and are therefore promising in vivo agents; however, they also suffer from the limitations mentioned above. Because the  $\beta$ CDPs are amine-terminated, these polymers were initially modified by coupling to the polymer endgroups segments of PEG. However, the  $\beta$ CDPs are, on average, 5-mers and modification of the polymer even with small molecules can disrupt DNA binding. Thus, a different method of polyplex modification must be developed for  $\beta$ CDPs.

Cyclodextrins are capable of forming inclusion compounds with hydrophobic moieties (Fig 5.1). For some molecules, this association can be quite strong. For example, adamantane derivatives have  $\beta$ -cyclodextrin association constants ( $K_a$ ) on the order of  $10^4$ - $10^5$  (11,12). Here, I make use of this cyclodextrin/hydrophobic compound complexation as a method for modifying  $\beta$ CDP-based polyplexes. The hypothesis is that utilizing the cyclodextrin cups for modification would cause minimum disturbance to pre-formed polyplexes. The  $\beta$ CDPs bind to DNA via electrostatic interactions of the cationic amidine groups on the  $\beta$ CDP and the anionic phosphate groups on the DNA. The cyclodextrin cups should therefore be available on the polyplex surface for complexation.

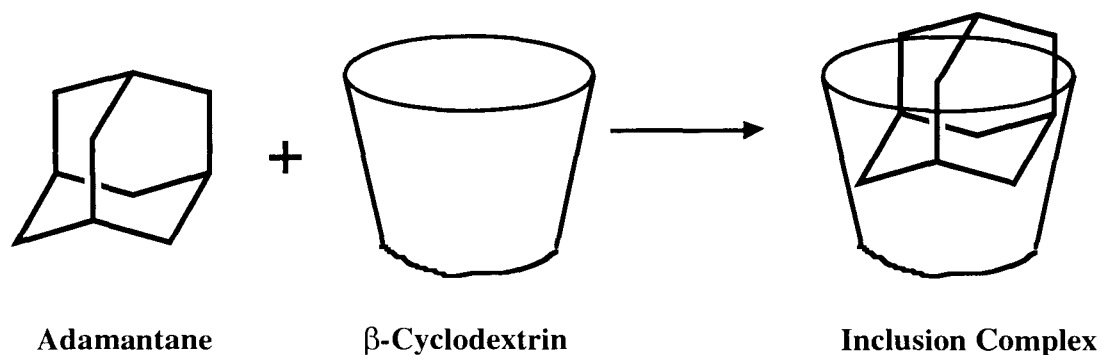


**Figure 5.1. Schematic illustration of inclusion complexation of adamantane with  $\beta$ -cyclodextrin.** Adamantane displaces associated water molecules from the hydrophobic cyclodextrin cavity to form the inclusion complex.

To test the hypothesis listed above, adamantane was selected as the hydrophobic complexation agent because it has a high binding constant with  $\beta$ -cyclodextrin ( $10^4$ - $10^5$ ). GALA, a highly anionic peptide, was used as the modifying agent. The anionic nature of the peptide allows for monitoring of polyplex modification by zeta potential measurements. In addition, GALA is a water-soluble peptide that becomes fusogenic at low pH (13,14). GALA has been shown to enhance transfection efficiencies, possibly by acting as an endosomal disrupting agent at low pH (15). Therefore, GALA modification may also be useful for increasing transfection efficiencies. Here, it is shown that adamantane-conjugated GALA (GALA-Ad) successfully modifies  $\beta$ CDP6-based polyplexes without disrupting polymer/DNA binding. Modification of the polyplexes results in highly anionic particles with inhibited cellular uptake.

### 5.3. MATERIALS AND METHODS

#### 5.3.1. Polymer and Peptide Preparation

*$\beta$ -cyclodextrin-DMS copolymer ( $\beta$ CDP6) preparation.*  $\beta$ CDP6 was synthesized according to previously described procedures (10). In brief,  $\beta$ -CD dicycstamine and an equimolar amount of dimethyl suberimidate (DMS, Pierce, Rockford, Illinois) were dissolved in 0.5 M  $\text{Na}_2\text{CO}_3$  and stirred overnight at room temperature. The pH of the resulting solution was brought below 5.0 by the addition of 1 M HCl and dialyzed extensively against  $\text{dH}_2\text{O}$  in a MWCO 3500 dialysis membrane (Pierce) for 24 hours. The dialyzed solution was lyophilized to dryness to yield a white, fluffy solid, with typical yields around 25-30%.

*Peptide synthesis.* The GALA peptide (sequence: W-E-A-A-L-A-E-A-L-A-E-A-L-A-E-H-L-A-E-A-L-A-E-A-L-E-A-L-A-A, MW 3032) was synthesized by the Biopolymer Synthesis Facility (Beckman Institute, California Institute of Technology) using an automatic synthesizer. Before cleaving the peptide from the resin, one-third of the resin

was set aside for adamantane conjugation. Analysis of the peptide by HPLC indicated greater than 95% purity. 1-Adamantane-carboxylic acid (Aldrich) was conjugated to the N-terminal end of the GALA-peptide with DCC coupling chemistry. The resulting peptide (GALA-Ad, MW 3194) was cleaved from the resin. Analysis of the peptide by HPLC indicated greater than 90% purity. The identities of the peptides were confirmed by MALDI-TOF analysis (Biopolymer Analysis Facility, Beckman Institute, California Institute of Technology).

### **5.3.2. Polyplexes and Modifications with GALA Peptide**

*Plasmids and oligonucleotides.* Plasmid pGL3-CV (Promega, Madison, WI), containing the luciferase gene under the control of the SV40 promoter, was amplified by *Esherichia Coli* and purified using Qiagen's Endotoxin-free Megaprep kit (Valencia, CA). Fluorescein-labeled oligonucleotides (FITC-oligos, 25-mer, 5'-FITC-ACT GCT TAC CAG GGA TTTCAG TGC A-3') were synthesized by the Biopolymer Synthesis Facility (California Institute of Technology).

*Particle formation and characterization.* Polyplexes were prepared by mixing an equal volume of  $\beta$ CDP6 dissolved in dH<sub>2</sub>O with DNA (0.1 mg/mL in dH<sub>2</sub>O) at the appropriate charge ratios. The same volume of GALA or GALA-Ad dissolved in 50 mM phosphate buffered saline (PBS, pH 7.2) was then added to the complexes. For example, with particle characterization studies, 2  $\mu$ g of plasmid DNA (20  $\mu$ L) were complexed with  $\beta$ CDP6 (20  $\mu$ L) at a 5+/- charge ratio. 20  $\mu$ L of GALA solution, GALA-Ad solution or 50 mM PBS (for control samples) were then added to the complexes. The solution was then diluted with the addition of 1.2 mL dH<sub>2</sub>O. The size and charge of particles were determined by dynamic light scattering and zeta potential measurements, respectively, using a ZetaPals dynamic light scattering detector (Brookhaven Instruments Corporation, Holtsville, NY).

### 5.3.3. Cells and Transfections.

*Cell Culture.* BHK-21 cells were purchased from ATCC (Rockville, MD) and HUH-7 cells were generously donated by Valigen (Newtown, PA). Both cell lines were cultured in DMEM supplemented with 10% fetal bovine serum, 100 units/mL penicillin, 100  $\mu\text{g}/\text{mL}$  streptomycin, and 0.25  $\mu\text{g}/\text{mL}$  amphotericin in a humidified incubator operated at 37 °C and 5% CO<sub>2</sub> and passaged every 4-5 days. Media and supplements were purchased from Gibco BRL (Gaithersburg, MD).

*Polyplex uptake by cultured cells.* BHK-21 cells were plated in 6-well plates at 150,000 cells/well and incubated for 24 hours at 37 °C. 5  $\mu\text{g}$  of FITC-oligo were complexed with  $\beta\text{CDP6}$  at a 5 +/- charge ratio. After a 5 minute complexation time, 50  $\mu\text{L}$  of GALA or GALA-Ad in 50 mM of PBS (pH 7.2) were added to the complexes. Media was removed from the cells and cells washed with PBS. For transfection, 900  $\mu\text{L}$  of Optimem were added to each polyplex solution and the entire solution transferred to the cells. The cells were incubated with the transfection mixture for five hours before removing the media and washing the cells twice with PBS. The cells were collected by trypsinization and prepared for FACS analysis. Cells were washed twice in wash buffer (Hank's Balanced Salt Solution containing DNase and MgCl<sub>2</sub>) and resuspended in 500  $\mu\text{L}$  FACS buffer (Hank's Balanced Salt Solution, 2.5 mg/mL bovine serum albumin, 10  $\mu\text{g}/\text{mL}$  propidium iodide). FACS analysis was performed using a FACSCalibur flow cytometer (Becton Dickinson, San Jose, CA) and CellQuest software.

*Luciferase Transfection and Toxicity.* BHK-21 cells were plated in 24-well plates at 50,000 cells/well and incubated for 24 hours at 37 °C. 3  $\mu\text{g}$  of pGL3-CV plasmid were complexed with  $\beta\text{CDP6}$  at 5 +/- charge ratio. 30  $\mu\text{L}$  of Gala or Gala-Ad in 50 mM PBS, pH 7.2 were then added to the complexes. Media was removed from the cells prior to

transfection and cells washed with PBS. 600  $\mu\text{L}$  of Optimem were added to each polyplex solution and 230  $\mu\text{L}$  transfection solution of this transfection solution were added to each of 3 wells for four hours. After four hours, 800  $\mu\text{L}$  of complete media were added to each well. Media was changed 24 hours after transfection and cells were lysed in 50  $\mu\text{L}$  of Cell Culture Lysis Buffer (Promega, Madison, WI) 48 hours after transfection. Luciferase activity was analyzed using Promega's luciferase assay reagent and cell survival was measured by determining total cellular protein with Biorad's DC protein assay (Hercules, CA) as described previously (10).

## 5.4. RESULTS

**5.4.1. Particle Size of Modified Complexes.** The hydrodynamic diameter of  $\beta\text{CDP6/pGL3-CV}$  polyplexes prepared at 5+/- was measured by dynamic light scattering and found to be 260 nm. The GALA peptide undergoes a transition from a water-soluble random coil conformation at pH 7.5 to a water-insoluble helix at pH 5 (14). Therefore, the GALA and adamantane-modified GALA (GALA-Ad) peptides were dissolved in 50 mM PBS (pH 7.2) and added to the polyplexes at various peptide/cyclodextrin ratios. The amount of peptide added is reported as mol/mol of GALA peptide to cyclodextrin. The mixture was diluted with  $\text{dH}_2\text{O}$  and particle sizes determined by dynamic light scattering (Fig 5.2). Because the particle count rate remains the same for all concentrations of peptide added, the addition of peptide does not appear to disrupt the polyplexes. The particle size profiles as a function of GALA and GALA-Ad addition are very similar. The hydrodynamic diameter increases from 250 nm (1% GALA or GALA-Ad) to 400 nm (10% GALA or GALA-Ad). As more peptide is added, the particle size again decreases to that of the unmodified polyplex. The diameter returns to around 250 nm with the addition of 30% or more GALA-Ad and 50% or more GALA.

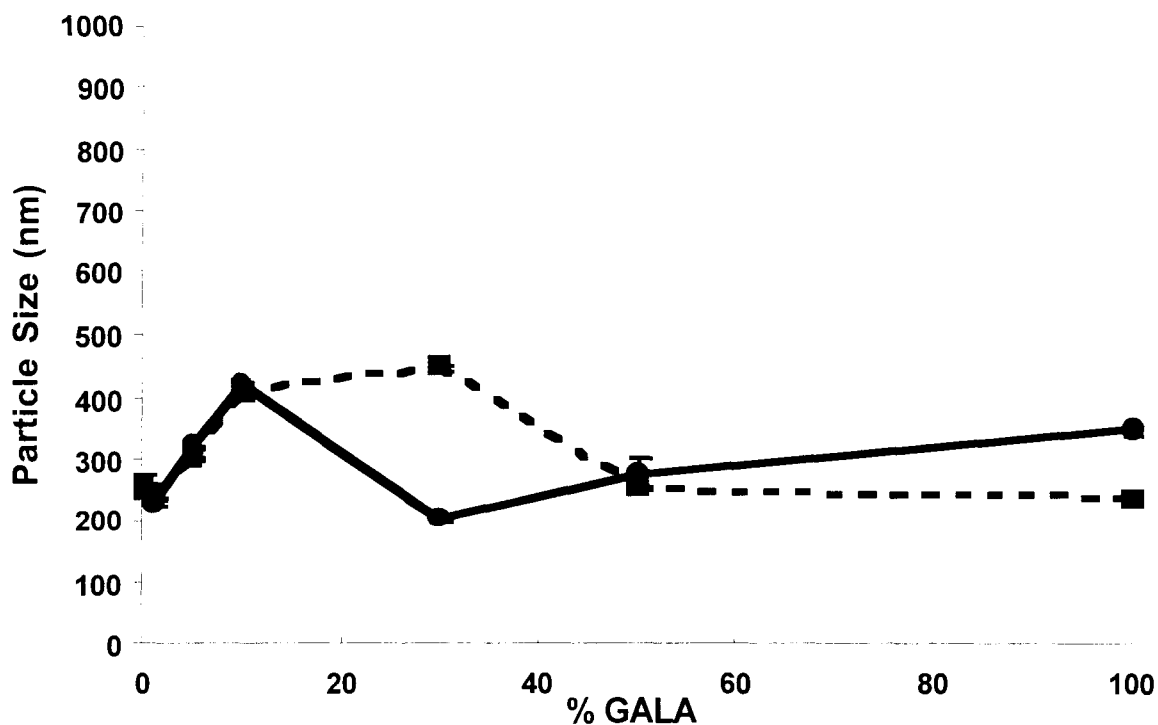


**Figure 5.2. Hydrodynamic diameter of GALA (dashed line) and GALA-Ad (solid line)-modified polyplexes.**

2  $\mu\text{g}$  of plasmid DNA in 20  $\mu\text{L}$  were mixed with an equal volume of  $\beta\text{CDP6}$  at 5+/. Various ratios of GALA or GALA-Ad were then added to the particles. Hydrodynamic diameter was determined by light scattering measurements. Results are presented as mean  $\pm$  standard deviation of three measurements.

**5.4.2. Zeta Potential of Modified Complexes.** The particle charge of  $\beta\text{CDP6/pGL3-CV}$  polyplexes at 5+/- was determined by zeta potential measurements and found to be +13 mV. GALA or GALA-Ad was added to polyplexes at various peptide/cyclodextrin ratios before dilution with  $\text{dH}_2\text{O}$ . The zeta potential of the particles in the presence of the peptides was determined and shown in Fig 5.3.

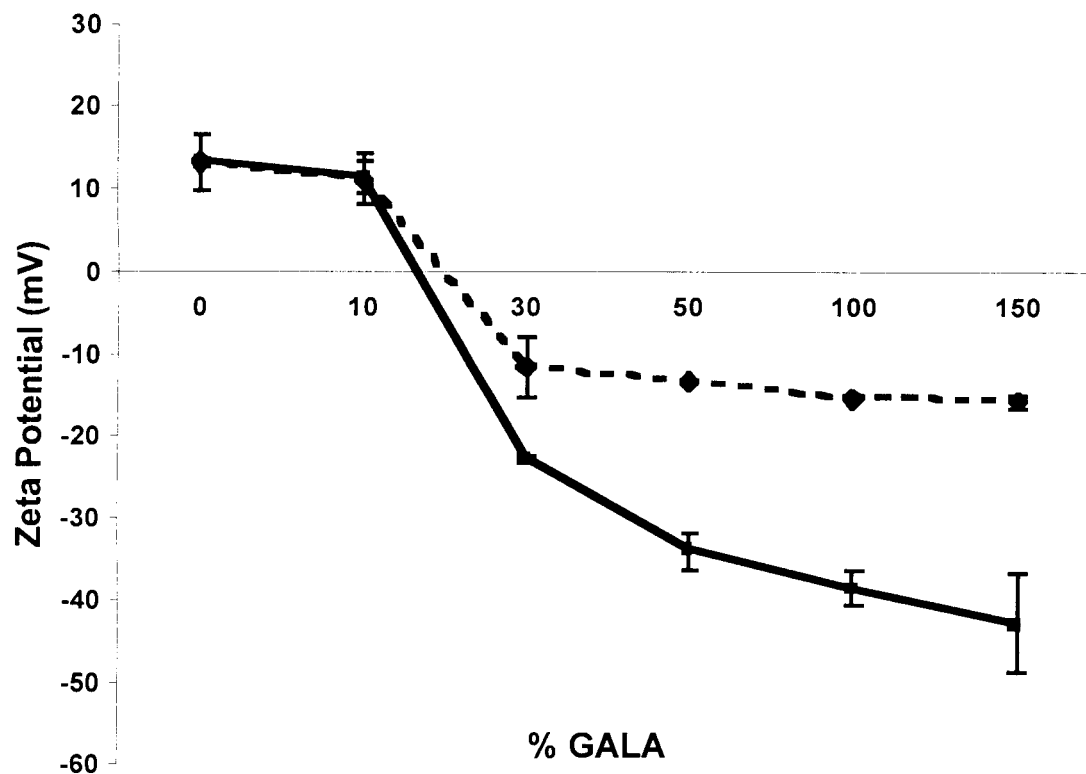


**Figure 5.3. Zeta potential of GALA (dashed line) and GALA-Ad (solid line)-modified polyplexes.**

2  $\mu\text{g}$  of plasmid DNA in 20  $\mu\text{L}$  were mixed with an equal volume of  $\beta\text{CDP6}$  at  $5\pm$ . Various ratios of GALA or GALA-Ad were then added to the particles. Particle charge was determined by electrophoretic mobility measurements and presented as particle zeta potential in mV. Results are presented as mean  $\pm$  standard deviation of three measurements.

Because the GALA peptide is an anionic peptide at pH 7.2 (contains several glutamic acid residues), the association of GALA and GALA-Ad with the polyplexes decreases their zeta potential. The polyplexes become negatively charged by 30% GALA (-11 mV) or GALA-Ad (-23 mV). The zeta potential of GALA + polyplex solutions plateaus at this point; adding more GALA only increases the zeta potential slightly (-15 mV at 150% GALA). However, the particles become more negatively charged with higher GALA-Ad

concentrations. Polyplexes with the addition of 150% GALA-Ad have zeta potentials of  $-42$  mV.

**5.4.3. DNA Delivery Efficiency of Modified Complexes.** The DNA delivery efficiency of GALA and GALA-Ad modified polyplexes was determined by flow cytometry. BHK-21 cells were exposed for 5 hours to fluorescein-labeled oligos (FITC-Oligos) complexed with  $\beta$ CDP6 at 5+/- and modified with 50% GALA or GALA-Ad. DNA uptake levels for individual cells were then determined by recording the fluorescein fluorescence intensity in each cell. The fluorescence profiles are presented in Fig 5.4. The parameters of the instrument were set such that the background fluorescein fluorescence of all BHK-21 cells resides in the first decile (Fig 5.4a).  $\beta$ CDP6-transfected cells show over 99% DNA uptake with average fluorescence levels around  $10^3$  (Fig 5.4b). Over 99% of cells exposed to  $\beta$ CDP6/FITC-Oligo/50% GALA also uptake FITC-Oligo with average fluorescence around  $10^3$  (Fig 5.4c). However, these cells have a broader fluorescence distribution than the cells transfected with  $\beta$ CDP6 alone. 80% of cells exposed to  $\beta$ CDP6/FITC-Oligo/50% GALA-Ad uptake the polyplexes. In addition, the mean fluorescence of BHK-21 cells transfected with  $\beta$ CDP6/FITC-Oligo/50% GALA-Ad is 2 orders of magnitude lower than  $\beta$ CDP6 and  $\beta$ CDP6/FITC-Oligo/50% GALA-transfected cells (Fig 5.4d).

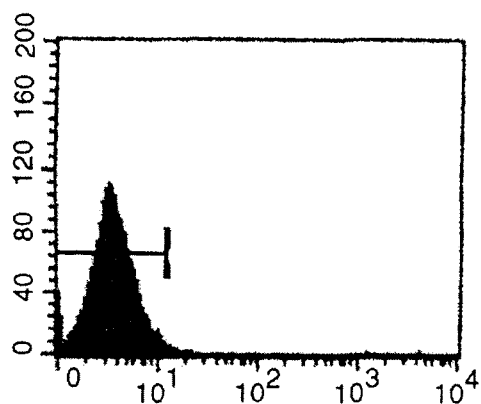


**Fig 5.4a. Untransfected BHK-21 cells**

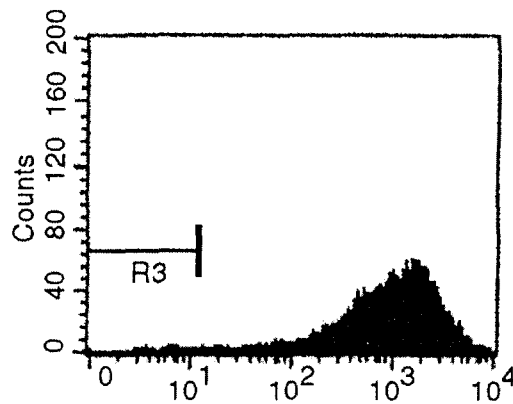


**Fig 5.4b. BHK-21 cells transfected with  $\beta$ CDP6/FITC-Oligo at 5+/-**

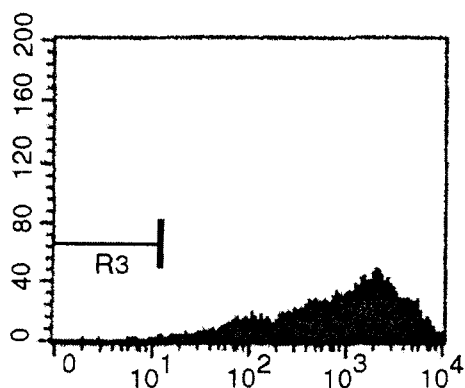


**Fig 5.4c. BHK-21 cells transfected with  $\beta$ CDP6/FITC-Oligo/50%GALA**

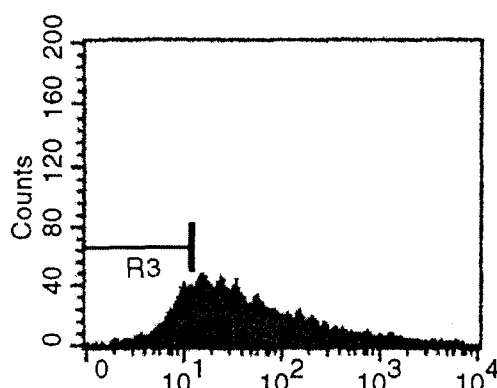


**Fig 5.4d. BHK-21 cells transfected with  $\beta$ CDP6/FITC-Oligo/50%GALA-Ad**

**Fig 5.4. Uptake of GALA-Ad and GALA modified polyplexes by BHK-21 cells.**

BHK-21 cells (4a) were transfected with  $\beta$ CDP6/FITC-Oligo (4b),  $\beta$ CDP6/FITC-Oligo/50%GALA (4c) and  $\beta$ CDP6/FITC-Oligo/50%GALA-Ad (4d). Polyplex uptake was determined by flow cytometry analysis. Data is presented as fluorescence profiles, with cell count number plotted along the y-axis and fluorescein fluorescence intensity plotted along the x-axis.

A hepatoma cell line, HUH-7, was also transfected with  $\beta$ CDP6/FITC-Oligo at 5 +/- and  $\beta$ CDP6/FITC Oligo/50% GALA-Ad polyplexes. DNA uptake was monitored as described for BHK-21 cells. The fluorescence profile for untransfected HUH-7 cells lies in the first decile (Fig 5.5a). FITC-Oligo was successfully delivered to 95% of HUH-7 cells with  $\beta$ CDP6 (Fig 5.5b). The addition of 50% GALA-Ad to the polyplexes inhibits FITC-Oligo uptake by two orders of magnitude, as observed with the BHK-21 cells (Fig 5.5c).

**5.4.4. Transfection Efficiency of Modified Complexes.** The transfection ability of GALA and GALA-Ad modified polyplexes was determined by delivery of a luciferase reporter gene to cultured cells. BHK-21 cells were plated in 24-well plates and transfected with 1  $\mu$ g of pGL-CV3 (a plasmid that contains the luciferase gene) complexed with  $\beta$ CDP6 at a charge ratio of 5+/- . These complexes were modified with the addition of GALA or GALA-Ad at various peptide/cyclodextrin ratios. The cells were lysed 48 hours after transfection and analyzed for luciferase activity, with results reported in relative light units (RLUs) (Fig 5.6).

Cells were successfully transfected with  $\beta$ CDP6/pGL-CV3 polyplexes, with RLUs  $\sim 1 \times 10^5$ . The addition of GALA did not have a large effect on transfection efficiency; however, polyplex modification with GALA-Ad greatly inhibited transfection. The addition of 1% GALA increased transfection by two-fold to  $2 \times 10^5$  RLU, and  $\beta$ CDP6/pGL-CV3/10% GALA also resulted in slightly higher transfections ( $1.5 \times 10^5$  RLU). The addition of 100% GALA decreased transfection by 50% to  $5 \times 10^4$  RLU.

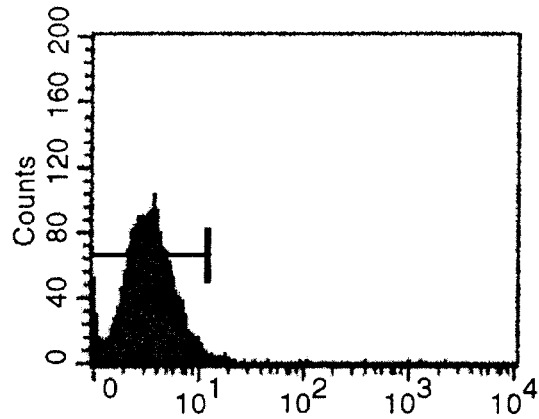


Figure 5.5a. Untransfected HUH-7 cells.

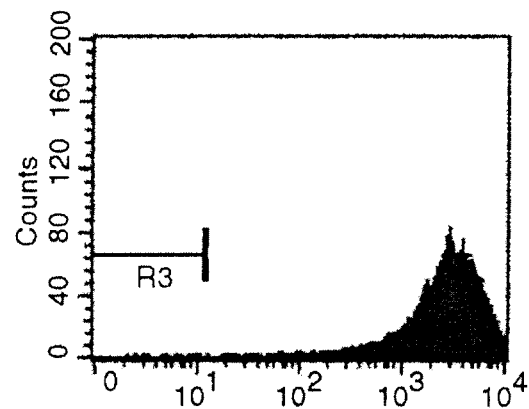


Figure 5.5b. HUH-7 transfected with  $\beta$ CDP6/FITC-Oligo at 5+/-.

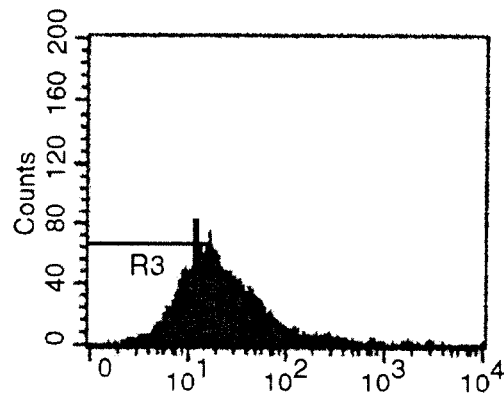
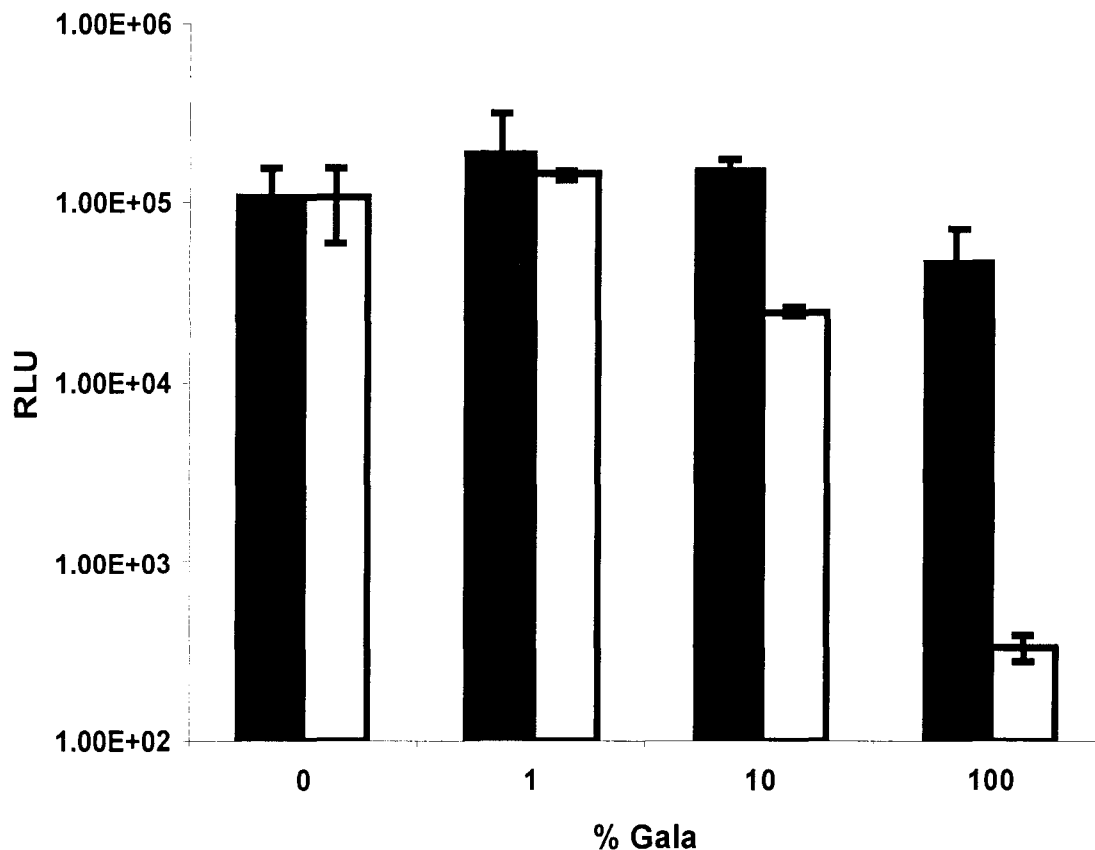


Fig 5.5c. HUH-7 transfected with  $\beta$ CDP6/FITC-Oligo/ 50% GALA-Ad.

**Figure 5.5. Uptake of GALA-Ad and GALA modified polyplexes by HUH-7 cells.** HUH-7 cells (5a) were transfected with  $\beta$ CDP6/FITC-Oligo (5b)  $\beta$ CDP6/FITC-Oligo/50%GALA-Ad (5c). Polyplex uptake was determined by flow cytometry analysis. Data is presented as fluorescence profiles, with cell count number plotted along the y-axis and fluorescein fluorescence intensity plotted along the x-axis.



**Figure 5.6.** Luciferase transfection of BHK-21 cells with  $\beta$ CDP-based polyplexes modified with GALA (shaded bars) and GALA-Ad (white bars).

BHK-21 cells were transfected with  $\beta$ CDP6/pGL-CV3 (at 5+/-) in the presence of various ratios of GALA and GALA-Ad. Transfection efficiency was determined by monitoring for luciferase activity and is reported in RLU. Data are reported as the mean  $\pm$ SD of three samples. Background =300 RLU.

The addition of 1% GALA-Ad to  $\beta$ CDP6/pGL-CV3 polyplexes also increased transfection ( $1.5 \times 10^5$  RLU). Increasing the GALA-Ad/cyclodextrin ratio further results in transfection inhibition.  $\beta$ CDP6/pGL-CV3/10% GALA-Ad decreases transfection by 1/4 to  $2.5 \times 10^4$  RLU.  $\beta$ CDP6/pGL-CV3/100% GALA-Ad eliminates nearly all transfection, with RLUs decreased by three orders of magnitude (500 RLU, background is 300 RLU).

**5.4.5. Toxicity of Modified Complexes.** The toxicity of GALA and GALA-Ad modified polyplexes was determined by measuring the protein concentrations of the cell lysates obtained in the transfection experiments. The protein concentrations of three replicates were averaged and divided by the average protein concentration of cells transfected with  $\beta$ CDP6/pGL-CV3 polyplexes alone and reported as fraction cell survival (Fig 5.7). The addition of GALA and GALA-Ad to the transfection solution resulted in no observable toxicity to BHK-21 cells.

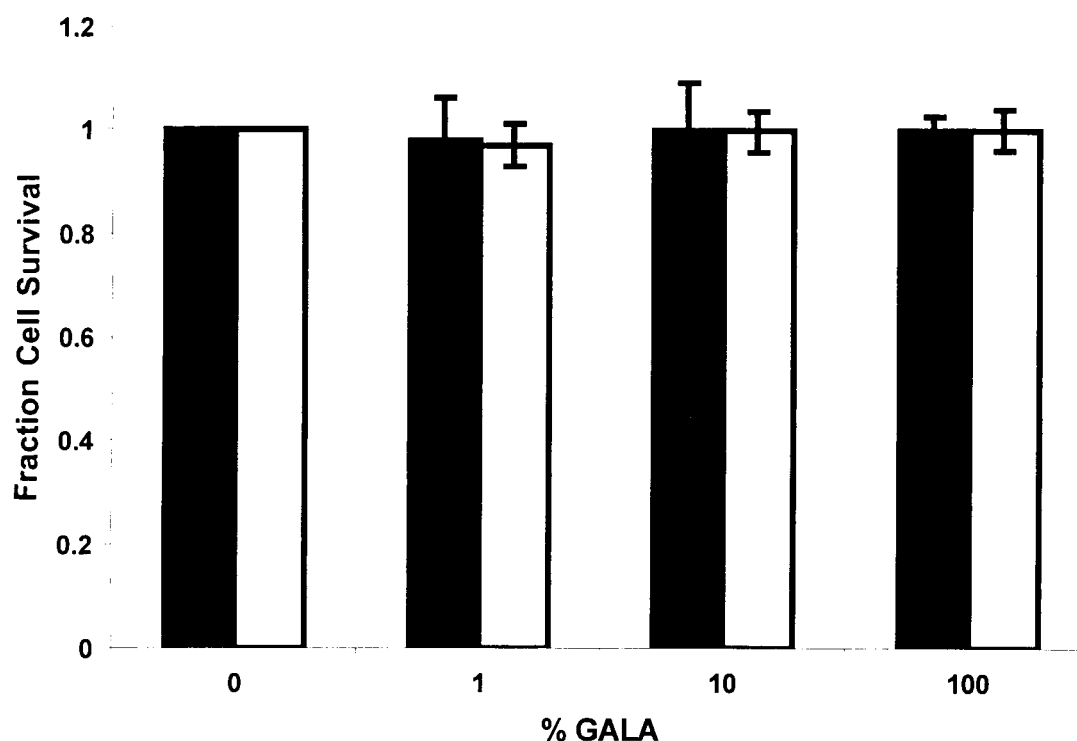


**Figure 5.7. Toxicity of GALA and GALA-Ad modified polyplexes to BHK-21 cells.** BHK-21 cells were transfected with 1  $\mu$ g of pGL-CV3 complexed with  $\beta$ CDP6 at 5+/. Prior to transfection, various ratios of GALA and GALA-Ad were added to the complexes. Cell survival for transfections in the presence of GALA (solid bars) and GALA-Ad (white bars) was determined by assaying for total protein concentrations 48 hours after transfection and normalizing each sample with protein levels for untransfected cells. Data are reported as the mean  $\pm$ SD of three samples.

## 5.5. DISCUSSION

The need exists for a method of modifying polymer/DNA particles for in vivo use after complexation without disrupting the polymer/DNA interactions that would result in a change in polyplex size. Cationic, cyclodextrin-based polymers have been used as efficient DNA delivery agents for cultured cells. The ability of cyclodextrins to form inclusion complexes with hydrophobic molecules provides a method of modifying cyclodextrin-based polyplexes. Here, adamantane is conjugated to a water soluble peptide. Adamantane is chosen as the cyclodextrin-inclusion compound because it is reported to have a binding constant with  $\beta$ -cyclodextrin of  $10^4$ - $10^5$  (11,12). GALA is selected as the modifying peptide because it is water soluble and highly anionic at physiological pH and has fusogenic abilities under acidic conditions.

The addition of GALA or GALA-Ad to  $\beta$ CDP6-based polyplexes does not disrupt DNA/polymer interactions, as evidenced by the consistency in particle count rate for all samples. However, GALA and GALA-Ad addition does influence polyplex size (Fig 5.2). The particle size changes can be explained by taking into account the zeta potentials of the particles (Fig 5.3). Particles with higher zeta potential magnitudes are less likely to aggregate due to electrostatic repulsion.  $\beta$ CDP6/plasmid DNA complexes prepared at 5+/- are stable with diameters of 260 nm and zeta potentials of +13 mV. GALA or GALA-Ad-modified  $\beta$ CDP6 polyplexes with zeta potentials between -11 and 11 mV have larger hydrodynamic diameters (~400 nm) as seen for  $\beta$ CDP6 polyplexes with 10% GALA, 30% GALA, or 10% GALA-Ad. These particles are less charged and have less electrostatic stabilization. Therefore, the increased diameter likely signifies particle coagulation. Particles with 50% or more GALA peptide added are more negatively charged (>-13 mV) and therefore return to smaller sizes (~250 nm). Similarly, particles with 30% or more GALA-Ad peptide are highly anionic and also have smaller particle diameters.

The GALA and GALA-Ad-modified polyplexes have similar zeta potential profiles at low peptide concentrations but the profiles diverge at high peptide concentrations. The zeta potential of GALA-modified polyplexes plateaus around  $-13$  mV above 30% GALA. Additionally, the zeta potential of GALA-Ad-modified polyplexes continues to decrease as GALA-Ad concentration increases.

Structures of  $\beta$ CDP6/DNA/GALA and  $\beta$ CDP6/DNA/GALA-Ad complexes are schematically proposed in Fig 5.8.  $\beta$ CDP6/DNA complexes (5+/-) are positively charged (Fig 5.8a). The anionic GALA peptide binds to the  $\beta$ CDP6/DNA complexes via electrostatic interactions. The addition of GALA at low ratios (up to 10%) begins to neutralize the polyplex charge, resulting in decreasing zeta potential (Fig 5.8b). As GALA concentration increases, the particles reach some point ( $\sim$ 50% GALA) where the positive charges are neutralized (Fig 5.8c). After this saturation point, an increase in GALA concentration doesn't have an affect on the particle zeta potential; the excess GALA remains in solution. The particles are slightly anionic, probably due to peptides that bind only partly to the complex to neutralize charge with the other part free in solution. GALA-Ad has two possible interactions with the  $\beta$ CDP6/DNA complexes: electrostatic interaction by charge and complexation of the adamantane with cyclodextrin to form inclusion compounds. At low ratios (up to 10%), the GALA-Ad probably interacts with the polyplexes by both mechanisms (Fig 5.8d). The structure of these particles is not much different from those of polyplexes with low ratios of GALA. At high ratios (30% GALA-Ad and higher), GALA-Ad is likely to interact by both charge and adamantane/cyclodextrin complexation (Fig 5.8e). This allows for a much higher saturation point for GALA peptides associated with polyplexes. The zeta potential continues to increase past 100% GALA-Ad because  $\sim$ 25% of the GALA-Ad is likely charge associated (estimated by the approximate saturation point of GALA). Assuming

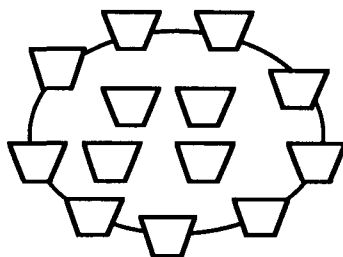


**Fig 5.8a.**  $\beta$ CDP6/DNA Complexes are positively charged at 5+/-.

### GALA Addition

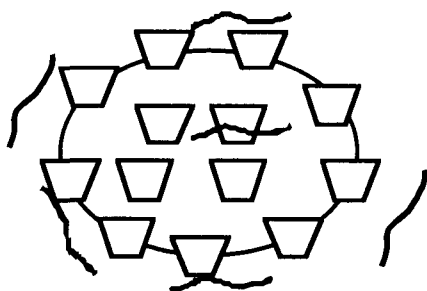


**Fig 5.8b.** At low ratios, the GALA peptide begins to neutralize polyplex charge.

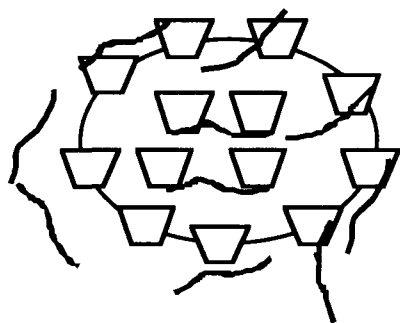


**Fig 5.8c.** At high ratios, the GALA peptides reach a “saturation” point. The positive charges are neutralized, leaving no more available binding opportunities.

### GALA-Ad Addition

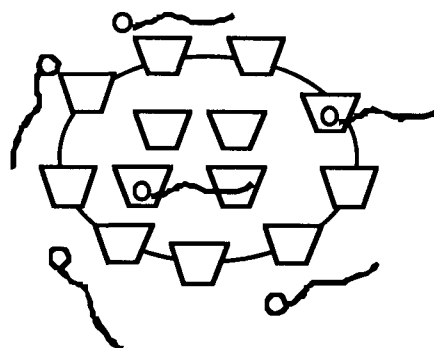


**Fig 5.8d.** At low ratios, the GALA-Ad likely interacts with the polyplex via electrostatic and complexation interactions

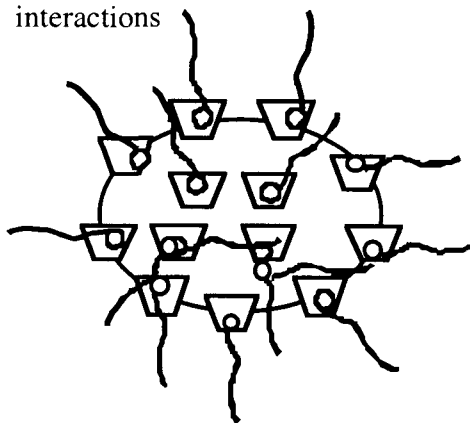


**Fig 5.8e.** At high ratios, most of the GALA-Ad is likely to interact by adamantane/cyclodextrin complexation, resulting in higher concentrations of peptide on the particle.

**Figure 5.8.** Proposed structures of GALA and GALA-Ad modified polyplexes.

very high affinity binding between adamantane and  $\beta$ -cyclodextrin, the zeta potential of the particles probably plateaus past 150% GALA-Ad.

GALA-modified polyplexes are able to efficiently deliver DNA to cultured cells (Fig 5.4c). Although  $\beta$ CDP6/DNA/50% GALA particles are negatively charged, the peptide/polyplex interaction is probably dynamic. Once the cell binds to the polyplex, the negatively charged glycoproteins on the cell surface may displace some GALA peptides from the polyplexes, resulting in stronger association and eventual uptake (5,16). The decreased zeta potential of GALA-modified polyplexes does have a small effect on DNA uptake, as evidenced by broader fluorescence distribution when compared to  $\beta$ CDP6/DNA transfected cells (Fig 5.4b). Polyplex modification with 50% GALA-Ad results in a two orders of magnitude decrease in polyplex uptake for both BHK-21 (Fig 4d) and HUH-7 (Fig 5.5c) cells. The uptake inhibition by Gala-Ad addition is probably a result of the highly negative zeta potential of the modified particles (-38 mV) that prevents the particles from close contact with the anionic cell surfaces. The GALA-Ad peptide, with MW=3194, may also provide a steric shield for the polyplexes against the cell surface, resulting in decreased uptake.

The protein expression of the delivered reporter gene is also greatly affected by GALA-Ad modification but not by GALA addition to the polyplexes (Fig 5.6). At low ratios (1% GALA), GALA or GALA-Ad addition enhances transfection by around 2-fold. The increase is probably due to the fusogenic properties of GALA at low pH. The GALA peptide has been shown to cause lipid vesicle leakage at pH 5 (14). Simoes et al. report a 5-fold increase in the transfection efficiency of HeLa cells due to the association of GALA peptide with lipoplexes (15). The fusogenic effect has not been optimized in this system; however, the increase in transfection efficiency at low ratios is nonetheless evident.

At higher peptide ratios (10% and 100%), GALA-Ad modification impedes DNA transfection, such that at 100% GALA-Ad, nearly all reporter gene expression has been

eliminated. As discussed previously, the anionic GALA-Ad complexes with the cyclodextrin molecules in the polymer and decreases particle uptake. Although some complexes are internalized, the number of intracellular complexes is two orders of magnitude lower than the amount of non-modified polyplexes internalized under the same conditions. The low number of internalized polyplexes, compounded with the low frequency of endosomal release (see previous chapter) likely results in the low transfection levels observed. DNA uptake and transfection inhibition ability is unique to adamantane modified GALA; addition of 100% GALA decreases transfection by only 50%.

GALA and GALA-Ad modification of polyplexes does not increase cellular toxicity (Fig 5.7). The addition of 100% GALA or GALA-Ad (corresponds to 20  $\mu$ M peptide in solution during transfection) to cells for 48 hours results in no change in cell proliferation.

In conclusion, this work has shown that  $\beta$ CDP6-based polyplexes can be modified by adamantane-containing conjugates without disrupting polymer/DNA binding interactions. In this proof-of-concept example,  $\beta$ CDP6-based polyplexes were modified by adamantane conjugated to an anionic, water-soluble peptide (GALA). The adamantane moiety formed inclusion compound with the cyclodextrins. The modified-polyplexes were highly anionic due to the attached GALA peptides, resulting in inhibition of polyplex uptake by cultured cells. One practical application of this system could be targeted gene delivery. Cationic polyplexes deliver genes to cells non-specifically. Coating the polyplexes with an anionic peptide such as GALA prevents nonspecific uptake. The polyplexes could then be modified with an appropriate ligand to allow for receptor-mediated uptake into targeted cells. Therefore, the ability to modify polyplexes provides a way to include multiple alterations, thereby increasing the suitability of polyplexes for systemic gene delivery. Some of the possible modifications will be discussed in the following chapter.

## 5.6. LITERATURE CITED.

- (1) Behr, J.-P. *Acc. Chem. Res. Synthetic Gene-Transfer Vectors* **1993**, *26*, 274-278.
- (2) Bielinska, A. U., Kukowska-Latallo, J. F., Jr., J. R. B. *Biochimica et Biophysica Acta* The interaction of plasmid DNA with polyamidoamine dendrimers: mechanism of complex formation and analysis of alterations induced in nuclease sensitivity and transcriptional activity of the complexed DNA **1997**, *1353*, 180-190.
- (3) Boussif, O., Lezoualch, F., Zanta, M. A., Mergny, M. D., Scherman, D., Demeneix, B., Behr, J.-P. *Proceedings of the National Academy of Sciences* A versatile vector for gene and oligonucleotide transfer into cells in culture and in vivo: Polyethylenimine **1995**, *92*, 7297-7301.
- (4) Felgner, P. L., Barenholz, Y., Behr, J. P., Cheng, S. H., Cullis, P., Huang, L., Jessee, J. A., Seymour, L., Szoka, F., Thierry, A. R., Wagner, E., Wu, G. *Human Gene Therapy* Nomenclature for synthetic gene delivery systems **1997**, *8*, 511-512.
- (5) Mislick, K. A., Baldeschwielder, J. D. *Proceedings of the National Academy of Sciences* Evidence for the role of proteoglycans in cation-mediated gene transfer **1996**, *93*, 12349-12354.
- (6) Dash, P., Read, M., Barrett, L., Wolfert, M., Seymour, L. *Gene Therapy* Factors affecting blood clearance and in vivo distribution of polyelectrolyte complexes for gene delivery. **1999**, *6*, 643-650.
- (7) Nishikawa, M., Takemura, S., Takakura, Y., Hashida, M. *J. Pharm. Exp. Ther.* Targeted delivery of plasmid DNA to hepatocytes in vivo: Optimization of the pharmacokinetics of plasmid DNA galactosylated poly(L-lysine) complexes by controlling their physicochemical properties **1998**, *287*, 408-415.

- (8) Choi, Y. H., Liu, F., Kim, J.-S., Choi, Y. K., Park, J. S., Kim, S. W. *Journal of Controlled Release* Polyethylene glycol-grafted poly-L-lysine as polymeric gene carrier **1998**, *54*, 39-48.
- (9) Ogris, M., Brunner, S., Schuller, S., Kircheis, R., Wagner, E. *Gene Therapy* PEGylated DNA/transferrin-PEI complexes: reduced interaction with blood components, extended circulation in blood and potential for systemic gene delivery **1999**, *6*, 595-605.
- (10) Gonzalez, H., Hwang, S. J., Davis, M. E. *Bioconjugate Chemistry* New class of polymers for the delivery of macromolecular therapeutics **1999**, *10*, 1068-1074.
- (11) Cromwell, W., Bystrom, K., Eftink, M. *J Phys Chem-US* Cyclodextrin Adamantanecarboxylate inclusion complexes-studies of the variation in cavity size **1985**, *89*, 326-332.
- (12) Eftink, M., Andy, M., Bystrom, K. *J Am Chem Soc* Cyclodextrin inclusion complexes-studies of the variation in the size of alicyclic guests **1989**, *111*, 6765-6772.
- (13) Parente, R. A., Nadasdi, L., Subbarao, N. K., Szoka, F. C. *Biochemistry* Association of a pH-sensitive peptide with membrane vesicles: Role of Amino Acid Sequence **1990**, *29*, 8713-8719.
- (14) Parente, R. A., Nir, S., Francis C. Szoka, J. *Biochemistry* Mechanism of Leakage of Phospholipid Vesicle Contents Induced by the Peptide GALA **1990**, *29*, 8720-8728.
- (15) Simoes, S., Slepshkin, V., Gaspar, R., Pedrosos de Lima, M., Duzgunes, N. *Gene Therapy* Gene delivery by negatively charged ternary complexes of DNA, cationic liposomes and transferrin or fusogenic peptides **1998**, *5*, 955-964.

(16) Ruponen, M., Yla-Herttuala, S., Urtti, A. *Biochemica et Biophysica Acta-Biomembranes* Interactions of polymeric and liposomal gene delivery systems with extracellular glycosaminoglycans: physicochemical and transfection studies **1999**, *1415*, 331-341.

## Chapter 6

# Applications of $\beta$ -Cyclodextrin Polymer-Containing Polyplexes Modified by Inclusion Complex Formation

### 6.1. ABSTRACT

Modifications of cationic polyplexes to impart salt stability, to add transfection enhancing agents, and to target delivery are plausible enhancements that may be required for transferring the use of these delivery systems from in vitro settings to in vivo systems. Here, the use of inclusion complex formation that was described in the previous chapter is applied to  $\beta$ CDP polyplexes in order to ascertain whether they can be suitably modified into agents suitable for in vivo use. While copolymers of PEG and  $\beta$ CDP6 are unable to condense DNA, pegylation of  $\beta$ CDP polyplexes by inclusion compound formation results in small, discrete particles that are salt-stabilized in a PEG length-dependent manner. In addition, fluorescein-labeled PEG (Peg-FITC) complexed with  $\beta$ CDP6 polyplexes ( $\beta$ CDP6/Ad-Peg-FITC) are preferentially delivered to cultured cells over uncomplexed Peg-FITC, demonstrating the possibility of co-delivery of small molecule therapeutics or transfection enhancement agents with  $\beta$ CDP polyplexes. Finally, hepatocyte-targeted delivery via galactose-modified  $\beta$ CDP6 polyplexes is investigated. Preliminary experiments suggest the need for a “spacer” between polyplex and ligand for effective delivery as well as a method for preventing non-specific, charge-mediated uptake. Thus, this chapter demonstrates and proposes variations to  $\beta$ CDP6 polyplexes to accommodate targeted in vivo delivery.

## 6.2 INTRODUCTION

The objective of this research was to apply the  $\beta$ CDP polyplex modification method described in the previous chapter towards the development of a suitable  $\beta$ CDP-based systemic delivery system. Three possible polyplex modifications will be discussed, each with important implications for in vivo applications: steric stabilization of polyplexes, co-delivery of transfection enhancement agents or small molecule therapeutics, and ligand attachment for targeted delivery.

Polyplexes need to be small and stable to accommodate sustained systemic circulation. Most unmodified polyplexes never arrive at their target site due to self-aggregation upon injection, trapping in extracellular matrices, and rapid elimination from the body by phagocytes (1). Nanoparticles are known to be unstable due to van der Waals attraction forces that become important when particles come in close contact with each other. When formulated in water, cationic polyplexes have a double layer of anionic counterions that serve to stabilize particles by repulsion. However, in aqueous salt, the electrostatic double layer around each particle is reduced. At physiological salt conditions, the double layer thickness of charged particles is usually reduced to  $< 1$ nm. The electrostatic repulsion at these concentrations is insufficient for overcoming van der Waals attractions, and results in rapid particle aggregation. In addition to self-aggregation, cationic polyplexes bind nonspecifically to extracellular matrices or blood proteins. The amount of blood proteins bound to particles correlates with in vivo clearance (2) and often results in complement activation (3). Charged particles are also a target for the phagocytic system (4).

One method of preventing self-aggregation or unwanted particle interactions is polymeric steric stabilization. Polymers attached to particle surfaces serve to stabilize particles by sterically inhibiting inter-particle, protein, and cell contact. This method has been successfully used in many colloidal systems (5). Polyethylene glycol (PEG) holds

particular interest for gene delivery applications due to its biocompatibility. PEG has been grafted to liposomes (6), poly-L-lysine (PLL, (7-9)), polyethylenimine (PEI, (10)), and various peptides (11,12). In general, pegylated particles show increased salt and serum stability with longer in vivo circulation.

Pegylation of  $\beta$ -cyclodextrin polymers ( $\beta$ CDPs) is discussed in the first section of this chapter. Three pegylation approaches were applied to  $\beta$ CDP6: pre-DNA-complexation pegylation, post-DNA-complexation pegylation by grafting, and post-DNA-complexation pegylation by inclusion compound formation. While the first two approaches result in disruption of polymer/DNA binding, post-DNA-complexation of  $\beta$ CDP6 polyplexes with an adamantane-modified PEG imparts salt stability to the particles.

The ability to co-deliver small molecules or transfection enhancing agents with  $\beta$ CDP polyplexes would increase the efficacy of the delivery system. For example, a delivery package with combinations of genes and small molecules could target several points in a disease pathway, resulting in a more effective treatment. The co-delivery of a fusogenic peptide or pH-sensitive polymer could assist in endosomal release of the polyplexes, thus enhancing gene delivery. In the second section of this chapter,  $\beta$ CDP polyplexes are modified with a polymer (PEG) covalently attached to a small molecule (fluorescein). Cultured cells exposed to the modified polyplexes show much higher fluorescein uptake than cells exposed to free fluorescein-PEG in the presence of polyplexes, thus demonstrating the potential of multicomponent therapeutic delivery systems.

Finally, systemic delivery calls for specific uptake to the cells of interest. One method of accomplishing selective gene transfer is via receptor-mediated targeting. Ligands such as folate, transferrin or galactose have been used in synthetic delivery systems to target cells expressing folate (13-15), transferrin (16,17), or asialoglycoprotein receptors (18-20) on their surface. Asialoglycoprotein receptors are expressed on the

surface of hepatocytes, and gene therapy systems targeting these receptors are known to be effective for in vivo delivery to the liver (21). The liver is an important target organ for several genetic diseases such as Crigler-Najjar, Pompe's disease, phenylketonuria, and hemophilia. The asialoglycoprotein receptor recognizes terminal galactose residues of oligosaccharides (22). The last section of the paper discusses possible approaches for targeting  $\beta$ CDP polyplexes to hepatocytes by galactose conjugation.

### 6.3 MATERIALS AND METHODS

#### 6.3.1 Synthesis of Adamantane Conjugates.

*Adamantane-PEG<sub>3400</sub>-NH<sub>2</sub> (Ad-PEG<sub>3400</sub>-NH<sub>2</sub>).* 266 mg of Fmoc-PEG<sub>3400</sub>-NHS (78.2  $\mu$ mol, Shearwater Polymers, Huntsville AL) were added to a glass vial equipped with a magnetic stirbar. 10 eq. of 1-adamantane-methylamine (1.5 mmol, Aldrich) dissolved in 3 mL of DCM were then added and the solution stirred overnight at room temperature. The solvent was removed in vacuo and water was added to the remaining solution to dissolve the PEG product. The solution was centrifuged at 20K rcf for 10 minutes, whereupon the adamantane-methylamine phase-separated as a denser liquid. The aqueous portion was collected and water removed in vacuo. The remaining viscous liquid was redissolved in 20% piperidine in DMF for Fmoc deprotection and stirred for 30 minutes at room temperature. The solvent was removed in vacuo, washed several times with DMF, redissolved in water, and run on an anionic exchange column to remove unreacted PEG. The first fractions were collected and lyophilized to yield 222 mg of a white, fluffy powder (76% yield). The desired product was confirmed by MALDI-TOF analysis.

*Adamantane-PEG<sub>3400</sub>-Lactose (Ad-PEG<sub>3400</sub>-Lac).* 60 mg of Ad-PEG<sub>3400</sub>-NH<sub>2</sub> (16.8  $\mu$ mol) and 5.0 eq of lactose-monosuccidimyl (50 mg, Pierce, Rockford, IL) were added to a

glass vial equipped with a stirbar. 2 mL of 50 mM NaHCO<sub>3</sub> was added and the resulting solution stirred overnight. The reaction of the amine was monitored by TNBS assay, that determines amine concentrations (23). Upon full reaction of the amine (99% amine reacted), the solution was transferred to a dialysis tubing (Slide-A-Lyzer, MWCO=3500, Pierce), dialyzed for 24 hours against water, and lyophilized to yield 65.1 mg of a fluffy white powder (93% yield).

*Adamantane-PEG<sub>5000</sub> (Ad-PEG<sub>5000</sub>)*. 279 mg of PEG<sub>5000</sub>-NHS (53 μmol, Shearwater Polymers) were added to a glass vial equipped with a magnetic stirbar. 8 eq. of 1-adamantane-methylamine (420 μmol, Aldrich) dissolved in 3 mL of DCM were then added and the solution stirred overnight at room temperature. The solvent was removed in vacuo and water was added to the remaining solution to dissolve the PEG product. The solution was centrifuged at 20K rcf for 10 minutes, whereupon the adamantane-methylamine phase separated as a denser liquid. The aqueous portion was collected and dialyzed for 24 hours (Slide-A-Lyzer, MWCO=3500) against water. The solution was lyophilized to yield 252 mg of a white, fluffy powder (92% yield) .

*Adamantane-(PEG<sub>5000</sub>)<sub>2</sub> (Ad-(PEG<sub>5000</sub>)<sub>2</sub>)*. 315 mg of (PEG<sub>5000</sub>)<sub>2</sub>-NHS (30 μmol, Shearwater Polymers) were added to a glass vial equipped with a magnetic stirbar. 10 eq. of 1-adamantane-methylamine (300 μmol, Aldrich) dissolved in 3 mL of DCM were then added and the solution stirred overnight at room temperature. The solvent was removed in vacuo and water was added to the remaining solution to dissolve the PEG product. The solution was centrifuged at 20K rcf for 10 minutes, whereupon the adamantane-methylamine phase separated as a denser liquid. The aqueous portion was collected and dialyzed for 24 hours (Slide-A-Lyzer, MWCO=3500) against water. The solution was lyophilized to yield 286 mg of a white, fluffy powder (91% yield) .

*Adamantane-PEG<sub>3400</sub>-Fluorescein (Ad-PEG<sub>3400</sub>-FITC)*. 20 mg of Ad-PEG<sub>3400</sub>-NH<sub>2</sub> were dissolved in 3 mL of 0.1M Na<sub>2</sub>CO<sub>3</sub> in a glass vial equipped with a magnetic stirbar. To this solution were added 3 eq of fluorescein isothiocyanate (FITC, Sigma) in DMSO (4 mg/mL, 1.6 mL) and the resulting solution was stirred in the dark overnight before transferring to dialysis tubing (MWCO=3500) and dialyzing in the dark for 48 hours against water. The solution was collected and lyophilized to yield 23 mg of a yellow fluffy solid. PEG<sub>3400</sub>-FITC was synthesized as a control polymer from PEG<sub>3400</sub>-NH<sub>2</sub> (Sheaterwater Polymers) with the same protocol to yield 23 mg.

### 6.3.2 Synthesis of Cyclodextrin-based Polymers.

*β-cyclodextrin-DMS copolymer (βCDP6)*. The β-cyclodextrin-DMS copolymer was prepared as described previously (24). In brief, β-CD dicysteamine and an equimolar amount of dimethyl suberimidate (DMS, Pierce, Rockford, Illinois) were dissolved in 0.5 M Na<sub>2</sub>CO<sub>3</sub> and stirred overnight at room temperature. The pH of the resulting solution was brought below 5.0 by the addition of 1 M HCl and dialyzed extensively against dH<sub>2</sub>O in a MWCO 3500 dialysis membrane (Pierce) for 24 hours. The dialyzed solution was lyophilized to dryness to yield a white, fluffy solid, with typical yields around 25-30%.

*Lactose-CDP6 (Lac-CDP6)*. βCDP6 (20.5 mg, 3 μmol), 10 eq of α-lactose (21 mg, 60 μmol, Sigma), and 18.6 mg of sodium cyanoborohydride (300 μmol) were added to a glass vial. 1 mL of borate buffer, pH 8.5 was added to the solids and the resulting solution was vortexed briefly before incubating in a 37 °C water bath for 30 hours. The solution was acidified to pH 6.0 with the addition of 1M HCl and dialyzed against water (28) for 24 hours. TNBS assay for polymer amines revealed 87% conjugation.

*Lactose-(CH<sub>2</sub>)<sub>6</sub>-CDP6 (Lac-C6-CDP6)*. βCDP6 (43.2 mg, 7.4 μmol) and 5.6 eq of mono(lactosylamido) mono(succinimidyl) suberate (50 mg, 84 μmol, Pierce) were added

to a glass vial equipped with a magnetic stirbar and dissolved in 2 mL of 50 mM  $\text{NaHCO}_3$ . The resulting solution was stirred overnight. The reaction was followed by monitoring the disappearance of the polymer amine endgroups by TNBS assay, which revealed 90% conjugation. The solution was acidified to pH 5.0 by the addition of 1M HCl and resulting solution dialyzed against water in Pierce MWCO 3500 Slide-A-Lyzer for 2 days before lyophilization. A white, fluffy powder was obtained in 70% yield.

*PEG<sub>3400</sub>-CDP6*. 20.3 mg of  $\beta\text{CDP6}$  (3  $\mu\text{mol}$ ) and 10 eq of Fmoc-Peg<sub>3400</sub>-NHS (190 mg, 60  $\mu\text{mol}$ ) were added to a glass vial equipped with a magnetic stirbar and dissolved in 1 mL of 50 mM  $\text{NaHCO}_3$ , pH 8.5. The solution was stirred in the dark at room temperature for 20 hours and then lyophilized. The solid was dissolved in 0.5 mL of 20% piperidine in DMF and stirred for 30 minutes for Fmoc deprotection. The solvent was removed in vacuo and the remaining viscous liquid dissolved in water and the pH brought below 6.0 with 0.1 M HCl. The polymer was separated from unreacted PEG by anion exchange chromatography and lyophilized to yield a white fluffy powder.

### 6.3.3. Polyplex Preparation and Characterization.

*Plasmids and Oligos*. Plasmid pGL3-CV (Promega, Madison, WI), containing the luciferase gene under the control of the SV40 promoter, was amplified by *Esherichia Coli* and purified using Qiagen's Endotoxin-free Megaprep kit (Valencia, CA). Oligonucleotides with a random sequence (25-mers, 5'-ACT GCT TAC CAG GGA TTTCAG TGC A-3') and fluorescein labeled oligos with the same sequence (FITC-Oligo) were synthesized by the Biopolymer Synthesis Facility (California Institute of Technology).

*Particle Sizing*. 2  $\mu\text{g}$  of pGL3-CV in 600  $\mu\text{L}$  of  $\text{dH}_2\text{O}$  were mixed with an equal volume of  $\beta\text{CDP6}$  (in  $\text{dH}_2\text{O}$ ) at a charge ratio of 5+/- . Particle size was measured using a

ZetaPals dynamic light scattering detector (Brookhaven Instruments Corporation, Holtsville, NY).

*Post-DNA-complexation Pegylation by Grafting.* The procedure used was modified from Ogris et al. (10). 5  $\mu\text{g}$  of pGL3-CV in 500  $\mu\text{L}$  of  $\text{dH}_2\text{O}$  were mixed with an equal volume of PEI (in  $\text{dH}_2\text{O}$ ) at 3+/- or 6+/- .  $\beta\text{CDP6}$  complexes were prepared in the same manner at a charge ratio of 5+/- . The polyplex diameters were measured by dynamic light scattering (DLS). After complex formation, PEG<sub>5000</sub>-SPA (10 mg/mL in DMF) was added to the solution mixed at room temperature for two hours. After particle size determination, 500  $\mu\text{L}$  of PBS, pH 7.2, were added to the solution. The solution was incubated for 30 minutes at room temperature before final particle sizes were measured by DLS.

*Post-DNA-complexation Pegylation by Inclusion Compound Formation.* 2  $\mu\text{g}$  of pGL3-CV in 600  $\mu\text{L}$  of  $\text{dH}_2\text{O}$  were mixed with an equal volume of  $\beta\text{CDP6}$  (in  $\text{dH}_2\text{O}$ ) at a charge ratio of 5+/- . The desired amount of Ad-PEG (10 mg/mL in  $\text{dH}_2\text{O}$ ) was added and particle size determined by DLS. 600  $\mu\text{L}$  of PBS, pH 7.2, were added to the solution and particle size monitored in 2 minute intervals for 8 minutes.

#### **6.3.4. Cell Culture and Transfection Experiments.**

*Cells.* BHK-21, baby hamster kidney cells, were purchased from ATCC (Rockville, MD) and HUH-7, human hepatoma cells, were generously donated by Valigen (Newtown, PA). Both cell lines were cultured in DMEM supplemented with 10% fetal bovine serum, 100 units/mL penicillin, 100  $\mu\text{g}/\text{mL}$  streptomycin, and 0.25  $\mu\text{g}/\text{mL}$  amphotericin in a humidified incubator operated at 37 °C and 5%  $\text{CO}_2$  and passaged every 4-5 days. Media and supplements were purchased from Gibco BRL (Gaithersburg, MD).

*$\beta$ CDP6/Ad-PEG<sub>3400</sub>-FITC Polyplex Formation and Delivery to Cultured Cells.* BHK-21 cells were plated in 6-well plates at 200,000 cells/well and incubated for 24 hours at 37 °C. 3  $\mu$ g of Junk-oligo (0.1 mg/mL in dH<sub>2</sub>O) were complexed with an equal volume of  $\beta$ CDP6 (2 mg/mL in dH<sub>2</sub>O) at a 5 +/- charge ratio. After a 5 minute complexation time, 1.5  $\mu$ L of PEG-FITC or Ad-PEG-FITC (10  $\mu$ g/mL in dH<sub>2</sub>O) were added to the complexes. Media was removed from the cells and cells washed with PBS. For transfection, 940  $\mu$ L of Optimem were added to each polyplex solution and the entire solution transferred to the cells. The cells were incubated with the transfection mixture for 4 hours before removing the media, washing the cells with PBS, and adding in 4 mL of complete media. The cells were incubated for another 24 hours at 37 °C before media was removed and cells washed twice with PBS. The cells were collected by trypsinization and prepared for FACs analysis. Cells were washed twice in wash buffer (Hank's Balanced Salt solution containing DNase and MgCl<sub>2</sub>) and resuspended in 500  $\mu$ L FACS buffer (Hank's Balanced Salt Solution, 2.5 mg/ml bovine serum albumin, 10  $\mu$ g/mL propidium iodide). FACS analysis was performed using a FACSCalibur flow cytometer (Becton Dickinson, San Jose, CA) and CellQuest software.

*Luciferase Transfection.* HUH-7 cells were plated in 24-well plates at 50,000 cells/well and incubated for 24 hours at 37 °C. 3  $\mu$ g of pGL3-CV plasmid (0.1 mg/mL in dH<sub>2</sub>O) were complexed with an equal volume of  $\beta$ CDP6 or Lac- $\beta$ CDP6 at various charge ratios. Media was removed from the cells prior to transfection and cells washed with PBS. 600  $\mu$ L of Optimem were added to each polyplex solution and 230  $\mu$ L transfection solution of this transfection solution were added to each of 3 wells for 4 hours. After four hours, 800  $\mu$ L of complete media were added to each well. Media was changed 24 hours after transfection and cells were lysed in 50  $\mu$ L of Cell Culture Lysis Buffer (Promega, Madison, WI) 48 hours after transfection. Luciferase activity was analyzed using Promega's luciferase assay reagent.

## 6.4 RESULTS AND DISCUSSION

### 6.4.1. Polyplex Stabilization by Pegylation.

Pegylation has been used to confer *in vivo* stability to lipoplexes and polyplexes. In this section, three methods of pegylating  $\beta$ CDPs are discussed: pre-DNA-complexation pegylation, post-DNA-complexation pegylation by grafting, and post-DNA-complexation pegylation by inclusion compound formation.

*Pre-DNA-complexation pegylation.* PEG<sub>3400</sub>-NHS was coupled to the  $\beta$ CDP6 amine endgroups to give the polymer shown in Fig 6.1 ( $\beta$ CDP6-PEG<sub>3400</sub>).

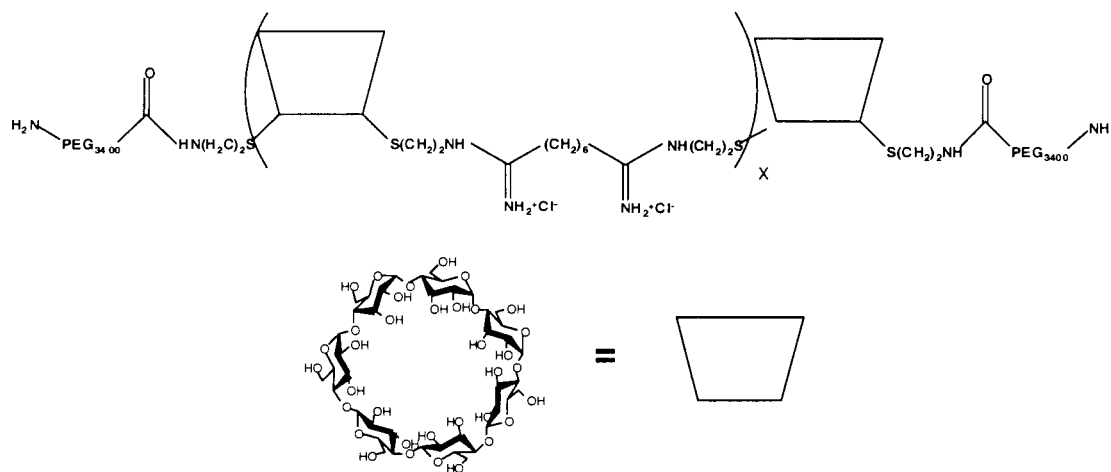
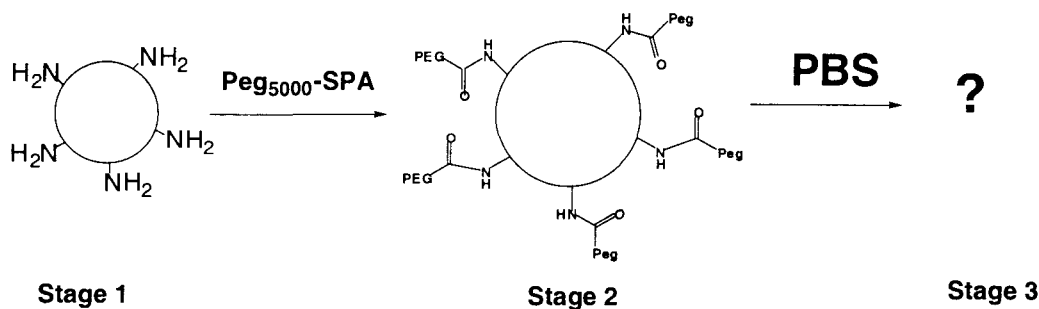


Figure 6.1. Structure of  $\beta$ CDP6-PEG<sub>3400</sub>.

The pegylated polymer was mixed with plasmid DNA for particle size measurements. While  $\beta$ CDP6 condenses plasmid DNA to uniform particles with hydrodynamic diameter  $\sim$ 130 nm, pegylated  $\beta$ CDP6 is unable to condense DNA. The presence of PEG at the

polymer termini disrupts DNA binding. Choi et al. report successful albeit reduced DNA binding with pegylated PLL (7). However, they used PLL with MW 25,000, that contains on average 170 amines/polymer strand. The higher charge density results in a higher DNA binding constant. The  $\beta$ CDP6 contains on average 10 charges/polymer strand. Although the number of charges per polymer strand is unchanged, pegylation doubles the molecular weight of each polymer. Therefore, it is not surprising that pegylation of the  $\beta$ CDPs reduces the polymer charge density, thereby eliminating DNA binding ability.

*Post-DNA-complexation pegylation by grafting.* Ogris et al. pegylated transferrin/PEI and PEI after complexation with plasmid DNA by reacting the primary amino groups in PEI with PEG<sub>5000</sub>-SPA (10). The pegylated polyplexes were stable in salt, whereas the unpegylated polyplexes aggregated upon addition of PBS. This method of pegylation was applied to  $\beta$ CDP6-based polyplexes. PEI-based polyplexes were also used as a control. A schematic of the experimental method used is shown in Fig 6.2. In Stage 1, PEI/DNA or  $\beta$ CDP6/DNA complexes were formed in 1.2 mL dH<sub>2</sub>O. The sizes of the particles were determined by dynamic light scattering (DLS). PEG<sub>5000</sub>-SPA was added to the polyplex solutions in Stage 2 and allowed to react with the polymer primary amino groups for 1 hour. The sizes of the pegylated samples were measured by DLS. For Stage 3, 600  $\mu$ L of PBS, pH 7.2, were added to each sample to test the salt stability of pegylated particles. The particle sizes were determined 30 min after salt addition to determine the extent of particle aggregation.



**Figure 6.2. Scheme for post-DNA-complexation pegylation by grafting.**

Polyplexes are prepared in  $\text{dH}_2\text{O}$  in Stage 1 and diluted in  $\text{dH}_2\text{O}$  for light scattering measurements. The particles are pegylated in Stage 2 by reacting  $\text{PEG}_{5000}\text{-SPA}$  onto the primary amine groups. PBS is then added to the polyplexes and the extent of salt-induced aggregation is determined after 30 minutes by dynamic light scattering.

PEI polyplexes were formulated at 3+/- and 6 +/- and  $\beta\text{CDP6}$  polyplexes were formulated at 5+/- for Stage 1.  $\text{PEG}_{5000}\text{-SPA}$  was added to PEI at 10:1 w/w according to the procedure published by Ogris et al (10).  $\beta\text{CDP6}$  was pegylated with 100%, 150% and 200% PEG:amine (mol%). As a control, unreactive PEG was also added to  $\beta\text{CDP6}$  at 100%. The particle diameters at each stage are presented in Table 6.1. The PEI polyplexes increased slightly in size upon pegylation (58 nm to 65 nm for 3+/- and 55 nm to 60 nm for 6+/-). Pegylation protected the PEI polyplexes against salt-induced aggregation. While unmodified PEI particles increase in diameter to ~800 nm after salt addition, pegylated PEI polyplexes increased slightly in size to 78 nm (for 6+/-) and 115 nm (for 3+/-).

Polyplex	PEG	Stage 1 (nm)	Stage 2 (nm)	Stage 3 (nm)
PEI 3+/-	10:1	58	65	115
PEI 6+/-	10:1	55	60	78
$\beta$ CDP6 5+/-	100%	70	67.4	303
$\beta$ CDP6 5+/-	150%	70	X*	N/A
$\beta$ CDP6 5+/-	200%	70	X	N/A
$\beta$ CDP6 5+/-	100% PEG**	67	81	700

\*Poor correlation function; no size measurements possible.

\*\*Free PEG added instead of PEG<sub>5000</sub>-SPA

**Table 6.1. Particle sizes of PEI and  $\beta$ CDP6 polyplexes during post-DNA-complexation pegylation by grafting.**

For Stage 1, 5  $\mu$ g of DNA plasmid (in 500  $\mu$ L of dH<sub>2</sub>O) was mixed with PEI or  $\beta$ CDP6 (in 500  $\mu$ L of dH<sub>2</sub>O) at the indicated ratios. PEG<sub>5000</sub>-SPA (10 mg/mL in DMF) was then added to the polyplexes in Stage 2. The PEG<sub>5000</sub>-SPA was allowed to react with the polymer primary amines. After 2 hours, 500  $\mu$ L of PBS, pH 7.2, was added to solution. The solution was incubated for 30 minutes before particle size measurement. All particle sizes were determined by dynamic light scattering and reported as the mean of three measurements.

The addition of 150% and 200% PEG<sub>5000</sub>-SPA to  $\beta$ CDP6-based polyplexes results in particle disruption; particle counts drop drastically and no consistent correlation function was observed. Pegylation of  $\beta$ CDP6 likely prevents polymer/DNA binding. The particle size is maintained at 67 nm after pegylation with 100% PEG<sub>5000</sub>-SPA. However, monitoring of particle size as a function of time revealed that the particles were disrupted for approximately 30 seconds after PEG addition, after which the small particles were again observed. Therefore, the addition of 100% PEG<sub>5000</sub>-SPA may pegylate a fraction of the  $\beta$ CDP6. Because the polymer is added in excess with respect to the DNA (at a 5+/-), the particles could then rearrange such that the unmodified polymers form polyplexes with the plasmid DNA while most of the pegylated polymer remain free

in solution. Salt addition to these particles results in particle aggregation (300 nm), although not to the extent of unmodified  $\beta$ CDP6 polyplexes (700 nm). In summary, post-DNA-complexation pegylation by reaction with polymer primary amino groups is likely to be effective for high MW polymers with high charge densities. However, reaction with  $\beta$ CDP6, even post-DNA complexation, results in lack of salt stabilization at 100% PEG<sub>5000</sub>-SPA addition and particle disruption with higher PEG<sub>5000</sub>-SPA concentrations.

*Post-DNA-complexation pegylation by inclusion compound formation.* Another approach to post-complexation pegylation is to use the ability of cyclodextrins to form inclusion complexes with guest molecules. Therefore, adamantane, that has a  $10^4$ - $10^5$  binding constant with cyclodextrin, was conjugated to various PEGs (Fig 6.3).

The adamantane-PEG (Ad-PEG) molecules were added to solutions of preformed polyplexes at 100% adamantane to cyclodextrin (mol%). PBS was then added to the solutions and the particle size monitored by DLS in 2 minute intervals (Fig 6.4). The average diameter of unpegylated  $\beta$ CDP6 particles increases from 58 nm to 250 nm within 8 minutes after salt addition. The presence of free PEG in solution does not prevent aggregation (average diameter of 240 nm after salt addition). However, pegylation with linear Ad-PEG molecules reduces particle aggregation in a length dependent matter. 8 minutes after salt addition, particles pegylated with Ad-PEG<sub>3400</sub> aggregate to 210 nm in diameter while particles with Ad-PEG<sub>3400</sub>-Lac aggregate to 200 nm. Particles pegylated with Ad-PEG<sub>5000</sub> only increase in diameter to 90 nm 8 minutes after salt addition and to 160 nm 2 hours after salt addition (data not shown). Modification with Ad-(PEG<sub>5000</sub>)<sub>2</sub> had a small effect on aggregation (particle diameter of 200 nm after salt addition).

Pegylation of polyplexes alleviates salt-induced aggregation by providing a steric layer around the particles. The steric layer prevents close contact between particles by keeping the van der Waals attraction forces, that is dependent on the interparticle

distance, lower than the thermal energy of the particles. Therefore, there should be a critical polymer length greater than the range of van der Waals attraction between particles that results in polymer stabilization. For many colloidal systems, the necessary distance is  $\sim 5$  nm. The length of PEG<sub>3400</sub> and PEG<sub>5000</sub> is estimated to be 3.5 nm and 4.3 nm, respectively (5). PEG<sub>5000</sub> is sufficient in length for stabilizing  $\beta$ CDP polyplexes in 50 mM salt. Ad-PEG<sub>3400</sub>- Lac (that has an effective polymer MW of 4000) and PEG<sub>3400</sub> do not provide enough steric stabilization under the experimental conditions. Interestingly, Gref et al., working with PEG-coated poly(lactic acid) (PLA) nanoparticles of 160-270 in diameter, also found 5000 to be the minimum PEG molecular weight necessary for significant reductions in the plasma protein binding to the nanoparticles (11).

The polymer density on the particle surface is another important factor in steric stabilization. The branched PEG compound, Ad-(PEG<sub>5000</sub>)<sub>2</sub>, probably has a much lower packing density than the linear PEG compounds. Also, the binding constant of Ad-(PEG<sub>5000</sub>)<sub>2</sub> with  $\beta$ -cyclodextrin is likely much lower than that of Ad-PEG<sub>5000</sub> due to the bulkiness of the branched PEG group. Indeed, Ad-(PEG<sub>5000</sub>)<sub>2</sub> is not nearly as effective as Ad-PEG<sub>5000</sub> in providing steric stabilization.

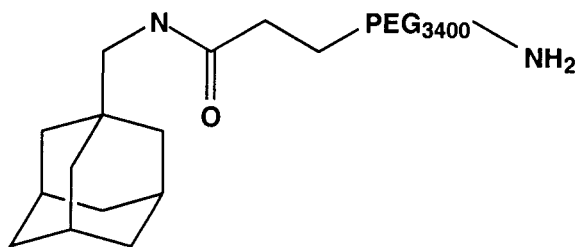


Figure 6.3a Ad-PEG<sub>3400</sub>

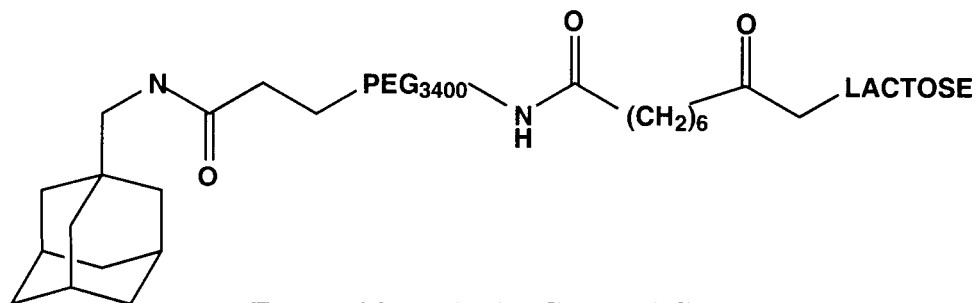


Figure 6.3b Ad-PEG<sub>3400</sub>-LAC

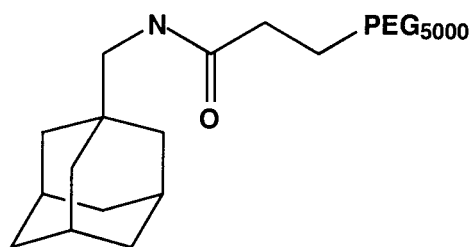


Figure 6.3c Ad-PEG<sub>5000</sub>

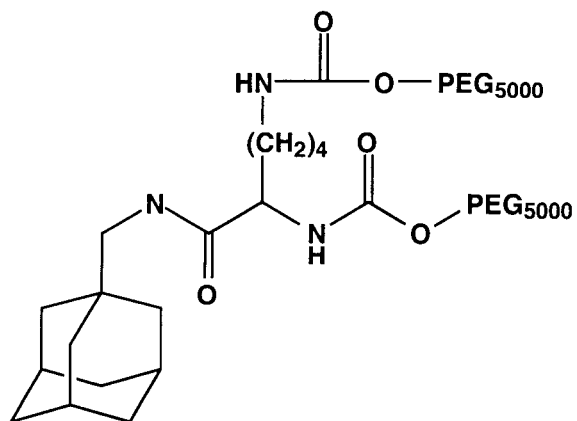
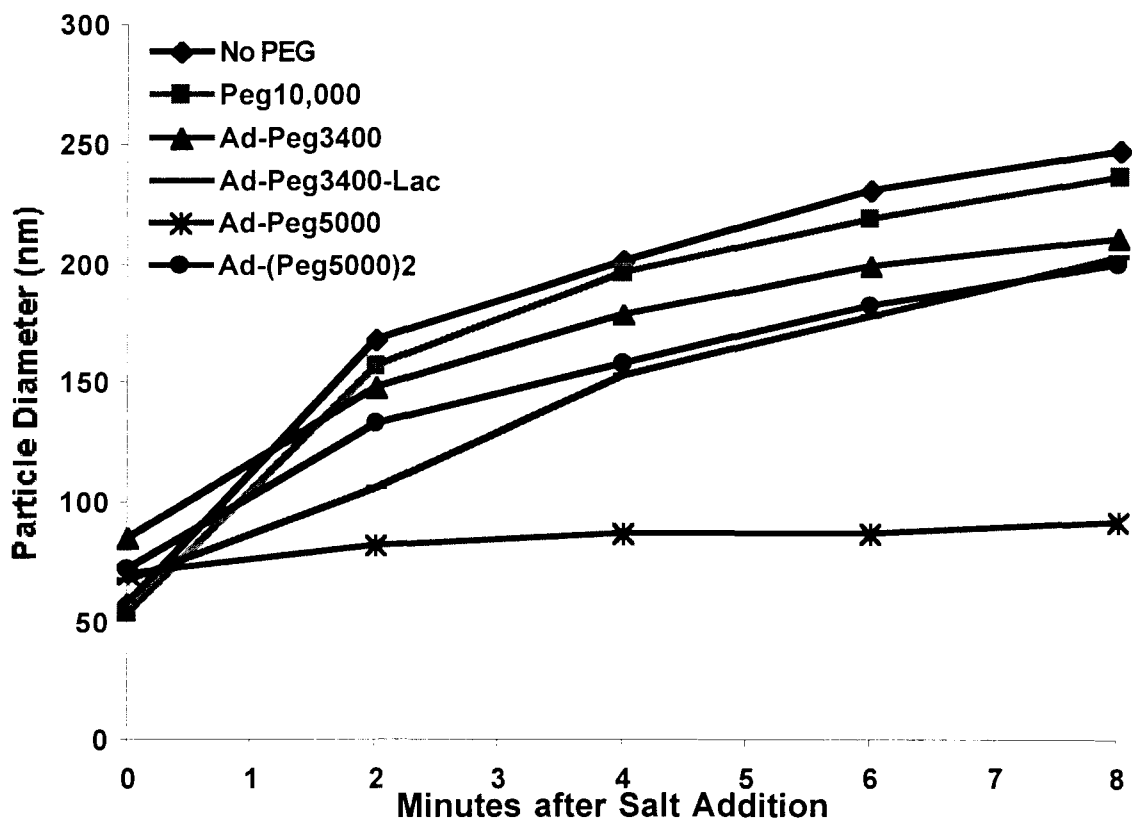


Figure 6.3d Ad-(PEG<sub>5000</sub>)<sub>2</sub>

Figure 6.3. Structures of Various Adamantane-PEG molecules.



**Figure 6.4. Salt stabilization of polyplexes by pegylation.**

2  $\mu\text{g}$  of plasmid DNA was mixed with  $\beta\text{CDP6}$  at 5+/- and then PEG compounds (100 mol% of cyclodextrin) was added to the complexes to a total volume of 1200  $\mu\text{L}$ . 600  $\mu\text{L}$  of PBS was added to the solutions and the particles sizes monitored by dynamic light scattering for 8 minutes after salt addition.

Polymers are capable of stabilizing colloidal particles by steric stabilization or depletion stabilization (5) (Fig 6.5). Steric stabilization is a result of macromolecules attached to the particle surface while depletion stabilization results from macromolecules free in solution. If the Ad-PEG<sub>5000</sub> were imparting stabilization by depletion stabilization, then an equal concentration of unmodified PEG should have the same stabilization effect. However, no enhanced stabilization was observed with the addition of an equal concentration of PEG<sub>10,000</sub> in solution. Therefore, Ad-PEG<sub>5000</sub> prevents salt-induced aggregation of  $\beta\text{CDP6}$  polyplexes by steric stabilization.

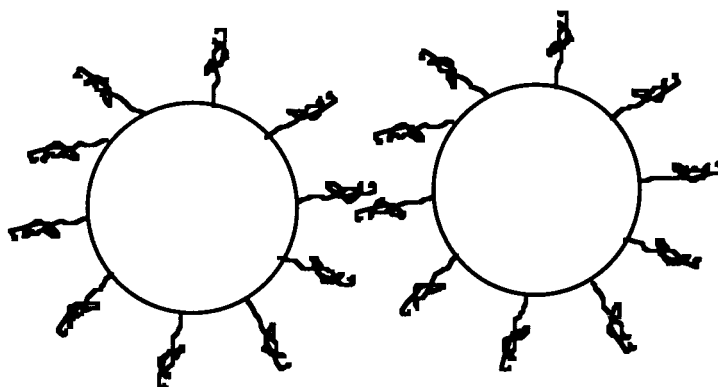


Figure 6.5a Steric Stabilization

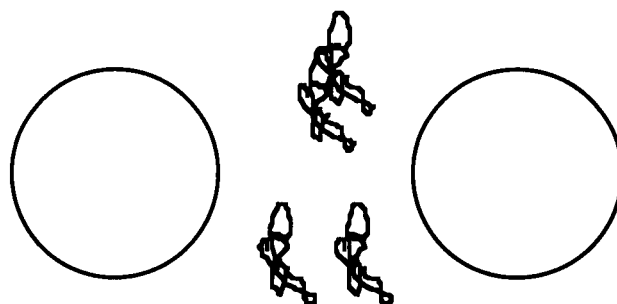


Figure 6.5b Dispersion Stabilization

**Figure 6.5. Steric stabilization versus dispersion stabilization.**

Despite the preliminary stabilization success with Ad-PEG<sub>5000</sub>, this system of polymer modification still requires improvement. In particular, the binding constant between the Ad-PEG<sub>5000</sub> and cyclodextrin molecules needs to be increased. This is evident from two experiments. First, stabilization of PEI or PLL polyplexes by grafting PEG requires a much lower PEG density on the particle than the necessary concentration of Ad-PEG<sub>5000</sub>. Gref et al. observe stabilization of PLA particles at 5 wt% PEG (11), Ogris et al. show that pegylation of every third to fourth primary amine in PEI imparts

particle stability (10), and Choi et al. pegylate up to 25% of the  $\epsilon$ -amino groups in PLL(7). Because Ad-Peg<sub>5000</sub> does not pegylate by covalent attachment to the particle, the Ad-Peg<sub>5000</sub> is in dynamic equilibrium between the solution and the particle surface. Therefore, it is unknown how much of the added Ad-Peg<sub>5000</sub> is actually particle-associated at a given time. Based on the PLA, PEI, and PLL stabilization results,  $\beta$ CDPs should be stabilized by less than 50% PEG (to cyclodextrin) on the particle surface. However, stability of  $\beta$ CDP6 polyplexes requires 100% Ad-PEG<sub>5000</sub> addition; 50% Ad-PEG<sub>5000</sub> only shows a minor advantage over the unpegylated particles. This result suggests that Ad-PEG<sub>5000</sub> is substantially partitioned into the solution phase.

Second, although Ad-PEG<sub>5000</sub> modification of  $\beta$ CDP6 polyplexes prevents particle uptake by cultured cells on short time scales (15 minutes), Ad-Peg<sub>5000</sub>/ $\beta$ CDP6 polyplexes are efficiently endocytosed into >95% of cells if incubated with cells for 4 hours. These data indicate that the Ad-PEG<sub>5000</sub> initially shields  $\beta$ CDP6 polyplexes from cell surface interactions; however, because the pegylation is reversible, the particles are eventually pegylated at a subcritical density, allowing for cell surface interaction and uptake. A systemic delivery system requires circulation times longer than 15 minutes. Therefore, the binding constant between Ad-Peg<sub>5000</sub> and cyclodextrin needs to be increased.

One method of increasing the complexation constant is to functionalize the PEG<sub>5000</sub> with two adamantane molecules. If spaced correctly, the adamantanes could complex with two cyclodextrins on the polyplex. The bi-dentate binding should greatly increase the association constant between the Peg modification and the  $\beta$ CDP-based polyplex. Another possibility is to include an anionic region near the adamantane to increase binding to the cationic polyplex. The modification of polyplexes with the anionic GALA-Ad conjugate presented in Chapter 5 decreases polyplex uptake by 2 orders of magnitude. The higher prevention of cell uptake by GALA-Ad modified polyplexes is probably due to the negative zeta potential imparted by the GALA peptide and to an increased binding constant of the peptide to the polyplex surface. While Ad-

PEG<sub>5000</sub> binds to the  $\beta$ CDP-based polyplex by inclusion complex formation, GALA-Ad interacts by both inclusion complex formation and electrostatic interaction. Therefore, the inclusion of an anionic region in Ad-PEG<sub>5000</sub> should increase its binding to the polyplex and thus promote a more effective particle stabilization.

#### **6.4.2. Adamantane-mediated co-delivery of small molecules and peptides.**

Postcomplexation modification of  $\beta$ CDP polyplexes could potentially be used to co-deliver small molecule therapeutics or transfection-enhancing agents to cells. In a proof-of-concept experiment, adamantane was conjugated to fluorescein via a PEG<sub>3400</sub> linker (Ad-PEG<sub>3400</sub>-FITC). Ad-PEG<sub>3400</sub>-FITC or PEG<sub>3400</sub>-FITC was added to  $\beta$ CDP6 polyplexes at 10% mol. (to cyclodextrin) ratio and incubated with BHK-21 cells. Fluorescein uptake was monitored by flow cytometry. Polyplex modification with Ad-PEG<sub>3400</sub>-FITC resulted in substantially increased fluorescein uptake over  $\beta$ CDP6 polyplexes incubated with PEG<sub>3400</sub>-FITC (43% vs. 14%, Fig 6.6). Free PEG<sub>3400</sub>-FITC in the media may be taken into the cell as part of the pinocytotic or endocytotic pathway. However, Ad-PEG<sub>3400</sub>-FITC is also able to enter cells when complexed to  $\beta$ CDP6. Ad-PEG<sub>3400</sub>-FITC modification of  $\beta$ CDP6 polyplexes at low ratios (10%) is unlikely to inhibit polyplex internalization. Rather, the  $\beta$ CDP6 polyplexes bind readily to the cell surface and co-delivers Ad-PEG<sub>3400</sub>-FITC to the cells as they are internalized. The  $\beta$ CDP6 polyplex-assisted delivery results in higher fluorescein fluorescence observed in  $\beta$ CDP6/ Ad-PEG<sub>3400</sub>-FITC transfected cells. This method could be applied for the co-delivery of a small molecule therapeutic along with the gene of interest.

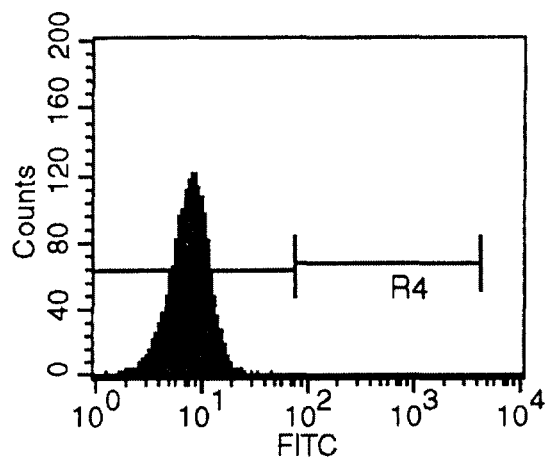


**Fig 6.6a Untransfected HUH-7**

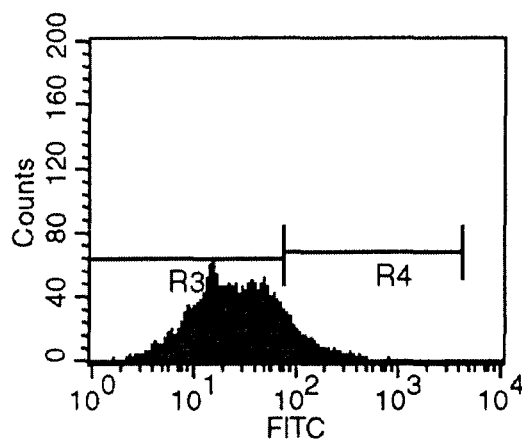


**Fig 6.6b HUH-7 transfected with  $\beta$ CDP6/Oligo + free PEG<sub>3400</sub>-FITC**

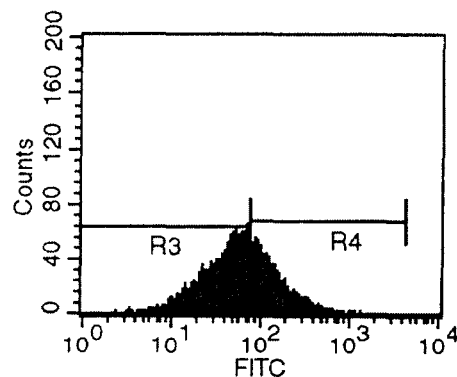


**Fig 6.6c HUH-7 transfected with  $\beta$ CDP6/Oligo/Ad-PEG<sub>3400</sub>-FITC**

**Fig 6.6. Co-delivery of  $\beta$ CDP6 polyplexes with PEG<sub>3400</sub>-FITC.**

BHK-21 cells were transfected with  $\beta$ CDP6 polyplexes in the presence of PEG<sub>3400</sub>-FITC or complexed with Ad-PEG<sub>3400</sub>-FITC. Uptake of FITC was determined by flow cytometry analysis.

$\beta$ CDP polyplexes could also be modified with agents such as fusogenic peptides or pH-sensitive polymers in order to enhance transfection efficiencies. After internalization, these peptides could assist in endosomal release of the polyplexes by changing conformations in the acidic compartments and mediating membrane destabilization or pore formation. GALA is one example of such a peptide (25). The GALA peptide undergoes a transition from a random coil at physiological pH to an amphipatic  $\alpha$ -helix in the acidic endosomes. Thus, GALA has been used to enhance transfection efficiencies in synthetic gene delivery systems (26).

Adamantane can be easily conjugated to GALA via the formation of a peptide bond. In the previous chapter, GALA-Ad was shown to associate readily with  $\beta$ CDP6 polyplexes by inclusion compound formation with the cyclodextrin moieties. It is hypothesized that delivery of these GALA-modified polyplexes should result in efficient transgene expression. Indeed, GALA-modification of  $\beta$ CDP6 polyplexes increased transfection by 2-fold even at low GALA ratios. However, the effect of GALA modification was limited due to the negative zeta potential of the polyplexes that prevented charge-mediated uptake of the modified polyplexes. One possible approach is the addition of an appropriate ligand to the GALA-modified polyplexes for receptor-mediated delivery. Some preliminary work toward receptor mediated delivery is discussed in the next section.

#### **6.4.3. Galactose Conjugation for Targeted Delivery to Hepatocytes.**

Unlike in vitro transfection or direct injection where polyplexes are immediately exposed to cells of interest, systemic delivery requires cell-specific delivery. A good model system with important therapeutic applications is targeted delivery to hepatocytes. Polyplexes can be targeted to the asialoglycoprotein receptors on hepatocyte surfaces with several ligands such as asialoorosomuroid (20), multiantennary synthetic galactose derivatives (27) and galactose (28). Galactose was chosen here for conjugation to

$\beta$ CDP6 because of its simplicity. In addition, the presence of multiple galactose ligands attached to each polyplex may mimic the multidentate binding of the protein ligands and synthetic branched derivatives.  $\beta$ CDP6 polyplexes were modified with galactose by direct conjugation, linker conjugation to polymer termini and by inclusion compound formation with the cyclodextrin moieties.

*Lactose-CDP6.* Direct conjugation of galactose to  $\beta$ CDP6 was accomplished by a reductive amination reaction between lactose (Gal-Glu) and the amine endgroups of  $\beta$ CDP6 to form an imine linkage (Lac-CDP6, Zanta, Fig 6.7).

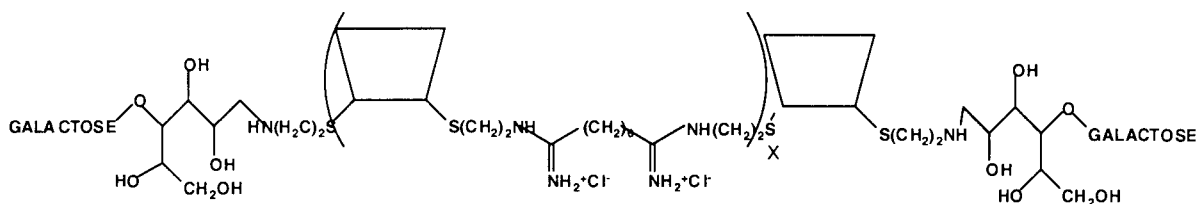


**Figure 6.7. Structure of Lactose-CDP6.**

Lac-CDP6 is able to bind and condense DNA to particles (data not shown); however, the particles have slightly larger diameters than those formed with the parent  $\beta$ CDP6 polymer (for example, particle diameter of 162 nm for Lac-CDP6 versus 130 nm for  $\beta$ CDP6 at 6+/-). To test the ability of Lac-CDP6 polyplexes to deliver to hepatocytes, HUH-7 cells (human hepatoma cell line with high levels of asialoglycoprotein expression) were transfected with Lac-CDP6 and  $\beta$ CDP6 complexed with the fluorescently labeled oligos or the luciferase plasmid at low charge ratios.

Lac-CDP6 and  $\beta$ CDP6-based polyplexes are nearly neutral when formulated at 2+/- (data not shown). Therefore, at low charge ratios, unmodified  $\beta$ CDP6 polyplexes (that enter cells by charge) should have low transfection efficiencies when compared to Lac-CDP6 polyplexes (that enter cells by receptor mediated delivery). Transfection of

HUH-7 cells with fluorescently labeled oligos (FITC-Oligo) complexed with Lac-CDP6 and  $\beta$ CDP6 at low charge ratios were visualized by confocal microscopy. No difference in DNA uptake between the two polymers was observed. In addition, Lac-CDP6 polyplexes do not demonstrate increased luciferase reporter gene expression in HUH-7 cells, suggesting that Lac-CDP6 polyplexes are not being delivered by receptor-mediated endocytosis (Fig 6.8).

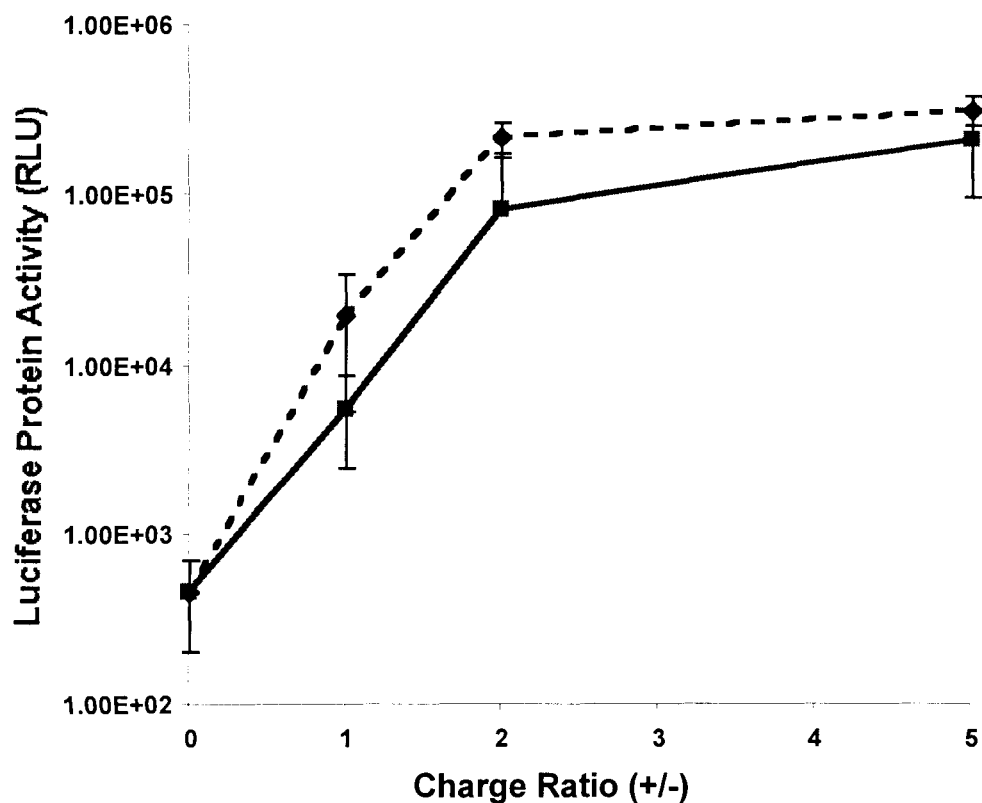


**Figure 6.8. Transfection of  $\beta$ CDP (dashed line) and Lac-CDP6 (solid line) polyplexes to HUH-7 cells.**

HUH-7 cells were transfected with 1  $\mu$ g of pGL3-CV complexed with  $\beta$ CDP and Lac-CDP6 at various charge ratios. Transfection efficiency was determined by assaying for luciferase protein activity and presented as relative light units. Results are presented as mean  $\pm$  standard deviation of three assays.

One explanation for the low Lac-CDP6 transfection is the inaccessibility of galactose conjugated directly to the polymer. Schaffer et al. describe the need for a spacer between polyplex and ligand for cellular uptake (29). Longer spaces, e.g., 3 nm, result in more efficient receptor-mediated uptake by alleviating steric hinderances. Receptor-mediated delivery to hepatocytes has been reported for lactosylated PEI (28) and PLL (19). However, while lactose was coupled to the terminal amines of branched PEI or to the amine side chains of PLL,  $\beta$ CDP6, a linear polymer, was lactosylated on the polymer backbone. Thus, the branching of PEI and side chains of PLL may serve as a spacer between the ligand and polyplex. Based on these results, lactose was conjugated to  $\beta$ CDP6 with a methylene spacer linkage.

*Lactose-(CH<sub>2</sub>)<sub>6</sub>-CDP6.* An amine-reactive methylene spacer with an extended lactosyl moiety was reacted with the  $\beta$ CDP6 end groups to give a lactosylated polymer with a 6-carbon cross-linker (Lac-C6-CDP6, Fig 6.9). Unlike Lac-CDP6, Lac-C6-CDP6 is unable to condense DNA into small discrete particles; therefore, Lac-C6-CDP6-mediated transfection of FITC-Oligo to HUH-7 cells resulted in greatly decreased uptake as compared to  $\beta$ CDP6 and Lac-CDP6 transfections (Table 6.2).

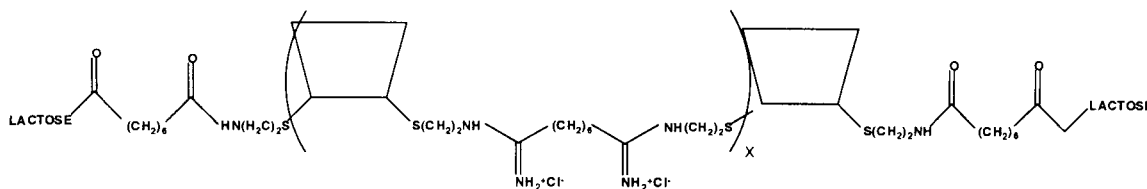


**Figure 6.9 Structure of Lac-C6-CDP6.**

Although conjugation of small molecules such as galactose or histidine (Chapter 4) to  $\beta$ CDP6 endgroups does not interfere with DNA binding and condensation, the attachment of larger entities such as the methylene linker or polyethylene glycol (Section 6.4.3) result in reduced DNA binding. Another point worth noting is that the chemistries

used for either direct lactose or histidine conjugation do not decrease the charge/polymer ratio. However, lactosylation with the methylene spacer occurs by peptide bond formation from the terminal polymer amines, reducing the average number of charges per polymer decreases from 10 to 8. The reduced charge density further decreases polymer/DNA binding. The results from Lac-CDP6 and Lac-C6-CDP6 mediated transfections suggest that direct ligand conjugation to polymer termini results in inefficient receptor-mediated uptake while ligand conjugation via a spacer group disrupts polymer/DNA binding. Therefore, receptor-mediated delivery of  $\beta$ CDPs needs to be approached from a different angle.

*Ad-PEG<sub>3400</sub>-Lac*.  $\beta$ CDP6/FITC-Oligo polyplexes were modified as described previously with 100% Ad-PEG<sub>3400</sub>-Lac. The Ad-PEG<sub>3400</sub>-Lac provides a hydrophobic guest molecule for cyclodextrin inclusion (adamantane), a spacer (PEG<sub>3400</sub>) and a galactose ligand (lactose). HUH-7 cells were contacted with 3  $\mu$ g of FITC-Oligo complexed with Lac-CDP6, Lac-C6-CDP6, and  $\beta$ CDP6 at 1+/- and 3+/- and  $\beta$ CDP6 polyplexes modified with Ad-PEG<sub>3400</sub>-Lac or Ad-PEG<sub>3400</sub>. Cellular uptake of the polyplexes was determined by flow cytometry. A summary of delivery efficiencies with the various polymers is presented in Table 6.2.

Polymer	Charge Ratio	Percent Uptake
$\beta$ CDP6	1+/-	72
$\beta$ CDP6	3+/-	94
Lac-CDP6	1+/-	70
Lac-CDP6	3+/-	97
Lac-C6-CDP6	1+/-	16
Lac-C6-CDP6	3+/-	41
$\beta$ CDP6/Ad-PEG <sub>3400</sub> -Lac	3+/-	94
$\beta$ CDP6 + Ad-PEG <sub>3400</sub>	3+/-	92

**Table 6.2 Lactose-mediated uptake into HUH-7 cells.**

HUH-7 cells were exposed to Lac-CDP6, Lac-C6-CDP6, and Ad-PEG<sub>3400</sub>-Lac-modified  $\beta$ CDP6 polyplexes delivering FITC-Oligo for 30 minutes. The polyplexes were prepared at 1+/- and 3+/. Uptake was determined by flow cytometry analysis.

The particles pegylated with Ad-PEG<sub>3400</sub> are endocytosed by HUH-7 cells as efficiently as the unmodified polyplexes (92% vs. 94%). Particles pegylated with Ad-PEG<sub>5000</sub> were delivered to cells with decreased efficiency only at short contact times (see Chapter 5). Therefore, the particles were contacted with HUH-7 cells for only 30 minutes. Because pegylation does not prevent charge-mediated delivery, even for particles formed near neutrality (Table 6.2, last row), the exact mechanism of Ad-PEG<sub>3400</sub>-Lac modified polyplex delivery remains ambiguous. It is clear from these experiments that in addition to attaching a targeting ligand, the  $\beta$ CDP6 polyplexes need to be modified to reduce charge-mediated uptake by cells. Chapter 5 discusses polyplex modification with an anionic peptide that protects particles from cellular uptake. This technique may be applied along with the lactosylated peg linker to prepare  $\beta$ CDP6 polyplexes for in vivo delivery to the liver.

In conclusion, this work has demonstrated the versatility of  $\beta$ CDP-based polyplex modification by inclusion compound formation. In the first section of this chapter, the modification method was successfully applied to pegylate  $\beta$ CDP6 polyplexes. Unlike direct conjugation methods that disrupt  $\beta$ CDP6/DNA binding, pegylation by inclusion compound formation results in discrete, small nanoparticles that are stable in salt solutions. The success of steric stabilization was found to depend on polymer length, with PEG<sub>5000</sub> providing the most stability. In the second section of this chapter, the possibility for co-delivery of small molecules or polymers was demonstrated.  $\beta$ CDP6 polyplexes assisted in Peg-FITC delivery to cultured cells by inclusion compound formation. This technique could be applied to co-deliver transfection enhancing agents such as fusogenic peptides for endosomal release or nuclear localization peptides to increase transport to the nucleus. Finally, the last section of the chapter involved the possibility for targeted  $\beta$ CDP6 polyplex delivery. Lactose directly conjugated to  $\beta$ CDP6 was found to be likely inaccessible to cell surface receptors while lactose conjugation via a spacer disrupts DNA condensation. Ad-PEG<sub>3400</sub>-Lac modification could provide for both the tether length and ligand for receptor-mediated uptake without altering the  $\beta$ CDP6/DNA interaction. In order to accomplish this, polyplexes need to be first made anionic to prevent non-specific uptake. The polyplexes could then be modified with PEG-Ligand compounds for ligand-specific delivery. By combining the particle stabilization, transfection enhancement and targeted delivery modifications discussed here, a polymeric system capable of systemic delivery becomes readily achievable.

## 6.5. ACKNOWLEDGMENTS

I thank Prof. John Brady (California Institute of Technology) for helpful suggestions regarding colloidal stabilization. I am also grateful to Jeremy Heidel for his help in running transfection experiments.

## 6.6. LITERATURE CITED

- (1) Niven, R., Pearlman, T., Wedeking, T., Mackeigan, J., Noker, P., Simpson-Herren, L. Smith, J. (1996) Biodistribution of radiolabeled lipid-DNA complexes and DNA in mice. *J. Pharm. Sci* 87, 1292-1299.
- (2) Chonn, A., Semple, S. Cullis, P. (1992) Association of blood proteins with large unilamellar liposomes in vivo. Relation to circulation lifetimes. *J Biol Chem* 267, 18759-18765.
- (3) Plank, C., Mechtler, K., Szoka, F. Wagner, E. (1996) Activation of the complement system by synthetic DNA complexes: a potential barrier for intravenous gene delivery. *Hum Gene Ther* 7, 1437-1446.
- (4) Woodle, M. (1998) Controlling liposome blood clearance by surface-grafted polymers. *Adv. Drug Del. Rev.* 32, 139-152.
- (5) Napper, D. *Polymeric Stabilization of Colloidal Dispersions*; Academic Press: London, 1983.
- (6) Woodle, M. Lasic, D. (1992) Sterically stabilized liposomes. *BBA* 1113, 171-199.
- (7) Choi, Y. H., Liu, F., Kim, J.-S., Choi, Y. K., Park, J. S. Kim, S. W. (1998) Polyethylene glycol-grafted poly-L-lysine as polymeric gene carrier. *Journal of Controlled Release* 54, 39-48.
- (8) Kwoh, D., Coffin, C., Lollo, C., Jovenal, J., Banaszczyk, M., Mullen, P., Phillips, A., Amini, A., Frabrycki, J., Bartholomew, R., Brostoff, S. Carlo, D. (1999) Stabilization of poly-L-lysine/DNA polyplexes for in vivo gene delivery to the liver. *BBA* 1444, 171-190.
- (9) Wolfert, M., Schact, E., Toncheva, V., Ulbrick, K., Nazarova, K. Seymour, L. (1996) Characterization of vectors for gene therapy formed by self-assembly of DNA with synthetic block co-polymers. *Hum Gene Ther* 7, 2123-2133.

- (10) Ogris, M., Brunner, S., Schuller, S., Kircheis, R. Wagner, E. (1999) PEGylated DNA/transferrin-PEI complexes: reduced interaction with blood components, extended circulation in blood and potential for systemic gene delivery. *Gene Therapy* 6, 595-605.
- (11) Gref, R., Luck, M., Quellec, P., Marchand, M., Dellacherie, E., Harnisch, S., Blunk, T. Muller, R. (2000) 'Stealth' corona-core nanoparticles surface modified by polyethylee glycol (PEG): influences of corona (Peg chain length and surface density) and of the core composition on phagocytic uptake and plasma protein adsorption. *Colloids and Surfaces B* 18, 301-313.
- (12) Kwok, K., McKenzie, D. L., Evers, D. Rice, K. G. (1999) Formulation of highly soluble Poly(ethylene glycol)-peptide DNA condensates. *J Pharm. Sci* 88, 996-1002.
- (13) Lee, R. J. Huang, L. (1996) Folate-targeted, Anionic Liposome-entrapped Polylysine-condensed DNA for Tumor Cell-specific Gene Transfer. *Journal of Biological Chemistry* 271, 8481-8487.
- (14) Lee, R. J. Low, P. S. (1994) Delivery of Liposomes into Cultured KB Cells via Folate Receptor-mediated Endocytosis. *Journal of Biological Chemistry* 269, 3198-3204.
- (15) Lee, R. J. Low, P. S. (1997) Folate-Targeted Liposomes for Drug Delivery. *Journal of Liposome Research* 7, 455-466.
- (16) Wagner, E., Zenke, M., Cotten, M., Beug, H. Birnstiel, M. L. (1990) Transferrin-polycation conjugates as carriers for DNA uptake into cells. *Proc. Natl Acad. Sci.* 87, 3410-3414.
- (17) Wightman, L., Patzelt, E., Wagner, E. Kircheis, R. (1999) Development of transferrin-polycation/DNA based vectors for gene delivery to melanoma cells. *J. Drug Targeting* 7, 293-303.

- (18) Martinez-Fong, D., Mullersman, J., Purchio, A., Armendariz-Borunda, J., Martinez-Hernandez, A. (1994) Nonenzymatic glycosylation of poly-L-lysine into hepatoma cells. *Nuc. Acids Res.* 21, 871-878.
- (19) Midoux, P., Mendes, C., Legrand, A., Raimond, J., Mayer, R., Monsigny, M. Roche, A. C. (1993) Specific gene transfer mediated by lactosylated poly-l-lysine into hepatoma cells. *Nuc. Acids Res.* 21, 871-878.
- (20) Wu, G. Y. Wu, C. H. (1987) Receptor-mediated in vitro gene transformation by a soluble DNA carrier system. *Journal of Biological Chemistry* 262, 4429-4432.
- (21) Chowdhury, N., Wu, C., Wu, G., Yerneni, P., Bommineni, V. Chowdhury, J. (1993) Fate of DNA targeted to the liver by asialoglycoprotein receptor-mediated endocytosis in vivo. Prolonged persistence in cytoplasmic vesicles after partial hepatectomy. *J. Biol. Chem* 268, 11265-11271.
- (22) Balaji, P., Qasba, P. Rao, V. (1993) Molecular dynamics study of asialoglycoprotein receptor ligands. *Biochemistry* 32, 12599-12611.
- (23) Hermanson, G. T. *Bioconjugate Techniques*; Academic Press: Rockford, Illinois, 1996.
- (24) Gonzalez, H., Hwang, S. J. Davis, M. E. (1999) New class of polymers for the delivery of macromolecular therapeutics. *Bioconjugate Chemistry* 10, 1068-1074.
- (25) Parente, R. A., Nadasdi, L., Subbarao, N. K. Szoka, F. C. (1990) Association of a pH-sensitive peptide with membrane vesicles: Role of Amino Acid Sequence. *Biochemistry* 29, 8713-8719.
- (26) Simoes, S., Slepishkin, V., Gaspar, R., Pedrosos de Lima, M. Duzgunes, N. (1998) Gene delivery by negatively charged ternary complexes of DNA, cationic liposomes and transferrin or fusogenic peptides. *Gene Therapy* 5, 955-964.
- (27) Wadhwa, M. S., Knoell, D., Young, A. Rice, K. G. (1995) Targeted gene delivery with a low molecular weight glycopeptide carrier. *Bioconj. Chem.* 6, 283-291.

(28) Zanta, M.-A., Boussif, O., Adib, A. Behr, J.-P. (1997) In Vitro gene delivery to hepatocytes with galactosylated polyethylenimine. *Bioconjugate Chemistry* 8, 839-844.

(29) Schaffer, D. V. Lauffenburger, D. A. (1998) Optimization of Cell Surface Binding Enhances Efficiency and Specificity of Molecular Conjugate Gene Delivery. *Journal of Biological Chemistry* 273, 28004-28009.

## Chapter 7

### Summary and Recommendations

#### 7.1. SUMMARY OF RESULTS

Most of the cationic polymers currently used for gene delivery are commercially available polycations that are tested and found to assist in DNA transfection. However, these off-the-shelf chemicals are not optimized for biological use and are therefore toxic to cells and deliver DNA with low efficiencies. In this work, a synthetic polymeric delivery system was developed by rational design. The complete system, formulated by self-assembly, consists of three components: the therapeutic gene-drug, a linear cyclodextrin-based polymer, and a modifier for in vivo stability and targeting.

Cyclodextrins (CDs) are discrete, sugar-based entities known to be non-immunogenic and tolerated at high doses in mammals. It was hypothesized that polymers synthesized from non-toxic starting materials would more likely be non-toxic as well. Therefore, cyclodextrins were incorporated into the backbone of linear, cationic polymers by co-polymerizing difunctionalized  $\beta$ -CD monomers with other difunctionalized comonomers. The  $\beta$ -cyclodextrin-based polymers ( $\beta$ CDPs) are able to bind to both plasmid DNA and oligonucleotides and condense into small particles of approximately 100-150 nm in diameter. When formulated with an excess of polymer, these particles are able to transfect cultured adherent cells with efficiencies comparable to other cationic polymers used in gene delivery. The  $\beta$ CDPs are also able to efficiently transfect suspension cell lines that are notoriously difficult to transfect. In addition, while other synthetic delivery vehicles are highly toxic to the cells, the  $\beta$ CDPs show low toxicity to all cell lines tested (Fig 7.1). The  $IC_{50}$ s of the  $\beta$ CDPs is roughly one order of magnitude above other cationic polymers and two orders of magnitudes above other cationic lipids used in gene delivery. The  $\beta$ CDPs are also relatively non-toxic in vivo. The  $LD_{50}$  of

$\beta$ CDP injected intravenously to mice is also an order of magnitude above those of cationic polymers such as polyethylenimine and poly-L-lysine. Thus, the  $\beta$ CDP can be used at a large range of concentrations without much concern for polymer-associated toxicities.

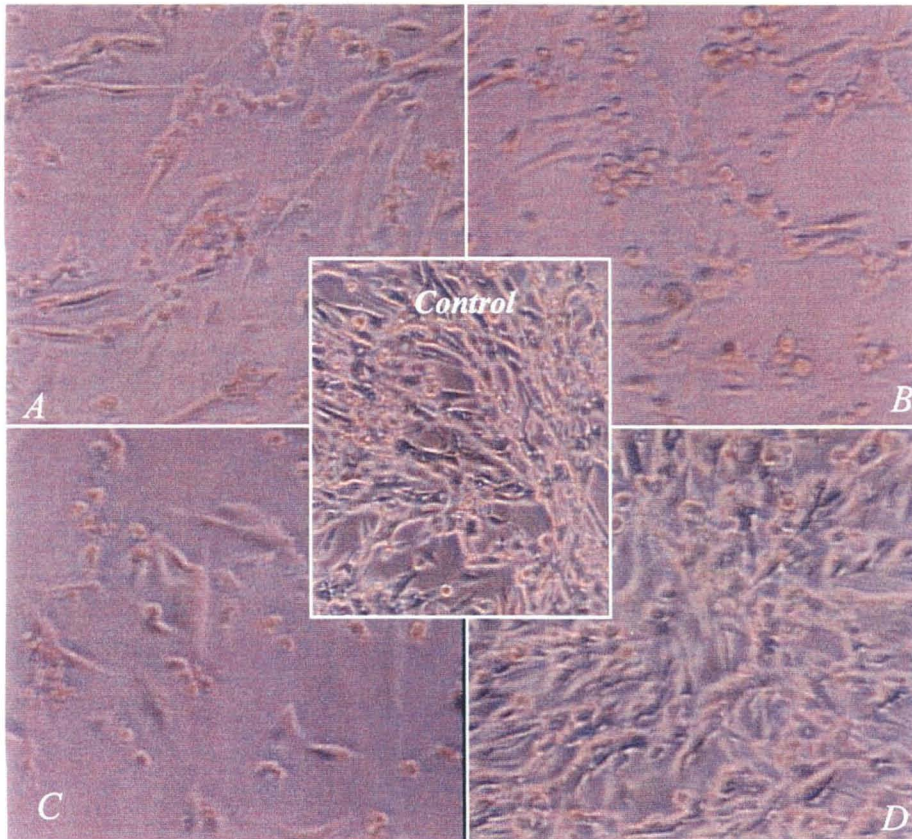


**Figure 7.1. Toxicity comparison of various non-viral vectors.**

BHK-21 cells were transfected with polyethylenimine (A), Lipofectamine™ (B), Superfect™ (C), and  $\beta$ CDP (D). The photographs are taken at vector concentrations that give approximately the same transgene activity. Untransfected BHK-21 cells are shown in the center panel.

The modular approach for synthesizing  $\beta$ CDPs facilitates a study on the effect of polymer structure on gene delivery and toxicity. Variations in the cyclodextrin comonomer verified the importance of cyclodextrins in the polymer. Incorporation of cyclodextrin into the backbone of polyamidine polymers decreases the  $IC_{50}$  of the polymers by up to three orders of magnitude. Spacer groups between the cyclodextrin moieties and the polymer amidine charge centers are also essential. The elimination of these spacer groups results in a polymer with no DNA binding ability while incorporation of a two methylene unit spacer group results in complete DNA binding, most likely by relieving steric hindrance from the bulky CD cups.

The effect of polymer charge density on polymer function was also studied by varying the length of the comonomer B units. DNA binding and condensation was achieved for all the polymers with minimal difference in polyplex sizes. However, the polymer function was greatly dependent on charge density, with up to 20-fold difference in transfection efficiency and one order of magnitude difference in polymer toxicity for the polymers studied. Incorporation of a reducible moiety in the polymer backbone had no effect on polymer toxicity and transfection. The optimum polymer for DNA transfection,  $\beta$ CDP6, was found to have a 2 methylene spacer between CD and amidine group and a 6 methylene spacer between adjacent amidine functionalities.

The basic  $\beta$ CDPs satisfied the first design criterion for a non-toxic polymer for DNA delivery. The next goal, increasing transfection efficiency, was achieved by conjugating pH-sensitive histidine molecules to the ends of the polymers. The imidazole group in histidine protonates below pH 6.0 and therefore could serve as a buffering agent in the endosomes. Buffering the endosomes delays degradation of the endosomal contents by nucleases and proteases in the lysosome. Indeed, the transfection efficiency of the histidylated polymer, Hist-CDP6, is 20-fold greater than unmodified  $\beta$ CDP6. Flow cytometry and confocal microscopy experiments suggest that Hist-CDP6

polyplexes are internalized with similar efficiencies as  $\beta$ CDP6 polyplexes but are accumulated at higher concentrations in the endosomes, most probably due to the histidine buffering effect. The higher polyplex concentration and delayed degradation allows for more opportunities for endosomal escape. Although histidylation reduces polymer solubility, no increase in toxicity is observed with Hist-CDP6. Thus, histidylation increases the transfection efficiency of  $\beta$ CDP6 without changing its toxicity profile.

The third objective was to modify the  $\beta$ CDP/DNA complexes for in vivo stability. A common strategy for modifying cationic polymers is conjugation of molecules of interest to polymer amines. However,  $\beta$ CDPs are short polymers and conjugation of other molecules directly to the polymer often disrupts polymer/DNA binding ability. The  $\beta$ CDP/DNA complexes were therefore modified by a third component, adamantane, that forms inclusion compounds with the cyclodextrin molecules. Adamantane conjugates are able to modify  $\beta$ CDP/DNA complexes without disrupting the core particles. Several applications of the polyplex modification with adamantane conjugates were investigated, including salt stabilization, co-delivery of genes and small molecules, and prevention of non-specific cellular uptake.

$\beta$ CDP/DNA complexes were modified with various adamantane-PEG conjugates and tested for salt stability. While PEGylated  $\beta$ CDP6 was unable to bind to DNA and grafting of PEG to pre-formed polyplexes by reaction with polymer endgroups resulted in complex disruption, adamantane-PEG molecules self-assembled with the cyclodextrin molecules without changing either particle size or zeta potential. The effectiveness of the PEG conjugates against salt-induced aggregation was length dependent; PEG<sub>5000</sub> was found to be the minimum applicable length for salt stabilization. The PEG-modified complexes were tested for cellular uptake. Although polyplex uptake was reduced at short time scales by PEGylation, longer incubation times resulted in efficient particle uptake. The PEGylation therefore appears to be reversible; the binding constant between

the PEG modifier and cyclodextrin polymer needs to be increased in order to prevent cell interactions.

The modifier component could also be used to co-deliver small molecules with the polyplex. One possible application could be the delivery of a tumor suppressor gene with a chemotherapeutic drug to tumor cells for cancer therapy. Another example involves the delivery of prodrugs. Because hundreds of small molecules could potentially be delivered with each polyplex, prodrugs could be delivered along with a gene coding for a catalytic protein. Expression of the protein would convert the prodrug into its therapeutically active form. As a proof-of-concept example,  $\beta$ CDP-based polyplexes were coated with adamantane-PEG-fluorescein molecules. Cells incubated with these particles were preferentially labeled over cells exposed to uncomplexed PEG-fluorescein molecules. These results demonstrate the feasibility of co-delivering small molecules and genes in one complex.

Finally,  $\beta$ CDP-polyplexes were modified with an anionic peptide (GALA) conjugated to adamantane. Modification resulted in highly negatively charged particles and prevented DNA uptake in cultured cells. The GALA-modified polyplexes were more efficient than the PEGylated particles in preventing non-specific uptake, probably due to the negative particle zeta potential. In addition, the GALA-adamantane conjugates are likely to have a higher polyplex binding constant due to the combination of adamantane/cyclodextrin complexations and electrostatic interactions between the anionic peptides and cationic polyplexes.

Thus, this work presents the development of a three component gene delivery system by rational design. The system described has clear advantages over other currently available synthetic vectors because of its low toxicity and adaptability for in vivo delivery.

## 7.2. RECOMMENDATIONS

The development of a polymeric gene delivery system with low toxicity opens up the possibility for systemic administration of gene-based therapeutics. Future improvements in the three components may result in a vector matching viral delivery efficiency while maintaining the advantages of a synthetic system. In addition, the modular self-assembly facilitates the adaptation of the designed system for different systems. A proposed vector design is presented here for targeted delivery to hepatocytes.

There are several genetic diseases that could be treated by gene delivery to the liver, including hemophilia, Crigler-Najjar, and phenylketonuria. In the case of hemophilia, the first component (the therapeutic gene-drug) could contain gene coding for a clotting factor. The second component would be a cationic, cyclodextrin-based polymer such as  $\beta$ CDP6.

The third component would consist of a mixture of adamantane conjugates assisting in stabilization and cell targeting, endosomal escape, and nuclear localization. The desired characteristics for each component will be discussed briefly and a proposed structure will be presented.

*Stabilization and cell targeting.* The results presented in this work demonstrate that the binding constant between a single adamantane molecule and  $\beta$ -cyclodextrin is too low for applications requiring sustained interactions. Thus, the third component should contain a small anionic region near the adamantane to increase the binding affinity between the polyplex and modifier. Polyethylene glycol should also be incorporated to provide salt and serum stability to the particles. For hepatocyte targeting, a ligand such as lactose needs to be conjugated to the ends of the PEG. Lactose binds specifically to asialoglycoprotein receptors expressed on hepatocytes. After internalization into the endosomes, the polyplexes should be released from the receptors. If the compound

contained a disulfide bond, reductase enzymes in the endosome would facilitate release of the polyplexes. A schematic for this component is shown in Fig 7.1.

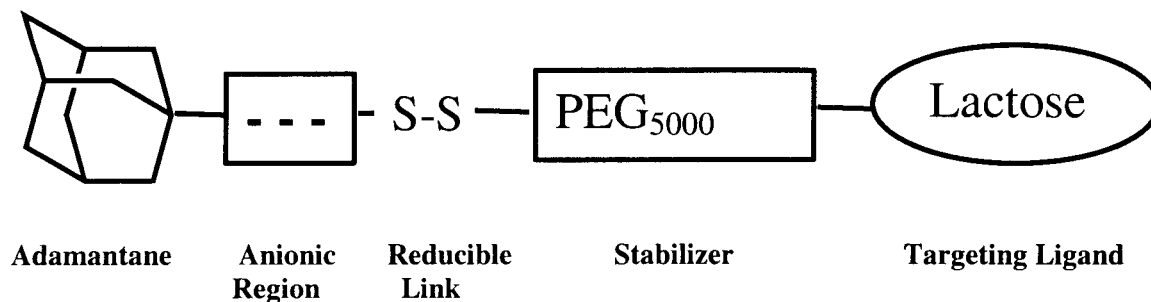


**Figure 7.1. Stabilization and cell targeting component.**

*Endosomal release.* As discussed above, the endosomal release component should contain a short anionic region near the adamantane. In addition, a pH-sensitive polymer or peptide could be used to enhance endosomal release. In this example, the GALA peptide (see Chapter 4) that undergoes a conformational change below pH 6.0 to become membrane lytic is selected for its water-solubility characteristic at physiological pH. Like the targeting component, the endosomal release peptide should be cleaved from the polyplex in the endosome to enhance its lytic abilities. Therefore, a disulfide bond should also be incorporated in the molecule.

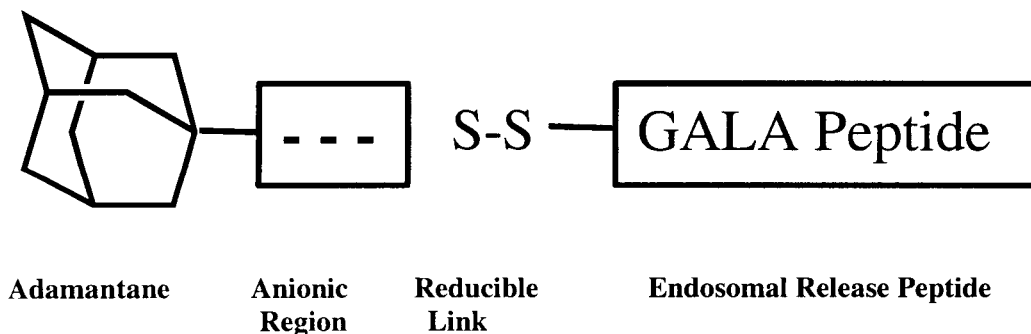


**Figure 7.2. Endosomal release component.**

*Nuclear localization.* The nuclear localization should also contain an anionic region for stronger binding to the polyplex. Several authors have published on effective nuclear localization sequences (NLS) for gene delivery. For example, Zanta et al. demonstrate that incorporation of a single NLS on a reporter gene enhances gene expression by to a thousandfold.(1) However, this component should stay on the polyplex after endosomal release; therefore, no disulfide bond should be incorporated. After release from the endosome, the polyplex should be coated with only NLS for efficient DNA translocation to the nucleus.

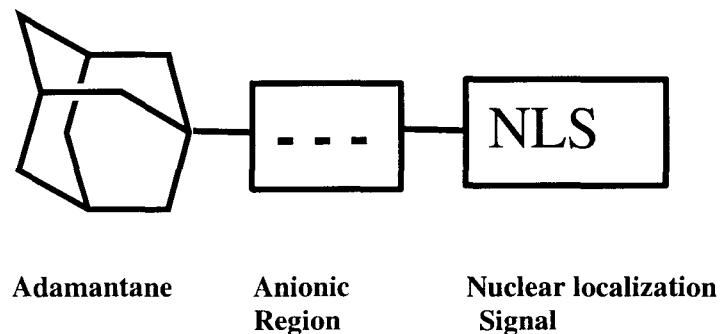


**Figure 7.3. Nuclear localization component.**

The final delivery vehicle is depicted in Fig 7.4. The optimal concentration of each entity added to the polyplex would have to be determined experimentally. However, this example demonstrates the modular approach to assembling a system for a specific target. The vehicle could be easily adapted to different targets by substituting in the desired ligand for the lactose. Once in vitro cell-specific targeting and delivery is achieved, in vivo testing could begin.

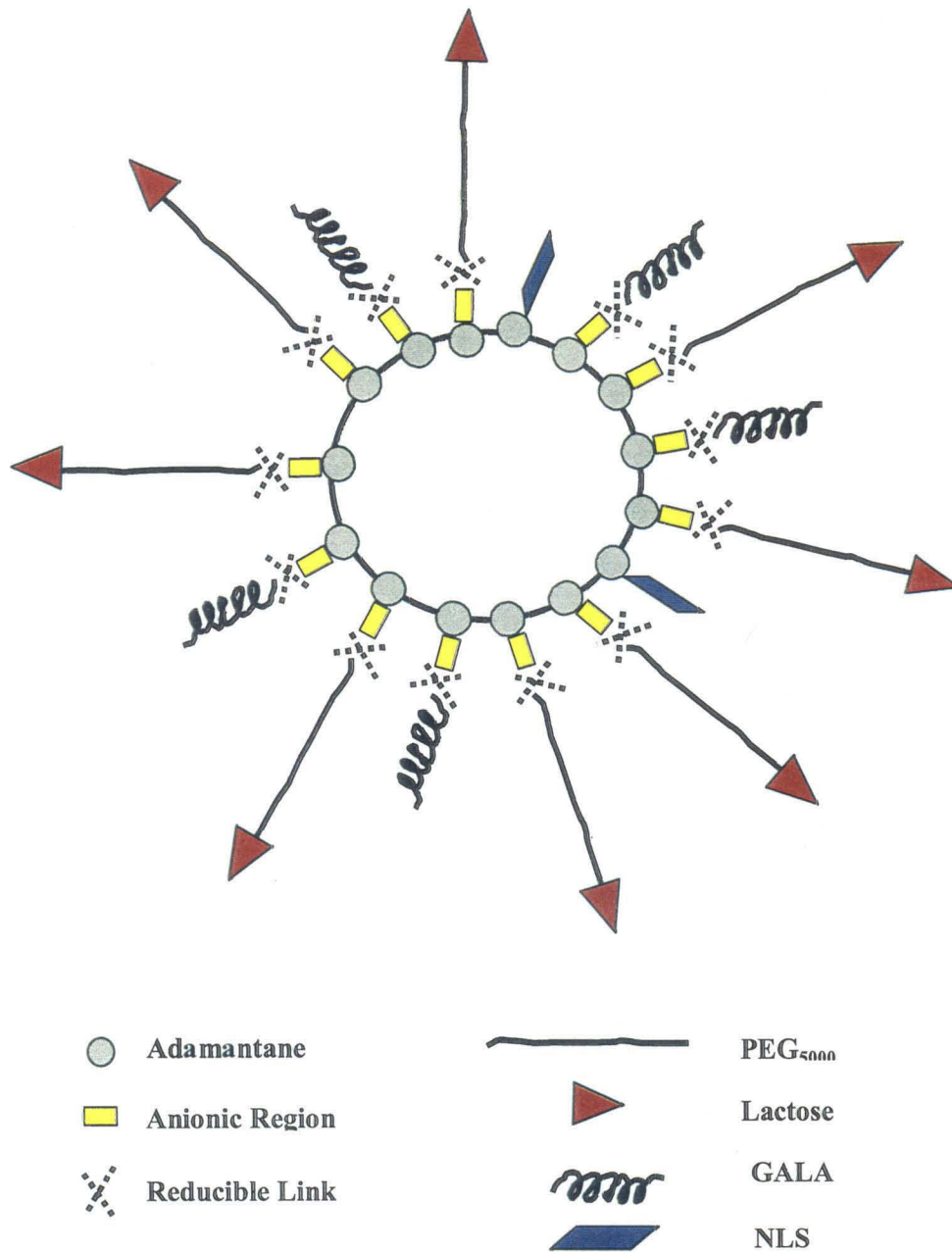


Figure 7.4. Proposed delivery vehicle for liver targeting.

### 7.3. LITERATURE CITED

1. Zanta, M., Belguise, P. and Behr, J. (1999) Gene Delivery: A single nuclear localization signal (NLS) peptide is sufficient to carry DNA to the cell nucleus. *Proc Natl Acad Sci USA*, **96**, 91-96.